Effects of Diluent Addition and Mixing Conditions on Solvent Deasphalting of Bitumen Emulsions

by

Aligulu Alili

A thesis submitted in partial fulfillment of the requirements for the degree of

Master of Science

in

Chemical Engineering

Department of Chemical and Materials Engineering
University of Alberta

Abstract

Unconventional oil reserves, such as Canada's oil sands, must replace dwindling conventional oil supplies to meet the globally increasing energy demands. Canada is home to the third largest oil reserves, primarily in the form of bitumen deposits. Unlike conventional oil, bitumen has some unique characteristics that render its extraction more challenging. As a consequence of its high asphaltene content, bitumen is substantially denser and more viscous than conventional oil, and thus, it gives rise to challenges in the forms of sedimentation, deposition, precipitation, fouling, coke formation, and catalyst deactivation in both upstream and downstream processes. By studying the effects of the solvent-to-bitumen ratio (S/B) and mixing conditions on the solvent deasphalting (SDA) of the steam-assisted gravity drainage (SAGD) extracted bitumen emulsion, the goal of this project is to support the design of a solvent deasphalting process to enhance the bitumen production and treatment processes in bitumen extraction sites. The particular objective of this study is to determine the effectiveness of the SDA process applied to bitumen emulsions produced during the SAGD process.

The experiments of this study were performed in a bench-scale windowed reactor, in which both mixing and settling were conducted. Both batch and semi-batch experiments were performed to assess the feasibility of the process for scale-up to a larger scale continuous process. Operating temperature and pressure were kept constant at 164 ℃ and 40 bars. The effects of S/B ratio (0.9 – 2.2), mixing intensity (0.1 – 0.5 W/kg), and mixing energy (0.1 – 1.6 kJ/kg) on asphaltene precipitation and deasphalted oil (DAO) quality were studied.

The effects of the S/B ratio on the solvent deasphalting of bitumen emulsion vary depending upon the value of the S/B ratio. Below the onset of asphaltene precipitation, no asphaltene precipitation

was detected and the addition of solvent merely diluted the bitumen and slightly reduced its density and viscosity. However, above the onset value, a substantial increase in asphaltene precipitation was observed with the addition of more solvent. For the studied solvent blends, the onset of the asphaltene precipitation was found to be below 0.9 and for the S/B ratio range studied here, the optimum S/B ratio for a commercial SDA process was determined to be about 1.8.

Almost no literature data is available regarding the impact of mixing parameters on asphaltene precipitation from bitumen emulsion upon treatment with paraffinic solvents. In the studied range of mixing intensity and mixing energy, it was revealed that the impact of changing mixing conditions on solvent deasphalting of bitumen emulsion is insignificant. Provided that a well-mixed bitumen emulsion and solvent stream has been achieved, the amount of mixing energy and mixing intensity does not perceptibly change the asphaltene precipitation yield and the deasphalted oil quality, at least for the conditions studied here.

It was proven that settling time has a substantial impact on the asphaltene content of deasphalted oil and higher quality oil can be obtained with longer settling times. This indicates that aggregates with a wide range of diameters and densities exist in the system. Nevertheless, after the first 10 minutes of the settling process, asphaltene aggregates settling significantly drops and the change in asphaltene content of DAO samples becomes less noticeable.

Finally, it was determined that from the perspective of a commercial-scale bitumen emulsion upgrading plant, a multistage SDA process is more favourable than a single-stage SDA with a high S/B ratio. The residence time in mixers and settlers can be significantly reduced to increase production rate and improve process economics.

Dedicated to Aya

Acknowledgements

I am indebted to several individuals for their assistance and support throughout my research; without them it would be impossible to accomplish this work. Firstly, I wish to express my deepest gratitude to my supervisor, Dr. Sean Sanders, for providing me with the opportunity to be a part of such an important research project and assisting me to develop myself professionally and to manage the project efficiently. I am thankful to him for all the support and valuable feedback that he provided throughout my research that substantially altered my work for the better.

I would like to extend my gratitude to Aya; this work would not have been possible without her continued support and care.

I have much appreciation for the Pipeline Transport Processes (PTP) research group, which I have had the honour of being a part of. In particular, I am very thankful to Dr. Marcio Machado for his valuable comments on the project and support to conduct the experiments. Moreover, I would like to pay my special regards to Dr. David Breakey and Aaron Cheung for their assistance at the start of my research. I would also like to acknowledge Ms. Terry Runyon for her administrative support.

Finally, I am thankful to CNOOC for providing financial support to realize the research project.

Table of Contents

List of Figures

List of Tables

List of Symbols

Symbol	Description	Units
δ	Solubility parameter	$MPa^{1/2}$
ΔH	Enthalpy of vaporization	J/mol
R	Universal gas constant	$kJ/(K.mol)$
T	Temperature	K
ν_i	Molar volume	m^3/mol
P	Power	W
N_P	Power number	–
m	Mass	kg
V	Volume	m^3
ρ	Density	kg/m^3
N	Impeller rotational speed	rev/s
D	Impeller diameter	m
ε_{mix}	Mixing intensity	W/kg
E	Mixing energy	kJ/kg
t_{mix}	Mixing time	s

List of Acronyms

DAO	–	Deasphalted oil
S/B	–	Solvent-to-bitumen ratio
SOR	–	Steam-to-oil ratio
SDA	–	Solvent deasphalting
SAGD	–	Steam-assisted gravity drainage
RPM	–	Revolution per minute
RT	–	Rushton turbine
PBT	–	Pitch blade turbine
PTP	–	Pipeline Transport Processes

1. Introduction

1.1 Background

Conventional crude oil reserves are in decline; therefore finding unconventional and long-lasting oil sources becomes critical to meet the world's rapidly growing energy demands.[1,2] One of the ways to meet these demands is the utilization of Canada's oil sands, which contain heavy oil and bitumen (i.e. extra heavy oil).[3] Compared to the conventional oil that has supplied the world with its primary energy source for more than a century, heavy oil is more viscous and denser: that is also where heavy oil gets its name.[4,5]

Canada holds the 3rd rank in the world for its recoverable oil reserves and more than 95%, or 169 billion barrels, of this oil is in the form of oil sands.[6–8] Canada's major oil sands deposits are located in northern Alberta; Athabasca, Peace River, and Cold Lake.[6,7,9,10] The Canadian oil sands industry had a production capacity of 3.6 Mbbl/day in 2018 and with the current growth rate, it is forecasted that it will reach a production capacity of 5 Mbbl/day in 2030.[11] However, the oil sands industry suffers from technological impediments. These challenges are primarily related to sustainable resource extraction and are encountered in the mining, extraction, transportation, and upgrading stages. Some of those challenges are introduced here.

Unlike conventional oil reserves, bitumen resides in reservoirs in the form of oil sands. Oil sands mainly are a combination of sand, bitumen, water, and clay.[9,12,13] Oil sands deposits may be close to the surface or deep under the ground and depending on the depth of reserves different extraction methods are used to extract bitumen.[9,10,14] If the deposits lie 75 m deep or closer to the surface, bitumen is extracted through open-pit mining. If the deposits are located much deeper then bitumen recovery takes place through in situ methods such as steam-assisted gravity drainage (SAGD).[9,10,14–16]

Of the recoverable Canadian oil sands deposits, 80% is too deep to be profitably extracted by surface mining and therefore can only be exploited using in situ methods.[12,17] The SAGD process and its variations are widely used in situ methods in the oil sands industry to efficiently extract bitumen.[18] In its basic form, the SAGD process involves two pipelines buried deep under the ground with a 5 m vertical distance in-between. High-pressure superheated steam is injected

through the upper pipeline into oil sands reservoir. In the reservoir, since hot steam significantly increases the reservoir temperature and reduces the bitumen viscosity, the bitumen flows under gravity into the second pipe running below the steam line. The mixture of bitumen and water that flows into the production pipe is then pumped to the surface.[18–21] The product obtained through the SAGD process mainly consists of bitumen and water; however, some small amounts of sand and clay may also present in the extracted product.[9] After the extraction stage, the purification of the product takes place, during which the majority of impurities and water are removed and the bitumen is obtained as the final product. It is noteworthy that a large amount of water is present in the SAGD product in the form of a water-in-bitumen emulsion, which is detrimental to oil quality. Therefore, one of the objectives of subsequent bitumen treatment processes is to minimize the emulsified water content of bitumen.[9,22]

The bitumen emulsion extracted from oil sands is significantly different from conventional oil: it is very viscous and contains high molecular weight hydrocarbons, heavy metals, sulphur, nitrogen, and emulsified water.[23,24] Bitumen properties may differ depending on the reservoir and also significantly depend on the ambient temperature.[25] Bitumen, in most general classifications, is referred to as an oil with a viscosity greater than 10 Pa.s, which is 4 orders of magnitude greater than water viscosity at room temperature.[23,26] Bitumen density is greater than 1000 kg/m^3 at room temperature and ambient pressure conditions.[23,26–28]

The presence of asphaltenes is the primary reason for bitumen's exceptionally high viscosity and density.[29,30] Asphaltenes are characterized by their low reactivity that causes catalyst deactivation and coke formation in refineries.[30–32] In addition, asphaltenes may precipitate and deposit in the wellbore, flowlines, and/or separation units due to sudden temperature, pressure, or composition changes.[29–35]

The primary challenge faced after the extraction process is the transportation of bitumen from an extraction site to refineries. For this reason, bitumen has to meet pipeline specifications to be transported through a pipeline. For oil transportation, the maximum allowable oil density and viscosity are 940 kg/m^3 and 350 mPa.s, respectively; however, the bitumen extracted from oil sands has a density of over 1000 kg/m^3 and viscosity of more than 10 000 mPa.s.[16,36,37] To overcome this challenge, the bitumen density and viscosity have to be reduced to meet pipeline

specifications and it can be accomplished through industrially proven bitumen treatment methods: dilution and upgrading. These are the two main methods employed in bitumen extraction sites to address the challenges associated with the presence of large asphaltenes fraction and facilitate the transportation of bitumen to refineries.[3,36,38]

Dilution of bitumen with a large amount of naphtha or natural gas condensate is a method that is employed to reduce the density and viscosity of bitumen to meet pipeline specifications and the product obtained through this method is called DilBit.[3,36,37] The drawback associated with this approach, however, is that a significant amount of diluent is required to decrease the density and viscosity of bitumen and that gives rise to a considerable reduction in pipeline capacity to transport bitumen.[3,37] The type of diluent used defines the diluent-bitumen blend ratio and to meet pipeline specifications this value may range between 20 – 50 % in volume.[3,39]

The other method is the upgrading of bitumen, which takes place through either heat treatment or paraffinic solvent treatment, or a combination of both.[37,40] Through heat treatment, the quality of bitumen is improved and the density and viscosity of bitumen are decreased as a result of chemical cracking reactions; however, this process often results in coke formation that is also a major challenge associated with asphaltenes.[38,41] Thus, a more common practice to partially upgrade bitumen is the treatment of the extracted bitumen with paraffinic solvents such as n-pentane or n-heptane that results in the precipitation of asphaltenes, which in turn significantly reduces the product density and viscosity and facilitates bitumen transportation.[36,37] The process of oil upgrading through paraffinic solvent treatment is also known as the solvent deasphalting (SDA) of bitumen and it is a commercially prevalent partial bitumen upgrading method.[37,42]

Depending on the amount of asphaltenes removed and required improvement in oil quality, partial or full bitumen upgrading can be performed. The product obtained through the full bitumen upgrading process is called synthetic crude oil (SCO) which contains almost no vacuum residue and possesses physical properties close to those of the light oil.[3] Full bitumen upgrading requires massive investment in facilities on the extraction sites. Therefore, partial upgrading of bitumen is usually a more desirable option, which costs less than half the investment required for full bitumen upgrading facilities.[3] As a result of the partial upgrading process, the diluent amount required to

facilitate bitumen transportation is substantially reduced and that enables the pipeline to be used with its maximum capacity.[37]

1.2 Solvent deasphalting (SDA)

Solvent deasphalting of the in-situ extracted product (i.e. bitumen emulsion) is a partial bitumen upgrading process that aims to remove water and impurities and minimize the asphaltene content of bitumen as a result of treatment with light paraffinic solvents.[37,43] Through the SDA process, the fluidity of bitumen is increased significantly and it leads to a substantial improvement in bitumen transportability by pipeline. Being one of the widely used partial bitumen upgrading processes, the solvent deasphalting process harnesses the low solubility of asphaltenes in order to precipitate them with the aid of paraffinic solvents. Asphaltenes are highly aromatic and poorly soluble in a paraffinic medium; that is why treating bitumen with light paraffinic solvents leads to the precipitation of asphaltenes.[34,44]

Figure 1.1 provides a high-level illustration of an SDA process that is used to upgrade the SAGD-extracted bitumen emulsion. It is noteworthy that prior to feeding the in-situ product to an upgrading unit, some of the free water is removed from the SAGD product in order to harness the maximum capacity of the solvent deasphalting unit. In an industrial-scale SDA process, bitumen emulsion and paraffinic solvent are mixed and the mixture is then pumped to a settler. The mixture is allowed to settle for a certain time, after which three distinct phases are expected to be observed in the settler: deasphalted oil (DAO) phase, asphaltenes-rich phase, and water phase. Being the lightest of the three components, the DAO is obtained as the top phase or overflow product. The DAO is the valuable product of the SDA process and it has a significantly lower density and viscosity compared to the feed (bitumen emulsion). The asphaltenes-rich phase is the low-value product that forms between the DAO and water phases. The asphaltenes-rich phase consists of asphaltenes, maltenes, and solvent and this phase is also referred to as the pitch phase; both terms are used interchangeably in the thesis. As is evident from Figure 1.1, asphaltenes are removed within the water phase from the bottom of the settler. The asphaltenes-rich phase has solid-like properties at room temperature and it cannot flow unless heated up to above 140 ℃.[45,46] The water inside the settler is used to remove the precipitated asphaltenes from the process units. Consequently, it is essential to feed enough water into the process with the bitumen emulsion in

order to facilitate continuous displacement of the pitch from the settler as a dispersed water-pitch mixture.

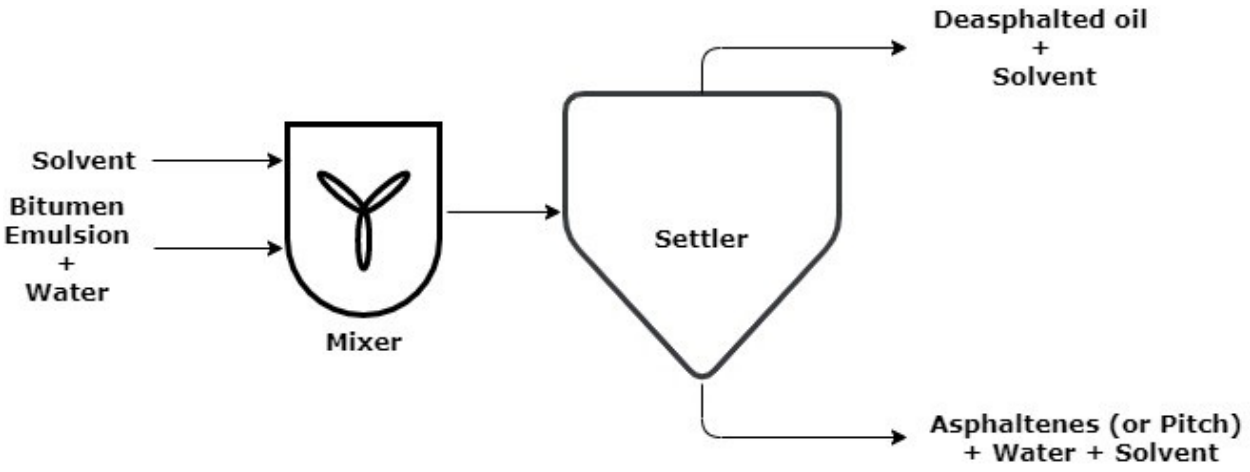

Figure 1. 1. A high-level overview of solvent deasphalting of bitumen emulsion

Figure 1.2 demonstrates a simplified version of the solvent deasphalting of the SAGD-extracted bitumen emulsion in a batch reactor.[47] Initially, the SAGD-extracted bitumen emulsion and water are fed to the reactor (Figure 1.2a). Then, the required solvent mass is calculated and added (Figure 1.2b). After the loading is complete, the reactor is sealed and the mixer is started, which continues until the required mixing has been achieved (Figure 1.2c). Finally, the vessel contents are allowed to settle for a certain amount of time (Figure 1.2d). Figure 1.2d illustrates the three phases that form inside the reactor at the end of the paraffinic solvent treatment process.

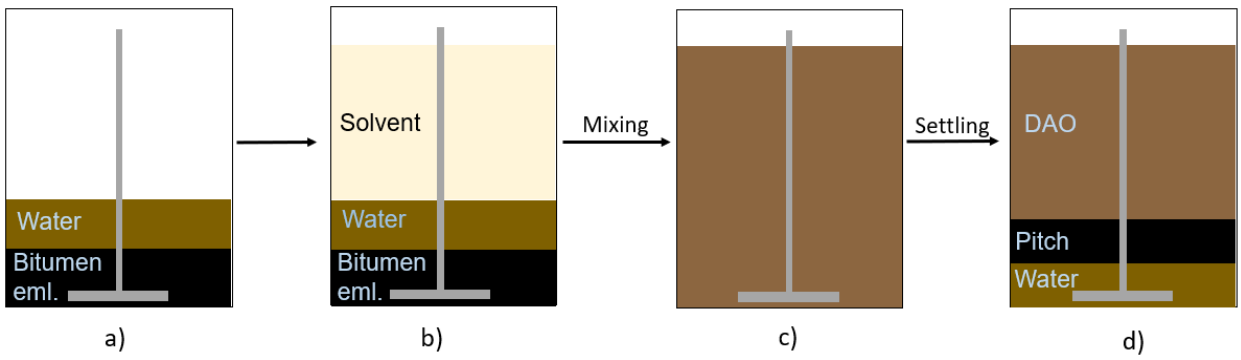

Figure 1. 2. Simplified laboratory-scale solvent deasphalting process: a) SAGD-extracted bitumen-water mixture, b) addition of paraffinic solvent, c) vessel contents during mixing, d) vessel contents after settling. Reproduced from Yarranton et al.[47]

The emulsified water amount and asphaltene content of deasphalted oil are indications of the quality of the SDA product. The product yield and product quality of the SDA process depend upon several factors, including temperature, pressure, solvent type, solvent-to-bitumen ratio (S/B), mixing intensity (energy dissipation per unit mass), and mixing energy (the product of mixing time and mixing intensity).[42,48,49] Numerous studies[9,45,50,51] have been performed to study the effects of temperature, pressure, and solvent addition on the partial bitumen upgrading process; however, little research has been conducted to understand the mixing and settling dynamics of the process. The available research data[8,35,52,53] suggest that the mixing parameters and settler residence time are essential optimization points that may help to improve process efficiency.

1.3 Problem statement

One of the main challenges for in situ bitumen producers is transporting their product to market. For North America, oil must have less than 350 mPa.s dynamic viscosity and its API gravity must be above 19 to meet pipeline specifications.[16,36,37] Prior to upgrading, the SAGD-extracted bitumen has an API gravity of less than 7 and viscosity of more than 10 000 mPa.s at 25 °C.[16,26,36] Therefore, a solvent deasphalting unit is employed to increase the fluidity of the bitumen to an extent that it does not require diluent addition to facilitate bitumen transportation through a pipeline. Recall from Section 1.1 that diluent addition significantly reduces the pipeline capacity to transport bitumen. Furthermore, the extracted bitumen also contains a significant amount of emulsified water that is very detrimental to the oil quality, and thus the emulsified water amount must also be minimized as much as possible during the solvent deasphalting process.

Initially developed to upgrade the vacuum residue and dry bitumen, solvent deasphalting technology has recently been introduced to the oil sands field, where it (in theory) would receive bitumen emulsion as feed.[8] However, little is known about the feasibility of the solvent deasphalting process that treats in-situ extracted bitumen emulsion. Furthermore, the concept of integration of the solvent deasphalting unit with the SAGD extraction process has recently been ventured by Nexen, where the SDA unit receives the feed directly from the SAGD process.[54] Although preliminary estimates indicate that it is a more viable option compared to the conventional use of the SDA process, a great deal of research is required to support this claim and establish the integration process as a viable technology.[54] The SAGD-SDA process is still in the

development stage and several concerns and questions are yet to be addressed: for example, the aggregation and precipitation of asphaltene particles, the impact of water to the mixing and asphaltene precipitation, mixing characterization of the bitumen emulsion-solvent stream, efficient removal of asphaltenes from the process, fluid dynamics of the pitch + water removal, building a commercial-scale plant etc.[8]

Research in many of these areas is still in progress and in fact, the objective of this study is to address some of these concerns and to support the development of a commercial-scale solvent deasphalting process.

1.4 Objectives

The objective of the project is to investigate the operating parameters of the solvent deasphalting unit in a bench-scale setup to gain information essential to scale up the SDA process and ultimately successfully develop a commercial-scale partial bitumen upgrading process. Several experiments will be performed in batch and semi-batch modes and the samples of DAO and pitch will be taken to study the impact of operating parameters on the SDA products. The investigation of the effects of S/B ratio, mixing parameters, and aggregates settling time on the asphaltene precipitation process is one of the initial stages of the SDA data collection process that will be accomplished within this study. The following are the detailed objectives of the project that will be investigated.

- **To study the effects of solvent-to-bitumen (S/B) ratio on asphaltene precipitation from bitumen.** In a bench-scale SDA unit, the SAGD-produced bitumen emulsion will be treated with different S/B ratios to find out the impact of varying solvent amounts on asphaltene precipitation from bitumen.
- **To study the effects of mixing conditions on asphaltene precipitation from bitumen.** Different mixing intensities and mixing energies will be used to study their impact on asphaltene rejection from the SAGD-extracted bitumen emulsion. No research performed to date can provide a comprehensive explanation in regard to the impact of mixing intensity and mixing energy on asphaltene precipitation from bitumen emulsion-solvent stream. The separate effects of both mixing energy and mixing intensity will be attempted to be studied under isolated experimental conditions.

- **To study the aggregates settling rate under various experimental conditions and the impact of settling time on the DAO quality.** The performed experiments will be recorded and by tracking the interface heights over time, the settling rate of asphaltene aggregates will be calculated. Besides, by retrieving several DAO samples at different settling times, the effects of settling time on the DAO quality will be determined.

1.5 Thesis outline

This section provides an outline for the thesis and introduces the main discussion points for each chapter. Chapter 1 gives background information about the project and elucidates the objectives of the project. It explains how the bitumen extracted from oil sands can cause challenges during transportation and refining. In addition, the objectives of the study and the main courses of action that can be taken to address these challenges are explained. This chapter also provides a high-level description of an SDA process and elaborates on how an SDA unit can be employed to minimize the asphaltene content of bitumen and increase the quality and value of oil.

Chapter 2 introduces detailed information about the essential research results hitherto obtained in the SDA field and analyzes the expected trends and limitations of the project. Moreover, it points out the gaps in the field of the SDA process and provides a strong foundation for the current study. The solvent deasphalting concept is explained and the parameters that can be manipulated to improve the asphaltene precipitation process are investigated.

Chapter 3 describes the materials that were used and the experiments that were conducted for the study. The major objectives of each set of experiments are laid out. The procedures followed to run each set of tests have been elaborated and the analyses made on the samples and the calculations performed to interpret results are elucidated in this chapter. Furthermore, this chapter provides detailed information about how the mixing and settling processes have been performed and the methods employed to calculate mixing parameters and aggregates settling rate.

In Chapter 4, the experimental results obtained with varying S/B ratios are introduced, discussed, and compared to the literature data. The impact of the solvent amount on the asphaltene precipitation process in terms of pitch yield and DAO quality is investigated. The densities of the

deasphalted oil samples taken at different S/B ratios are used as the supporting information for the conclusions.

Chapter 5 introduces the experimental results for the effects of different mixing conditions and investigates the possible interpretations and implications of those results to the solvent deasphalting field. The pitch yield and asphaltene quality of DAO are two parameters that are studied and compared to the literature data in order to determine the impact of mixing intensity and mixing energy on asphaltene precipitation from bitumen.

In Chapter 6, based on the images of the settling process, the asphaltene aggregates settling trends are studied, and the average settling rate is calculated for each experimental condition and the effects of experimental conditions on aggregates settling process are explained. Additionally, the DAO samples taken at different settling times are used to analyze the impact of settling time on the asphaltene content of DAO samples.

Chapter 7 summarises the major conclusions drawn from Chapters 4, 5, and 6. The significant contributions of the project are explained and the possible implications of the results to the commercial development of a SAGD solvent deasphalting are described. In addition, this chapter provides some recommendations to further investigate and improve the SDA process in the future.

1.6 Author's contribution

The bench-scale SDA setup was built by Dr. David Breakey and the author made necessary modifications to the existing bench-scale solvent deasphalting reactors' setup to be able to perform various batch and semi-batch experiments. Some of the major modifications made on the existing SDA setup are the commissioning of pressure equalization line, underflow cooling line, solvent heater, and solvent pump. The original safe work procedure (SWP) and operation checklist were written by Aaron Cheung and Dr. David Breakey, and of the twelve experiments mentioned in this study, five were conducted with their help. The author updated the SWP and operation checklist to meet new and improved design conditions. The remaining seven experiments were conducted with the help of Dr. Marcio Machado. The author generated the asphaltene aggregates settling graphs from the recorded settling images and calculated the average aggregate settling rate for all the SDA experiments conducted in the current study. The settling images were analyzed using a

MATLAB code written by Dr. David Breakey. All the results and interpretations provided in the thesis are the original work of the author.

The initial test matrices for the project were built by Dr. Sean Sanders, Dr. David Breakey, and Milan Todorovic (CNOOC representative). The author was responsible to run the experiments, collect and analyze the experimental results, make PowerPoint presentations about the performed experiments, and propose improvements to the following experiments. The author carried out the sampling of the SDA products, performed the density measurements for the taken samples, and sent the DAO samples for water and asphaltene content analyses. The water content analysis of the DAO samples was performed by Dr. Marcio Machado and asphaltene content analysis was performed in an external laboratory.

2. Literature Review

2.1 Introduction

This chapter introduces the solvent deasphalting concept for in-situ extraction and the most recent developments in the field of heavy oil upgrading. As the SDA is a new technology in the field of partial bitumen upgrading, little research has been performed to understand and improve this process that receives feed from the SAGD extraction. The available research results regarding the asphaltene precipitation and partial bitumen upgrading processes will be provided and their importance to the current study will be elaborated. Several important process parameters have significant impacts on asphaltene precipitation, including operating temperature, operating pressure, solvent type, solvent-to-bitumen ratio (S/B), mixing intensity, and mixing energy.[48,49] In this chapter, the effects of each parameter on the asphaltene precipitation process as described in the literature will be discussed.

2.2 Solvent deasphalting (SDA)

Solvent deasphalting is a process originally developed to treat heavy feedstock vacuum residue with light solvents at around the mid-twentieth century.[8,55] The process involves a paraffinic solvent (such as n-pentane or n-heptane) that dissolves light oil fractions from the vacuum residue and precipitates pitch that mainly consists of asphaltenes. Asphaltenes are the fraction of the oil that is insoluble in paraffinic solvents and soluble in aromatics such as toluene.[23,46,53] The pitch obtained from the solvent deasphalting of vacuum residue is a low-value product that is usually used for paving roads and the DAO is sent to refineries to be converted into gasoline and other valuable oil fractions.[56,57] The introduction of solvent deasphalting technology to the oil sands industry stems from the need for the upgrading of the SAGD-extracted bitumen emulsion so as to reduce its asphaltene content and facilitate bitumen transportation.[58] The main difference between the conventional SDA process and its use for the SAGD process is that the feed stream from the SAGD extraction contains water, in the form of both emulsion and free water.[8] Typical vacuum residue that is treated in an SDA process, however, does not contain water.[8]

The idea behind the solvent deasphalting process is that it harnesses the disequilibrium created as a result of the introduction of lightweight paraffinic solvents.[59] Treating bitumen with light

paraffinic solvents breaks the resin-asphaltene equilibrium and leads to the accelerated aggregation and precipitation of asphaltenes.[59] Consequently, asphaltene aggregates settle under gravity and leave behind a cleaner, lighter, and higher quality product, i.e. deasphalted oil.

As explained in Section 1.2, during the solvent deasphalting of the SAGD-extracted bitumen emulsion, the feed is mixed with a paraffinic solvent. Upon mixing, asphaltene aggregates form as a result of collisions among asphaltene particles. After sufficient turbulence and homogeneity in the vessel contents have been achieved, the mixture is allowed to settle. As a result, the vessel contents separate into three distinct phases: deasphalted oil, asphaltenes-rich, and water.[8,54] The arrangement of the phases with respect to one another can clearly be seen in Figure 1.2d: DAO is the top phase, the pitch (asphaltenes-rich) phase is in the middle and the water phase forms at the bottom of the vessel. The drawback of the solvent deasphalting of bitumen emulsion is such positioning of the phases, which poses problems for a continuous solvent deasphalting process.

For a continuous SDA process, DAO is withdrawn from the top of the settler and water is withdrawn from the bottom. Since the pitch phase is very viscous and cannot be displaced from the reactor separately, it will gradually grow and block both outlets of the vessel. To prevent this from happening, a method has to be devised to continuously withdraw the pitch phase from the vessel. However, solvent deasphalting of the SAGD-extracted bitumen is a relatively new concept and little research has been performed to improve the viability of this process and little is known about this technology. A recently performed study proposed to employ a partial mixer to mix pitch and water phases to displace both phases simultaneously.[8] The purpose is to create a homogenous pitch + water underflow stream without entraining any DAO from the overflow. The experiments performed in a glass vessel revealed that partial mixing can be achieved with an impeller of any size and geometry, on the condition that the impeller is fully submerged in the bottom phase. If the impeller is at the interface or above, then it will result in the entrainment of DAO in the underflow.[8]

The main focus of this study is also the solvent deasphalting of SAGD-extracted bitumen emulsion, with particular emphasis on the effects of the mixing conditions and solvent addition on asphaltene precipitation. Figure 2.1 illustrates a two-stage continuous solvent deasphalting process that receives feed from the SAGD extraction site. Initially, the bitumen emulsion + water mixture and

solvent are fed to the mixer. After the required homogeneity in the mixture has been obtained, the mixture is pumped to the first settler where aggregates settling and phase separation take place. In the subsequent stage, the DAO is displaced from the top and the pitch + water phase is displaced as a mixture from the bottom of the settler. The DAO from the first settler is rich in solvent that is why it is fed into another vessel operating at a lower pressure to flash and recover the solvent and recycle back to the first stage of the process to minimize the make-up solvent amount. Then, the DAO is displaced as the main product from the bottom of the vessel. To make the pitch phase lean in maltenes, it is pumped to a second mixer and mixed with some solvent. The mixture is then pumped into a second settler where it separates into three phases: washings, pitch, and water. The washings are pumped into the solvent recovery tank. The pitch + water mixture is then withdrawn from the bottom of the settler. In later stages of the SDA process, a series of separation units such as a centrifugal decanter, flash, and distillation columns may be used to improve the efficiency of the product separation. After the initial solvent deasphalting stage, the succeeding stages may be different for different plants. For instance, some plants may use ultrasonic vibrations field or integrated SDA and mild-thermal cracking unit followed by settlers and centrifuges for enhanced removal of the pitch from the slurry phase.[60–62]

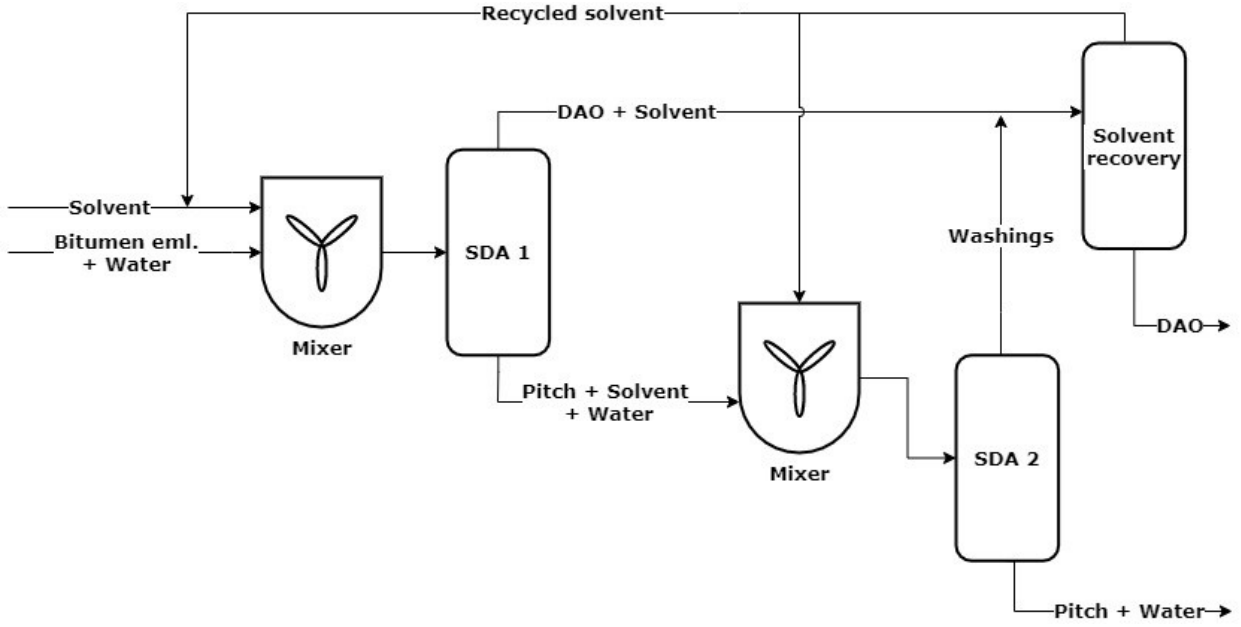

Figure 2. 1. Simplified process flow diagram for a two-stage solvent deasphalting process

One of the most recent innovations in solvent deasphalting of bitumen emulsion is the Nexen BituMax process. The objective of the invention is to reduce the cost and greenhouse gas (GHG) emissions associated with the partial bitumen upgrading process as a result of coupling the upgrading unit with the SAGD extraction process. Figure 2.2 illustrates a simplified BituMax process that is aimed to be built in an in-situ extraction site.[54,63] The key difference from the other bitumen upgrading process is that it involves a mild thermal cracking unit after the solvent deasphalter to further improve the quality of the DAO produced.[54] Furthermore, the water is separated from hydrocarbons and impurities, and directly recycled back to the extraction stage. The SDA process illustrated in Figure 2.1 corresponds to the separation block described in Figure 2.2.

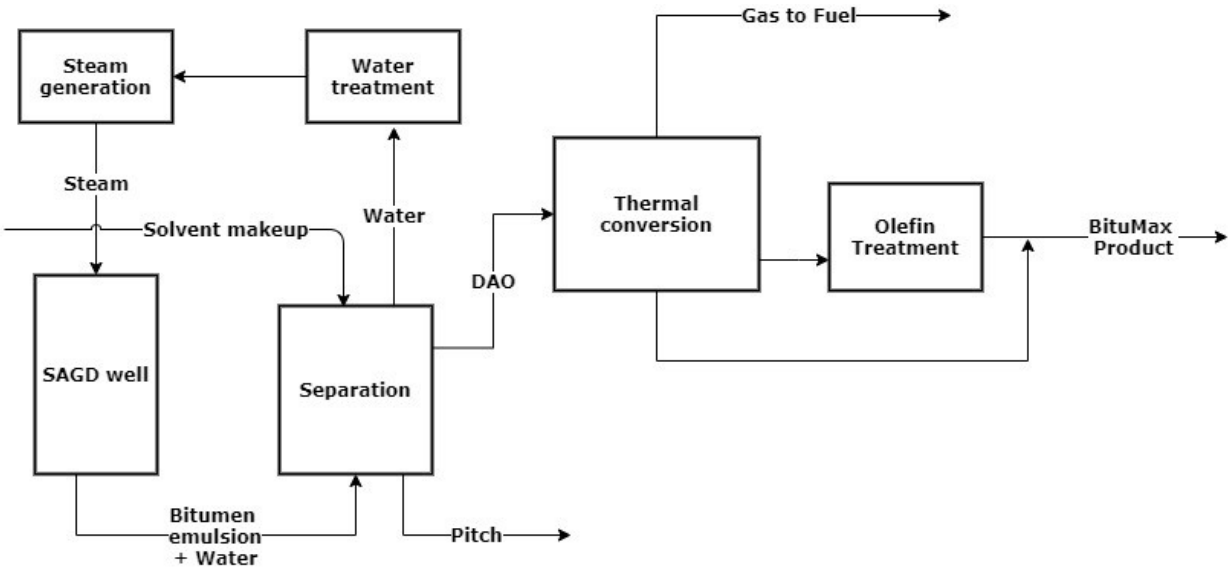

Figure 2. 2. Schematics of the Nexen BituMax process. Regenerated from Gieseman and Keesom.[54,63]

2.3 Solvent deasphalting process parameters

This section summarizes the findings from the literature regarding the effects of main operating parameters on asphaltene precipitation from heavy oil. Operating temperature, operating pressure, solvent choice, solvent amount, mixing intensity, and mixing energy are the parameters that will be discussed in the following subsections. The impact of each parameter on asphaltene precipitation will be explained and the feasible operating range for each parameter will be determined. Additionally, the mixing equipment frequently encountered in the chemical industry will be given and their utilization in the solvent deasphalting field will be explained.

2.3.1 Temperature

Based on the literature, the effect of temperature is not monotonic on the asphaltene precipitation from heavy oil.[34] As the temperature of bitumen increases, asphaltenes solubility also increases and for a given solvent-to-bitumen ratio, asphaltene precipitation reaches a minimum.[9,34,44] Zhao and Wei[34] mention this minimum to be between 80 – 100 ℃ for the heavy oil that was received from Cold Lake, Alberta, Canada. Another study performed by Xu[44] mentions that, for a given S/B ratio, asphaltenes yield decreases with increasing temperature in a range of 25 – 125 ℃ and the minimum is achieved between 75 – 100 ℃ for n-pentane and iso-pentane. With further increase of temperature, however, the solubility of asphaltenes decreases and asphaltene precipitation starts to increase.[34,44,45]

Figure 2.3 summarises the above-discussed relationship between temperature and asphaltenes solubility and illustrates how this information can be harnessed to improve the performance of a solvent deasphalting unit. It is evident from the results of Figure 2.3 that asphaltenes solubility is at its peak at around 100 ℃, which implies that this temperature is the most unfavourable condition for asphaltene precipitation. Away from this temperature, asphaltenes solubility decreases, whereas the drop is sharper at higher temperatures. For an SDA process, low solubility asphaltenes are preferred to facilitate the precipitation process; therefore, based on Figure 2.3, temperatures above 140 ℃ are favourable for most upgrading units, where the asphaltenes solubility is the lowest.[9]

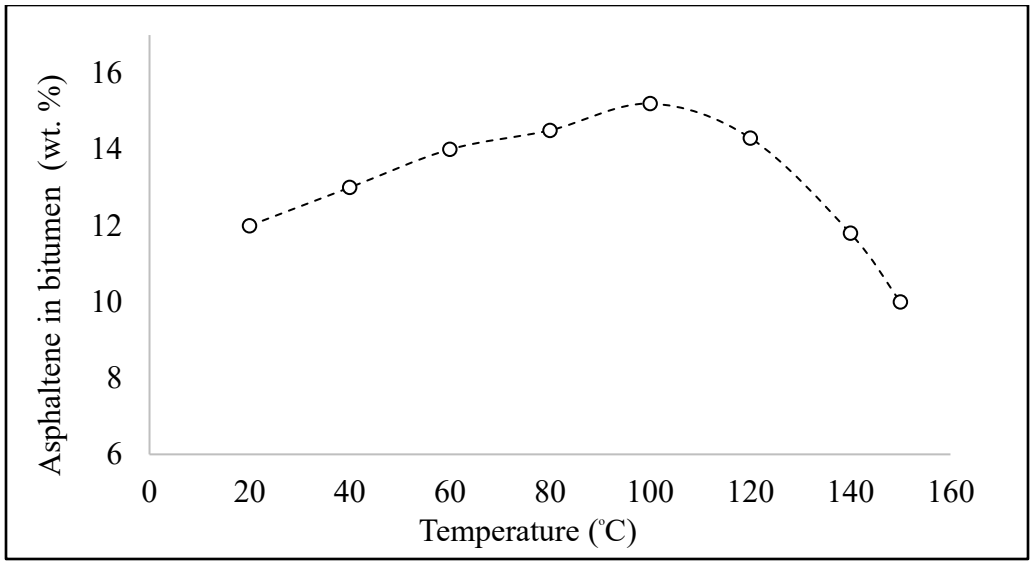

Figure 2. 3. Asphaltene solubility in bitumen as a function of the operating temperature. Reproduced from Long et al.[9]

Aggregate diameter is another important parameter that has a substantial impact on the asphaltene precipitation process: the larger the asphaltene aggregates are, the faster the settling of the aggregates becomes.[53] It is also noteworthy that a high aggregate settling rate is essential for commercial-scale SDA applications because the settler size and plant production capacity depend primarily upon the settler residence time. Consequently, formation of large aggregates is favourable for a solvent deasphalting process. Previous studies reveal that the asphaltene aggregate diameter is directly related to the operating temperature of the upgrading process.[53,64] The experiments performed by Long et al.[64] at a temperature range of 30–75 °C demonstrated that, at elevated temperatures, asphaltenes are more prone to aggregation and formed aggregates tend to be denser than the aggregates formed at low temperatures. Similar results were also observed by other researchers; Casas et al.[53] mentioned in their study that at elevated temperatures the obtained asphaltene aggregates are less porous and much denser.[53,65] Besides, it is a well-established fact that viscosity is also a temperature-dependent parameter and the viscosity of oil decreases with increasing temperature, which in turn positively affects the settling of asphaltene aggregates.[27,66]

To summarize, elevated temperatures are favourable for the enhanced deasphalting process, provided that it is not too high so as not to affect the chemistry of bitumen emulsions and turn

paraffinic solvent into a gas by surpassing its critical temperature.[30,34,67] Sufficiently high temperatures will not only improve the asphaltene aggregation and precipitation, but also accelerate aggregates settling rate because of the reduced friction during settling, reduced aggregate porosity, and increased aggregate density.[52,53,64]

2.3.2 Pressure

In a solvent deasphalter, the operating pressure is defined by the solvent volatility.[34] Based on a small amount of data, asphaltenes solubility is also believed to be pressure-dependent.[68,69] Johnston et al.[45] explain that asphaltenes can precipitate from live oil once displaced from the reservoir, due to sudden pressure drop.[45,68,69] Furthermore, depressurization of the crude oil is believed to be the major reason for the asphaltene deposition on well-bore pipes.[70] However, this is believed to be the case only under the reservoir conditions for undersaturated oil and as far as the partial bitumen upgrading process is concerned, asphaltenes solubility is essentially constant and the operating pressure has an imperceptible impact on the asphaltenes solubility and precipitation.[44] The primary purpose of the operating pressure is to keep the paraffinic solvent in liquid phase to enhance the mixing of bitumen with solvent and facilitate aggregation of asphaltene particles as a result of the dissolution all the remaining oil fractions.[34] Therefore, the system pressure always has to be slightly higher than the vapour pressure of the solvent to keep the mixture in liquid phase.[34,44]

The impact of the operating pressure is limited to maintaining two liquid phases in the solvent deasphalter. Figure 2.4 illustrates the combinations of operating pressure and S/B ratio that lead to favourable phase formations for a mixture of bitumen and solvent to enable asphaltene removal. Different phases may be observed with different combinations of these two parameters. Note that depending on the operating temperature and paraffinic solvent, the values on the axes may change; however, the observed trend is essentially the same for every occasion. From Figure 2.4, it is evident that below the onset of asphaltene precipitation only one liquid phase can be obtained and no asphaltene precipitation can be achieved. Above the precipitation onset, depending on the pressure, either two liquid phases or a vapour-liquid equilibrium can be achieved. In the latter case, the vapour phase formation is due to the high vapour pressure of the paraffinic solvent; therefore, the operating pressure of the solvent deasphalting unit has to be above the vapour pressure of the

solvent employed to keep all the materials in liquid phase. To achieve an effective asphaltene precipitation process, two liquid phases have to be obtained.[45]

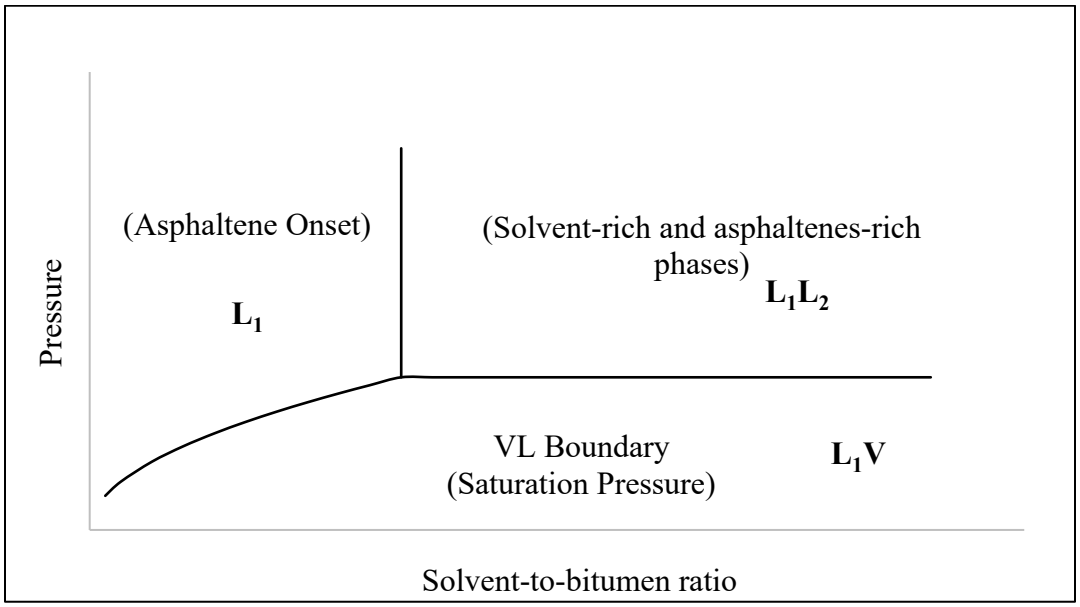

Figure 2. 4. Phase boundaries of the solvent-bitumen mixture. Reproduced from Johnston et al.[45]

2.3.3 Solvent type

Many solvents have been studied as asphaltene precipitating agents and it has been proven that to different extents, most paraffinic solvents can precipitate asphaltenes from heavy oils.[9,44,50,51] In this chapter, research results for the first seven members of the alkanes family will be introduced and the effect of increasing carbon number, i.e. molecular mass, on alkanes precipitation capability will be investigated.

Based on the literature, the yield and physical properties of the precipitated asphaltenes may differ significantly depending upon the type of solvent employed.[50,51] In solvent deasphalting of the in-situ extracted bitumen emulsion, the chosen paraffinic solvent serves several purposes; it is an anti-solvent that precipitate asphaltenes, density and viscosity reducing agent that facilitates water/hydrocarbon separation, a solvent that dissolves and washes away oil from asphaltenes.[30] Since each solvent yields different asphaltene products and distinct product specifications, in the realm of science, it is a common practice to name asphaltenes based on the solvents used for the

precipitation purpose such as C5-asphaltenes (n-pentane insolubles), C6-asphaltenes (n-hexane insolubles), C7-asphaltenes (n-heptane insolubles).[46,71]

The experiments performed by Mehrotra and Svrcek[72] with methane and ethane have revealed that methane-bitumen and ethane-bitumen systems essentially provide vapour-liquid (VL) multiphase behaviour due to their very high volatilities. Starting from propane, higher carbon number alkanes start to yield more than one liquid phase that is favourable for the solvent deasphalting process.[45,72] Recall from Section 2.3.2 that two liquid phases (LL) must be obtained in order to achieve asphaltene precipitation; however, with methane and ethane, two liquid phases cannot be achieved.[45,72] Therefore, they are unsuitable to be used as precipitants in a solvent deasphalter.

Luo et al.[51] studied three light paraffinic solvents, namely propane, n-pentane, and n-heptane, to test the impact of each on asphaltene precipitation from Canadian heavy oil. It was revealed that asphaltene precipitation yield is higher for lighter paraffinic solvents: of the three solvents that were studied, propane precipitated most asphaltenes under the same experimental conditions. It was also observed that the physical properties of the precipitated asphaltenes significantly depend upon the solvent used. Bright and black asphaltene particles were obtained with n-heptane, and with n-pentane and propane, the obtained asphaltenes are described as a dull, brown powder and very viscous, semi-solid like products, respectively.[51]

Xu[44] studied the butane and isomers of pentane as the potential precipitants for asphaltene rejection from bitumen. The experimental results revealed that neopentane and isopentane yield more asphaltenes than n-pentane. Moreover, the study also shows that butane is superior to n-pentane in asphaltene rejection from bitumen for the studied range of temperature and S/B ratio.

Calles et al.[50] investigated the asphaltene rejection capabilities of three alkanes. They used n-pentane, n-hexane, and n-heptane as the precipitants to remove asphaltenes from South American heavy oil residues at a temperature range of 25 – 50 °C. The paper states that lower asphaltene yield was obtained by using higher molecular weight alkanes for the given solvent amount. Zhao and Wei[34] also found that n-pentane is superior to n-hexane in the precipitation of asphaltenes from bitumen. Similar experimental results were obtained by Long et al.[9] using the same paraffinic solvents as Calles et al.[50] did for the precipitation of asphaltenes from bitumen under fixed

operating conditions. Long et al.[9] also confirmed that using n-pentane led to more asphaltene precipitation relative to the other heavier paraffinic solvents. A significant product quality difference was also observed such that asphaltenes obtained with n-pentane had a higher H/C ratio and was more aliphatic, whereas the asphaltene product obtained using n-heptane had a lower H/C ratio and was more aromatic. In addition, a careful review of the literature also shows that the asphaltenes obtained with heavier alkanes are denser and possess higher molecular weights compared to the asphaltenes obtained with light alkanes.[9,50,51]

To summarise, of the seven paraffinic solvents that were discussed, the first two, i.e. methane and ethane, are infeasible to be employed as solvents because of their very high vapour pressures that prevent the formation of two liquid phases upon mixing with bitumen. The following five members of alkanes and their isomers are suitable to be employed as asphaltene precipitating agents; however, the obtained product yield and product specification significantly depend upon the solvent used. In this study, a solvent mixture containing C4 – C7 alkanes will be used to precipitate asphaltenes from bitumen emulsion.

2.3.4 Solvent solubility parameter

It is not a coincidence that as the molecular weight of paraffinic solvents increases, their asphaltene precipitating ability decreases. The impact of the solvent on the asphaltene precipitation trend can be explained in terms of the solubility model approach. The solubility parameter (δ_i) of a solvent is calculated as[73]

$$\delta_i = \left(\frac{\Delta H_i - RT}{\nu_i}\right)^{\frac{1}{2}} \quad (2.1)$$

where ΔH_i is the enthalpy of vaporization of liquid solvent, R is the universal gas constant, T is the absolute temperature and ν_i is the molar volume of liquid solvent.

Numerous models have been developed over the past 20 years to characterize the behaviour of asphaltenes precipitation upon treatment with paraffinic solvents.[33,69,74–78] Equation 2.1 is the simplest formula that can be used to choose a suitable solvent to meet the upgrading unit product requirements. To put it simply, a higher solubility parameter corresponds to a higher dissolving capability of solvent. When a solvent with a high solubility parameter is mixed with bitumen, it

only rejects a small amount of asphaltene and dissolves most oil fractions. Therefore, a solvent with a low solubility parameter, i.e. a poor solvent, has to be used to be able to precipitate the majority of asphaltenes from bitumen.[33,44,79]

Figure 2.5 illustrates how the solubility varies depending on the molecular weight of alkanes at 25 ºC. The solubility parameter indicated on Y-axis is directly proportional to the solvating power of the corresponding solvent.[69,80] From Figure 2.5, it can clearly be seen that the solubility parameter of solvents increases, as the molecular mass of the solvents increases. Furthermore, based on the solvents studied in Section 2.3.3, it can be inferred that the asphaltenes precipitation yield is inversely proportional to the molecular mass of the solvent used. The same conclusion can also be derived from Figure 2.5: solvents with low molecular mass have low solvating power, therefore give rise to high asphaltene precipitation. For example, using propane will yield significantly more asphaltenes compared to the other paraffinic solvents that form LL (liquid-liquid) phases because propane has a much lower solubility parameter compared to the other solvents that have been studied.

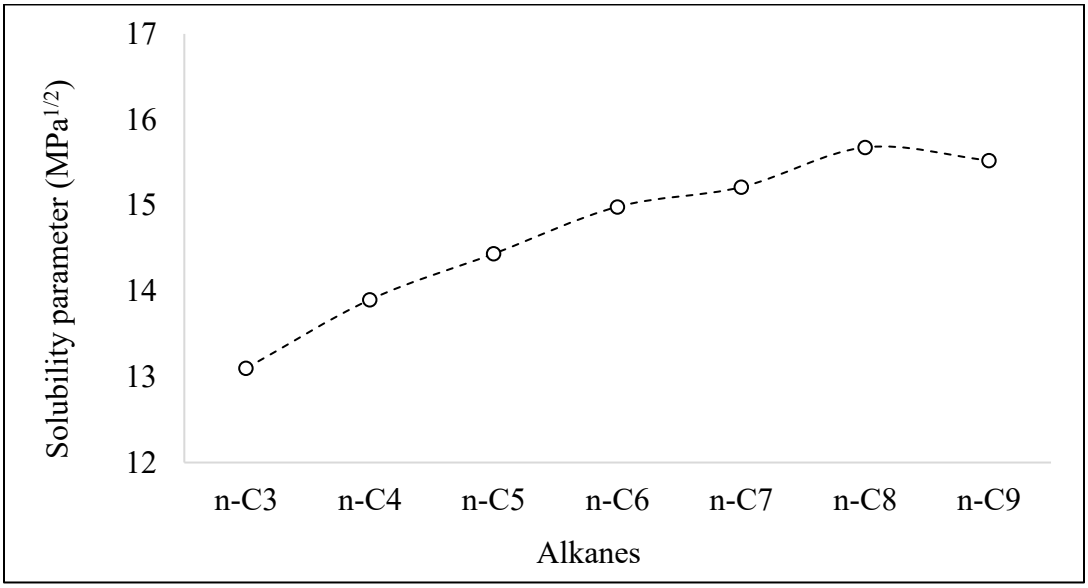

Figure 2. 5. Relationship between the solubility parameter and the molecular weight of paraffinic solvents. The graph was generated using the data from Yaws[81] and Oh and Deo[82]

Figure 2.5 summarises research results obtained by many researchers in the field of solvent deasphalting process and with the help of this figure, a suitable solvent for a solvent deasphalting process can more readily be determined. Using the recent and more advanced asphaltene precipitation models, graphs similar to Figure 2.5 can be generated with high accuracy for a wide range of paraffinic and non-paraffinic solvents to determine an optimum solvent blend for a particular SDA process.

2.3.5 Solvent-to-bitumen ratio

Experiments performed with various organic solvents on Canadian heavy oil demonstrate that increasing the S/B ratio accelerates the asphaltene aggregation process and increases asphaltene yield.[51,53] However, studies[82–84] also mention that asphaltenes precipitation is not feasible with any amount of solvent and there happens to be a threshold S/B value that initiates asphaltene precipitation. This critical value is known as the onset of asphaltene precipitation, at which the first precipitation is detected for the given operating conditions.[45,51] Furthermore, numerous studies[32,45,51] demonstrate that the onset of asphaltene precipitation and the asphaltene yield significantly depend on the solvent type and solvent nature. This critical value increases with the increasing aromaticity of solvents. Experimental results show that the onset of asphaltene precipitation is approximately 1.8 for paraffinic solvents and around 4 for naphthenic solvents at room temperature.[53,83–86]

The study performed by Xu[44] also confirms this finding and the paper states that the threshold value is slightly over 1 for n-pentane and for n-butane the onset of asphaltenes precipitation is approximately 0.8. Below this value, no perceptible asphaltene precipitation is observed. Experiments also showed that as the S/B ratio increases beyond the threshold value, the asphaltene yield also increases accordingly. Similar results were also found by Long et al.[9], whose results confirm an increasing asphaltene precipitation trend with increasing solvent amount for the same paraffinic solvent. Their study determined the onset of asphaltenes precipitation for n-pentane (1.0), n-hexane (1.35), and n-heptane (1.6) at 25 ºC.[9,44]

Zhao and Wei[34] used n-pentane and n-hexane to test the impact of changing the S/B ratio on the C5-asphaltenes precipitation from bitumen emulsion obtained from Cold-Lake, Alberta. The

experiments were performed at 20 ºC and as the S/B ratio was increased from 1.8 to 4.2, with n-pentane the asphaltene content of bitumen dropped from 15 wt. % to 1 wt. % and with n-heptane a drop from 16 wt. % to 5 wt. % was detected in the asphaltene content of bitumen. Furthermore, the paper states that in order to precipitate more than 95 wt. % of asphaltenes, the S/B ratio must be above 3.0.[34]

It is evident from the literature that increasing the S/B ratio will lead to an increase in asphaltene precipitation, but this increase is not always consistent and proportional. For sufficiently high S/B ratios, asphaltene precipitation may not perceptibly change by adding more solvent. Luo et al.[51] confirmed that by adding more solvent, the asphaltene yield increases to a maximum, and then reaches a plateau. They mentioned that when the S/B ratio reaches 20, the asphaltene precipitation levels off and no additional precipitation is observed for both n-pentane and n-heptane with the further addition of solvent, which is suspected to happen due to the oversaturation of the bitumen with solvent.

The amount of solvent required for a solvent deasphalting unit depends on the product requirements. With high S/B ratios, larger asphaltene aggregates will form that settle rapidly and a high asphaltene yield will be obtained. However, the DAO yield will be low because more solvent will cause precipitation of other heavy oil fractions too, which might be detrimental to DAO yield and process economics.[35] It has been proven experimentally that with 40:1 solvent-to-bitumen ratio, high purity asphaltene product can be attained, but this is very uneconomic and infeasible to implement to an operating plant.[87] For a commercial-scale process, depending on the product requirements, an S/B ratio of between 0.2 to 10 wt/wt can be used; however, for economic reasons, it is favourable to keep this ratio below 2.5 wt/wt.[30]

In addition to partially precipitating asphaltenes from heavy oil, paraffinic solvents can also improve the water removal process, through the promotion of coagulation and coalescence of emulsified water droplets.[9,34,83] Although the exact reason for this is unclear, it has been proven experimentally that beyond the onset of asphaltene precipitation, the water content of bitumen emulsion is also reduced.[9] It is a moot point whether asphaltene precipitation is a pre-condition for water removal or the water-in-bitumen emulsion happens to be destabilized at the same S/B ratio that asphaltenes start to precipitate.[9] It is believed that during the asphaltenes aggregation process,

water droplets are trapped within the aggregates which in turn increases the aggregate settling rate due to increased aggregate size.[9]

To summarise, it was established that the S/B ratio is a critical parameter for the solvent deasphalting of bitumen emulsion. This parameter affects the asphaltenes precipitation yield, asphaltenes aggregation, water removal, and settling of asphaltene aggregates.[9,51,83] The low limit of this parameter is defined by solvent nature and operating conditions: however, the highest S/B ratio that will be used for an SDA process requires rigorous optimization of all process parameters.[30,32,45] The optimum S/B ratio may vary depending on the operating conditions, product requirements, and process economics. One of the objectives of the current study is also to investigate the S/B ratio in a range and determine the favourable operating value for the S/B ratio under the given operating conditions.

2.3.6 Mixing equipment

Mixing is an essential part of nearly all chemical processes, both in lab-scale and commercial-scale applications. In the case of an SDA process, a well-mixed bitumen and solvent stream has to be achieved to maximize the process efficiency and facilitate asphaltene precipitation. Depending on the scale of process and operation mode, different mixers are employed to perform mixing.[88] For continuous processes, in-line static mixers are the most widely used method to achieve sufficient mixing over a short duration.[88] For batch processes, many different options are available, but stirred tanks are usually the primary choice because of the versatility and convenience in operation.[88]

Figure 2.6 demonstrates some different examples of static mixers. For static mixers to perform efficiently, constant fluid flow is required and thus static mixers are often used for continuous processes. They are fitted inside a pipe and the intricately designed parts of static mixers act as baffles to direct the flow and create turbulence.[88] Although static mixers can also be employed for lab-scale experiments, it is inefficient because some static mixers can only be used with certain types of fluid flow (i.e. laminar or turbulent).[8] Furthermore, it is challenging to adjust the mixing parameters using a static mixer, since the only parameter that can be adjusted is essentially the fluid flow. As a result, it is more favourable to use tanks equipped with impellers, i.e. stirred tanks, to better manage the mixing parameters for bench-scale processes.[8]

Figure 2. 6. Various types of static mixers. From left: vortex mixer (KVM), corrugated plate mixer (SMV), wall-mounted vanes (SMF), crossbar mixer (SMX), helical twist mixer (KHT), crossbar mixer (SMXL). Reproduced from Paul et al.[88]

Mixing can be performed through different mechanisms: mechanical agitation, gas sparging, jets etc.[88] Figure 2.7 demonstrates the configuration of a conventional stirred-tank that uses mechanical agitation to homogenize reactor contents. More than half of the bench-scale, as well as industrial-scale chemical production processes, involve these types of stirred tanks.[88] One of the main advantages of using a mechanically agitated tank to perform mixing is the ability and convenience to control flow patterns with high precision. Both laminar and turbulent flow conditions can readily be achieved through manipulating the power input to the motor.[88]

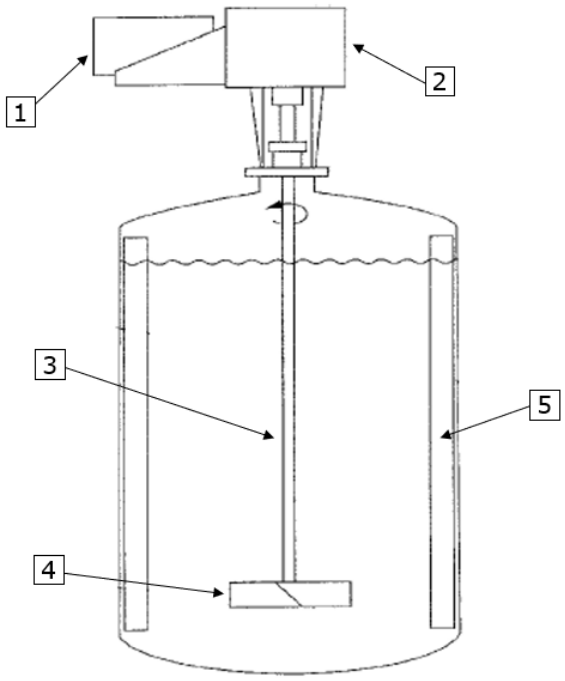

Figure 2. 7. Generic stirred tank configuration: motor (1), gearbox (2), shaft (3), impeller (4), wall baffles (5). Reproduced from Paul et al.[88]

Every commercial process initially passes through a bench-scale development stage, where process parameters are studied and optimized to improve process viability. Otherwise, it would be very costly and even unsafe to study reactor kinetics and optimization of operating parameters in a commercial-scale process.[89] The experiments conducted in a bench-scale setup provide answers to many questions concerning the process dynamics and operability. The results of the bench-scale study are used to rigorously evaluate a process to be able to improve its feasibility and profitability.[89]

One of the main challenges during the transition from a bench-scale process to a pilot-scale or a commercial-scale process is the scale-up of the mixing parameters.[90] To start with, the parameters that represent both scales have to be determined and used as a reference to make the transition from a bench-scale process to a larger scale. For this reason, dimensionless parameters (such as Reynolds number and Froude number) and geometric ratios of the process units are the most frequently used reference points to convert a bench-scale process into a commercial-scale.[90,91] Once the geometric similarities between both scales have been established, operating parameters

are adjusted for the new design. The adjustment of the mixing conditions usually involves parameters from bench-scale experiments such as flow regime, mixing time, and mixing intensity per unit mass.[91,92]

The scale-up of a continuous process is even more challenging than scaling up a batch process.[90] That is because most commercial-scale continuous processes involve in-line static mixers; however, bench-scale processes usually employ mechanically agitated tanks for both batch and continuous processes. At the time of scale-up, maintaining geometric similarities between bench-scale and commercial-scale units is impossible.[90] Thus, the only parameters that can be used as the representatives of bench-scale design are the mixing time and mixing intensity per unit mass.[90] In that case, the mixing time of a batch process is equivalent to the residence time in the pipe equipped with static mixers and the power consumption per unit mass is equivalent to the ratio of energy loss due to friction ($\Delta P/\rho$) to residence time.[90]

In the current study, through conducting experiments in a bench-scale SDA setup, the goal is to collect sufficient information to be able to characterize the mixing of an industrial-scale SDA process. The existing bench-scale setup contains a stirred tank reactor to perform mixing. Since the commercial-scale process will involve in-line static mixers, the major information from the laboratory design that can be applied to the scaled-up design will be the mixing time and power consumption per unit mass.

2.3.7 Mixing characterization

Mixing intensity and mixing energy are two fundamental parameters that determine the mixing efficiency of a process. Mixing intensity is calculated using

$$\varepsilon_{mix} = \frac{P}{m_{total}} \tag{2.2}$$

where ε_{mix} is the mixing intensity, P is the total mixing power and m_{total} is the total mass of the mixture.[88] Mixing power is calculated as

$$P = N_P \rho N^3 D^5 \tag{2.3}$$

where P corresponds to the mixing power, N_P is the power number, ρ is the mixture density, N is the rotational speed of the impeller (revolution per second), and D is the diameter of the impeller.[88] Mixing energy is the product of the mixing power and the time length that mixing is performed.[88]

Some literature sources[35,93,94] use shear rate to describe mixing; therefore, the relationship between the mixing power and the shear rate has to be established before introducing the research results for the effects of mixing parameters on asphaltene precipitation from bitumen. The shear rate is directly proportional to the mixing speed and this proportionality can be illustrated as

$$\gamma \sim K N \tag{2.4}$$

where γ is the shear rate, N is the rotational speed of the impeller (revolution per second), and K is the proportionality factor that depends on the impeller geometry and the distance from the tip of the impeller.[88]

From Equations 2.3 and 2.4, it is evident that mixing power is a function of the impeller speed cubed (N^3) and shear rate is proportional to the impeller speed (N); consequently, increasing mixing speed leads to an increase in both mixing power and the applied shear rate. In other words, increasing shear rate is an equivalent term to increasing mixing power.

2.3.8 Mixing effects

Few studies have been performed regarding the impact of mixing energy and mixing intensity on the asphaltene precipitation process. Even fewer studies have been undertaken to study the effects of the mixing conditions on asphaltene precipitation from the SAGD-extracted bitumen emulsion. Based on the studies performed to date, the impact of mixing intensity and mixing energy on asphaltenes settling and asphaltene aggregates formation is unclear and sometimes controversial.[53] While some studies state that the aggregate diameter decreases with longer mixing time for the given mixing intensity, others claim no appreciable change in aggregate size with changing mixing energy is observed.[8,35,53,95]

One of the most referred studies performed on asphaltene aggregates settling under various mixing conditions is Zawala et al.[52] They calculated the settling rate of asphaltene aggregates formed during a paraffinic froth treatment in a bench-scale stirred tank reactor. The paper states that as the mixing energy increases, the settling rate of the formed asphaltene aggregates also increases, however, an insignificant change in mean aggregate diameter was observed. It is explained that increasing mixing energy leads to the formation of nonporous and denser aggregates with no water content.[52] In another study, although similar observations were made in relation to the aggregates settling rate with changing mixing energy; however, completely different explanations were provided in terms of aggregate properties.[8] Cheung[8] also studied the effects of mixing parameters on asphaltene aggregates formation and aggregates settling rate using bitumen froth in a bench-scale stirred-tank reactor under similar operating conditions (700 – 1500 RPM). He also mentions that increasing mixing energy led to faster average individual aggregate settling. Contrary to what was mentioned by Zawala et al.[52], his study showed that formed aggregates size increases with mixing energy and as the aggregates get larger they become more porous and less dense.[8] Based on Stokes' law, the aggregate density and dimeter are two decisive factors that affect the aggregate settling rate ($u_{\propto} \sim \rho d^2$).[7,96] Calculations revealed that the change in asphaltene aggregate diameter is more impactful than the decrease in aggregate density; consequently, increasing mixing energy causes an increase in aggregates settling rate.[8] Unlike the claims made by Zawala et al.[52], no rapid water droplet coalescence upon stopping the mixing was observed and thus it is believed that water droplets were trapped within the formed asphaltene aggregates.[8]

It is also reported in the literature that even though aggregates settle more rapidly with increasing mixing intensity, no significant change in aggregate size was observed. Therefore, the increase in asphaltene aggregates settling rate with increasing mixing intensity was attributed to the changing aggregate properties.[52,53] It is believed that aggregates formed at higher mixing intensities are denser and nonporous because more solids become trapped inside asphaltene aggregates.[52,53] However, under similar experimental conditions, Cheung[8] found that changing mixing intensity affects aggregate diameter: decreasing mixing intensity results in the formation of larger asphaltene aggregates. It is explained that at high mixing intensities fragmentation rate of aggregates increases. Thus, for the same mixing energy input, lower mixing intensities lead to higher aggregate settling rates.[8]

Rahmani et al.[35] tested the effect of varying shear rates ($1.2 - 12.7\ s^{-1}$) on asphaltene aggregate formation in a Couette device. The solution was prepared by mixing solvent (toluene/heptane blend) with asphaltenes at 300 RPM for 15 s to achieve complete mixing. Then, the mixture was transferred to a Couette device to study the asphaltenes aggregation process under varying shear conditions. The results of the experimental study demonstrate that, initially, increasing shear rate causes an increase in the formed aggregate diameters; however, above a shear rate of $8.4\ s^{-1}$, the average aggregate size decreases with the increasing shear rate, this phenomenon is explained as the breakage of the formed large aggregates due to applied shear force. Recall from Section 2.3.7 that increasing shear rate is equivalent to increasing mixing intensity. Thus, the growth rate of aggregates is directly affected by the change in mixing intensity. In addition, the paper states that for the given shear rate, the aggregate diameter increases over time until it reaches a maximum at about 20 mins, after which the mean aggregate diameter starts to decrease due to aggregates breakage and the mean aggregate diameter reaches a steady-state condition. It is believed that the steady-state condition occurs because of the equal kinetic rates of competing aggregation and fragmentation processes.[35,93]

Results similar to those of Rahami et al.[35] were also observed by Soleimani-Khormakala et al.[94] They[94] performed a similar experiment in a Couette apparatus for a shear rate range of $129 - 1142\ s^{-1}$ for solvent (toluene/heptane blend) and asphaltenes mixture. The paper mentions that the average size of the asphaltene aggregates passes through a maximum before reaching the

steady-state condition. They[94] also observed that at the steady-state condition the mean aggregate diameter is larger for low shear; therefore, if the system is allowed to reach steady-state condition, a low shear rate (i.e. low mixing intensity) is preferable. However, the study also mentions that with higher shear rates the steady-state condition is achieved faster. For example, with 307 s^{-1} shear rate twice as much time was required to reach the steady-state aggregation process compared to 1142 s^{-1} shear rate.[35,94]

To summarise, some literature studies that investigated the effects of mixing energy and mixing intensity on asphaltene aggregates formation and aggregates settling processes provide conflicting results.[8,35,52,53] The experimental results of Cheung[8], Rahmani et al.[35,93], and Soleimani-Khormakala et al.[94] agree with one another and provide reasonable justifications for the effects of mixing conditions. Therefore, it is anticipated that the experimental results of the current study will be comparable to their findings. That is, larger aggregate diameters will be obtained with increasing mixing energy which will also affect the aggregate settling rate positively. Additionally, low mixing intensities are expected to yield relatively larger asphaltene aggregates that settle rapidly.[35,93,94] Nevertheless, it cannot be ruled out that completely different observations from those discussed in this section can also be made in the current study due to the utilization of a completely different bitumen feed. Experimental results provided in the literature are mostly applicable to bitumen froth which contains approximately 10 wt. % solids.[8,52] The bitumen emulsion that is used as the process feed in the current study, however, contains practically no solids. In that sense, the result of the current study may show the key differences between the mixing of bitumen froth treatment and solvent deasphalting of bitumen emulsion.

2.4 Summary and development of research objectives

The goal of the project is to study the solvent deasphalting of SAGD-produced bitumen emulsions in a bench-scale experimental setup to acquire essential research data to support the design of a commercial-scale integrated SAGD-SDA process. With the knowledge obtained from the literature review presented in this chapter, the objectives of the present study can be specified as follows:

- **To investigate the effects of S/B ratio on the asphaltene yield and deasphalted oil quality**
  - Compare the experimental results of the current study with the available literature data
  - Establish a relationship between the employed S/B ratio and the obtained deasphalted oil quality
  - Estimate the precipitation onset for the employed solvent blends and the optimum S/B ratio for a commercial-scale SDA process
- **To investigate the effects of mixing intensity and mixing energy on the asphaltene yield and deasphalted oil quality**
  - Analyze the asphaltene yield and DAO quality by conducting experiments using different combinations of mixing intensity and mixing time
  - Compare the obtained results for the effects of mixing intensity and mixing energy with the literature data
- **To determine the impact of asphaltene aggregates settling time on the deasphalted oil quality**
  - Calculate aggregates settling rate based on the images taken during experiments and establish a relationship between the operating conditions and the calculated aggregates settling rate
  - Analyze the asphaltene content of DAO samples taken at different settling times and determine the effects of settling time on the DAO quality

3. Experimental Method

3.1 Overview

This chapter introduces the materials used in the study and provides the operating procedures for experiments. Three sets of experiments (PB-A, PB-B, and PB-D) were performed and they were named in order of increasing complexity. The PB-A set experiments were performed in batch mode and the other two sets were performed in semi-batch modes. Necessary modifications were made to the existing experimental setup to meet the requirements of the following set. The main goal of the gradual increase in the complexity of the experimental setup was to assess the feasibility of building a continuous SDA process. The following paragraphs provide detailed information about the objectives of each set.

In the PB-A set experiments, the samples were taken after the reactor had completely cooled down to the room temperature. This set was critical to investigate the asphaltene aggregates settling process without any intervention. The PB-A set allowed analyzing the asphaltene content of DAO sample after a full day of uninterrupted settling process and it was compared to the results from the subsequent sets, in which DAO samples were taken during the experiments under operating temperature and pressure.

The objective of the PB-B set was to test whether DAO sampling could be executed at the operating pressure and temperature without significantly interrupting the aggregate settling process. In a commercial-scale plant, it is unfavourable to let settling take place for as long as a day; therefore, this set aims to assess the feasibility of significantly reducing the residence time in settler.

The objective of the PB-D set was to study the feasibility of solvent injection at operating temperature and pressure which is an essential step towards building a continuous solvent deasphalting process. Experiments of this set provide an insight into the mixing of bitumen emulsion and solvent during the solvent injection process. It helps to determine whether significant mixing occurs during the solvent injection process and if it causes any noticeable asphaltene precipitation.

3.2 Materials

3.2.1 Bitumen emulsion

The bitumen emulsion used for the experiments was supplied by CNOOC from their Fort McMurray, Alberta operation. The SAGD product was received in a 55-gallon steel drum as a mixture of bitumen emulsion and free water. Bitumen emulsion and water are two immiscible liquids that separate into two liquid phases when left still for a sufficiently long time. After receiving the mixture, it was separated into free water and bitumen emulsion. The free water was stored in 5-gallon plastic buckets and bitumen emulsion was stored in one-gallon metal cans. This separation process was essential to accurately control the amount of bitumen loaded into the reactor for each experiment. The analysis performed on the separated bitumen emulsion revealed that it had 12.5 wt. % emulsified water. The free water was added to the reactor based on the required steam-to-oil ratio (SOR) for each experiment, which is explained in Section 3.4 in more detail.

The bitumen emulsion was then sent to an external lab to be dewatered and tested for its physical properties and chemical composition. Table 3.1 provides the results for the properties of the dewatered bitumen at various temperatures. The results for the density and viscosity of the dewatered bitumen have been determined based on the analysis methods given in the third column. Three samples have been used to analyze each property and the average of the results is given in the last column. API gravity was calculated based on the dewatered bitumen density at 15.6 ℃ using[97]

$$\text{API} = \frac{141.5}{\text{specific gravity}} - 131.5 \qquad (3.1)$$

Table 3. 1. Physical properties of the dewatered bitumen used in the study*

Property	Analysis temperature (°C)	Method	Sample #			
			1	2	3	Avg
Density $\left(\frac{kg}{m^3}\right)$[98]	15.6	ASTM D70	1021.4	1021.7	1021.7	1021.6
Density $\left(\frac{kg}{m^3}\right)$[99]	100	ASTM D5002M	969.2	969.3	969.2	969.2
	130		950.2	950.2	950.2	950.2
	160		931.3	931.3	931.3	931.3
API Gravity[98]	15.6	Calculated	6.90	6.87	6.87	6.88
Dynamic Viscosity (cP)[98]	100	ASTM D5018	458.8	423.2	506.0	462.7
	130		131.2	118.4	110.7	120.1
	160		46.2	42.3	37.7	42.1

* These data were reported as obtained by the Pipeline Transport Processes (PTP) research group and insufficient information is available to determine the numbers shown in the table are as accurate as they appear.

Table 3.2 demonstrates the results for the SARA analysis of the dewatered bitumen. The results show that dewatered bitumen contains approximately 20.2 wt. % C5-insolubles and 11.6 wt. % C7-insolubles. The objective of the project is to minimize the fraction of C5-insolubles in bitumen. In this study, the asphaltenes refer to C5-insolubles, unless otherwise stated.

Table 3. 2. Composition of the dewatered bitumen used in the study*,[100]

Parameter	Method	Sample #			
		1	2	3	Avg
Saturates (wt. %)	ASTM D4124	15.0	-	-	15.0
Aromatics (wt. %)	ASTM D4124	26.6	-	-	26.6
Resins (wt. %)	ASTM D4124	38.1	-	-	38.1
C7-insolubles (wt. %)	ASTM D6560	11.4	11.7	11.6	11.6
C5-insolubles (wt. %)	ASTM D6560M	20.2	20.0	20.4	20.2

* These data were reported as obtained by the Pipeline Transport Processes (PTP) research group and insufficient information is available to determine the numbers shown in the table are as accurate as they appear.

3.2.2 Solvent

The solvent used in the current study is a blend of two condensates supplied by Keyera and Affiliates. Overall, three solvent blends were prepared and used for the experiments of this project. In addition, one experiment was performed only with n-pentane to compare the effects of n-pentane on solvent deasphalting of bitumen emulsion to the results obtained with the solvent blends. For this reason, n-pentane (CAS:109-66-0) from Fisher Chemical with 98% purity was used. Table 3.3 lists the compositions of each batch used. More detailed information about the composition of each batch can be found in Appendix A.

Table 3. 3. The composition of the solvent blends used in this project[101]

Composition	Batch 1 (wt/wt)	Batch 2 (wt/wt)	Batch 3 (wt/wt)
Iso-Pentane	0.58	0.56	0.63
n-Pentane	0.16	0.17	0.18
Hexanes	0.09	0.10	0.08
Heptanes	0.07	0.08	0.05
Octanes	0.05	0.05	0.03
Others	0.05	0.04	0.03

It is evident from Table 3.3 that more than 70 wt. % of batches are comprised of pentanes. Based on the discussion in Section 2.3.3, pentanes are the most powerful asphaltene precipitating agents in the mixture: therefore, the term pentane equivalent was established to interpret and compare experimental results. As such, the required solvent-to-bitumen ratio was estimated using the pentane equivalent basis; i.e. it was assumed that solvent batches consist of only pentane-type hydrocarbons (n-pentane and iso-pentane) and other components are inert materials that have a negligible impact on the experimental results. For example, for Batch 3, the total pentane fraction in the mixture is the sum of the corresponding fractions of n-pentane (0.63) and iso-pentane (0.18), which is $0.63 + 0.18 = 0.81$. If an S/B ratio of 2.4 is used from Batch 3, then the S/B ratio in the pentane equivalent is $2.4 \times 0.81 = 1.9$. In other words, using an S/B ratio of 2.4 from Batch 3 is equivalent to using an S/B ratio of 1.9 from pure n-pentane.

Note that a more complicated alternative would be using the solubility parameter approach to define each solvent blend. As discussed in Section 2.3.4, a solubility parameter can be calculated for each solvent blend based on the physical and chemical properties of each component as well as their interactions with other components in the blend.

Table 3.4 demonstrates the actual S/B ratio, the pentane equivalent S/B ratio as well as the solvent batch used for each experiment. Note that the pentane equivalent S/B ratio has been used to analyze and discuss all the results in the study, unless otherwise stated. The PB-D set experiments involve a small deviation in the injected solvent mass, due to the injection method. This deviation has been considered in the interpretation of the results and described in the respective graphs in following sections.

Table 3. 4. Solvent blends used for each experiment in the present study

Runs	Solvent used	S/B (wt/wt)	
		Actual	Pentane equivalent
PB-A-001	Batch 1	1.2	0.9
PB-A-002	Batch 1	1.2	0.9
PB-B-001	Batch 1	1.2	0.9
PB-B-002	Batch 1	1.7	1.3
PB-B-003	n-pentane	1.7	1.7
PB-B-004	Batch 2	2.4	1.8
PB-B-005	Batch 3	2.4	1.9
PB-B-006	Batch 3	2.4	1.9
PB-B-007	Batch 3	2.4	1.9
PB-B-008	Batch 3	2.4	1.9
PB-D-001	Batch 3	2.5 [a]	2.0
PB-D-002	Batch 3	2.7 [a]	2.2

[a] ± 0.1 deviation is applicable for the PB-D set experiments, due to the solvent injection method

3.3 Equipment

Two stainless steel 4560 series mini reactors purchased from Parr Instrument Company were used to perform the experiments. One of the reactors (model number: 4566B) is part of a future continuous SDA process and was used only for PB-D experiments as an intermediate solvent flow-through unit. It has a height of 203 mm, an internal diameter of 63.5 mm, and a total capacity of 600 ml. The other reactor (model number: 4567) was used as the main equipment to conduct the experiments, in which both mixing and settling processes were performed for all the experiments described in the thesis. The main reactor (model number: 4567) has a height of 152.4 mm with an internal diameter of 63.5 mm. It is equipped with two windows on opposite sides and has a total volume of 450 ml. Since all the experiments were performed in the windowed reactor, the term "reactor" refers to the model 4567 in the rest of the thesis, unless otherwise stated. The reactor has a pressure rating of 1900 psi and a temperature rating of 225 ℃.

Figure 3.1 demonstrates the detailed configuration of the reactor (model number: 4567), which was employed to perform all the experiments. As clearly seen in Figure 3.1, the reactor is a mechanically stirred tank that is also equipped with a dip tube to collect deasphalted oil samples and two impellers to perform mixing.

All the tubes, adapters, valves, and tools used for the commissioning of the experimental setup were purchased from Swagelok. Different dip dupe heights were required depending on the amount of material loaded to the reactor. Therefore, multiple dip tubes were made in the PTP laboratory using a tube cutter (part number: MS-TC-308), a tube deburrer (part number: MS-TDT-24), and a tube treader (MS-TK-4H). For this reason, ¼ inch stainless steel pipe was cut to the required length, deburred, and threaded.

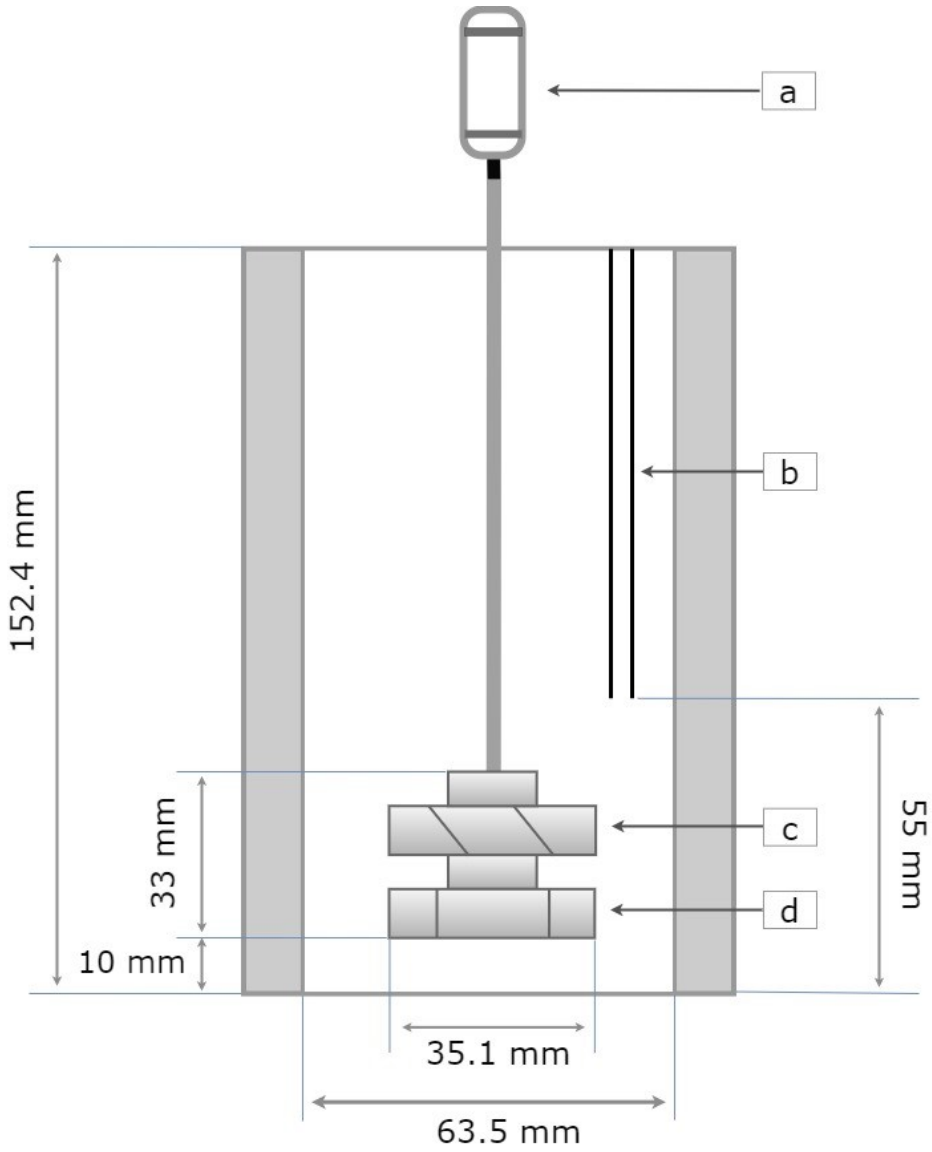

Figure 3. 1. Configuration of the reactor used for the CNOOC SDA experiments: motor (a), dip tube (b), pitch blade turbine (c), Rushton turbine (d)

The reactor is equipped with two six-blade impellers that were used to perform mixing. Figure 3.2 provides photographs of the impellers used. As described in Figure 3.1, the impellers were used one on top of the other with no gap in-between and there was a clearance of 10 mm between the bottom of the reactor and the impellers. The top impeller was a pitch blade downward turbine (PBT) with a 45-degree blade angle and the bottom impeller was a Rushton turbine (RT). Both impellers have the same diameters (35.1 mm). The PBT has a blade width of 1.5 mm and the RT

has a blade width of 3 mm. Two screws were used to mount them on the shaft as illustrated in Figure 3.2.

Figure 3. 2. Impellers that were used to perform mixing: Pitch blade turbine (on the left), Rushton turbine (on the right)

A Canon camera (model: EOS Rebel T3i) equipped with Canon EF 75-300 mm zoom lens was used to record the mixing and settling processes. A combination of two light sources, Dolan Jenner fiber-lite (model: PL-800) and NOMA Integrated Led (model: ST2SPT), was used to improve the visibility through the reactor window and take high-quality photos.

A Teledyne SSI positive displacement pump (part number: LS040SFP1A) was employed to transfer the solvent from the tank to the reactor. The pump was connected to a Parr heating mantle (part number: A2230HCEB) to increase the solvent temperature, prior to injection into the reactor. Tubes from the heating mantle to the reactor were wrapped with Omega silicone heating tapes (model: SRT051-040). Two heating tapes both with 0.5 in x 4ft dimensions were used to keep the solvent temperature inside the tubes at the operating temperature of the system. In addition, tubes were also wrapped with SORDIAL insulation cloth (model: 088114D1) to minimize heat loss. Parr thermocouples (part number: A470E2) were installed inside the reactors, heating mantle, and external tubes to transmit the temperature of the units to the controllers. The temperatures of reactors were controlled with Parr 4848B controllers and the temperature of the heating mantle was controlled using a Parr 4838 controller. Fisher brand (model: 4100 H21P) heating bath was used to heat the can of bitumen emulsion to sufficiently decrease bitumen viscosity to be able to weigh and load the required amount to the reactor.

HSW HENKE-JECT syringes of 20 ml were used to withdraw the DAO and water samples from the reactor. The syringes were also used to measure the exact amount of free water and solvent, prior to loading the reactor. Sartorius TE6101 lab balance was used to weigh both the materials loaded to the reactor and the taken sample. The balance has a maximum weighing capacity of 6100 g with readability of $\pm$ 0.1g. Fischer brand volumetric pipets (model: 136503L) were used to measure the density of the DAO and water samples. The pipets have a capacity of 10 ml with a tolerance of $\pm$ 0.02 ml.

Masterflex peristaltic pump (model: 77200-62) purchased form Cole-Parmer Instrument Company was used to circulate cold water around the pressure gauges and transducers to keep the instruments cool to prevent faulty pressure readings.

3.4 Experimental conditions

The operating conditions of the experiments that were performed for this study are provided in Table 3.5. As discussed in Section 1.4, the mixing conditions and S/B ratio are the primary parameters that were investigated in the current study. For that reason, the S/B ratio was varied in a range of 0.9 – 2.2. To study the mixing effects on SDA product quality, mixing time was varied between 2 – 60 mins and only two mixing speeds (515 and 258 RPM) were studied in this project.

The third column in Table 3.5 provides the amount of water (i.e. steam-to-oil ratio or SOR) used for each experiment. The SOR given in the table corresponds to the water-to-bitumen ratio that was used to calculate the required water mass to load the reactor. Initially, experiments were conducted with a SOR of 3 in order to imitate a real SAGD extracted bitumen product composition. However, as the experiments proved that water mass has no impact on SDA products' specifications, it was decreased to facilitate the use of higher S/B ratios.

As clearly seen in Table 3.5, the temperature of the system was essentially constant and the operating pressure deviated significantly from the target pressure. The reason for this deviation is that the reactor pressure depends on all the materials in the reactor (bitumen, solvent blend, water, nitrogen); however, it was impossible to consider the contribution of every component to the operating pressure. Therefore, only the main contributors (pentane, water, and nitrogen) were used to estimate the system pressure, which gave rise to considerable deviations in the operating

pressure. Nevertheless, as explained in Section 2.3.2, the objective of high pressure is only to keep the solvent in liquid phase and the operating pressure has no effects on the asphaltene precipitation process. All the given operating pressures in Table 3.5 are above the vapour pressure of the lightest solvent (iso-pentane) in the blend and therefore were enough to keep the solvent in liquid phase.

Table 3. 5. Test matrix for the experiments conducted during the present investigation

Runs	Pentane equivalent S/B ratio (wt/wt)	SOR[a] (wt/wt)	Mixing speed (RPM)	Mixing time (mins)	Pressure (bar)	Temperature (°C)
PB-A-001	0.9	3.0	515	60	46	165
PB-A-002	0.9	3.0	515	60	33	165
PB-B-001	0.9	3.0	515	60	31	165
PB-B-002	1.3	3.0	515	60	41	164
PB-B-003	1.7	3.0	515	60	42	164
PB-B-004	1.8	2.0	515	60	41	164
PB-B-005	1.9	1.9	515	30	38	164
PB-B-006	1.9	1.9	515	60	38	164
PB-B-007	1.9	1.9	515	2	36	164
PB-B-008	1.9	1.9	258	60	43	164
PB-D-001	2.0	1.9	515	10	37	164
PB-D-002	2.2	1.9	515	30	37	164

[a] SOR is equivalent to the water-to-bitumen ratio in the current study

3.5 Experimental procedures

Three sets of experiments were performed, and each set required a different equipment setup. The PB-A set experiments were performed in complete batch mode. The other sets, PB-B and PB-D, were conducted in semi-batch modes. The experimental procedures will be explained in order of increasing complexity of the sets. The main steps followed to perform each set of experiments will be described in the following subsection and more detailed Safe Work Procedures (SWP) can be found in Appendix D.

The experimental setup for the PB-D set is the most complex and was built by adding necessary modifications to the preceding setups. Figure 3.3 illustrates the process flow diagram of the experimental setup for the PB-D set. As explained in Section 3.3, mixer (4) and settler (6) are the two reactors that have been received from Parr Instrument Company. Both reactors are equipped with mixers and only one of them has windows. Note that mixer (4) and settler (6) are representative names for the units in Figure 3.3, both of them are essential parts of a future continuous SDA process. As mentioned in Section 3.3, for all the experiments, only the windowed reactor (6) was used to perform both mixing and settling processes, the detailed configuration of which is illustrated in Figure 3.1.

The pressure equalization line (5) was only part of the PB-D set experimental setup and it was used to enable the flow of solvent from the mixer (4) to the settler (6) under gravity. Note that it is critical that valves on both ends of the pressure equalization line (5) are open and both vessels are always at the same pressure to enable solvent injection into the main reactor (6). Otherwise, due to the pressure difference between vessels, some of the solvent might be trapped in the mixing vessel (4), which may produce an S/B ratio lower than that desired for the experiment.

In general, each experiment took thee days to complete. On the first day, loading and pressure testing of the reactor were carried out. On Day 2, the experiment was performed and the process data were recorded. For the PB-B and PB-D set runs, deasphalted oil samples were taken at operating temperature and pressure. On Day 3, the reactor was emptied, cleaned, and made ready for the next run.

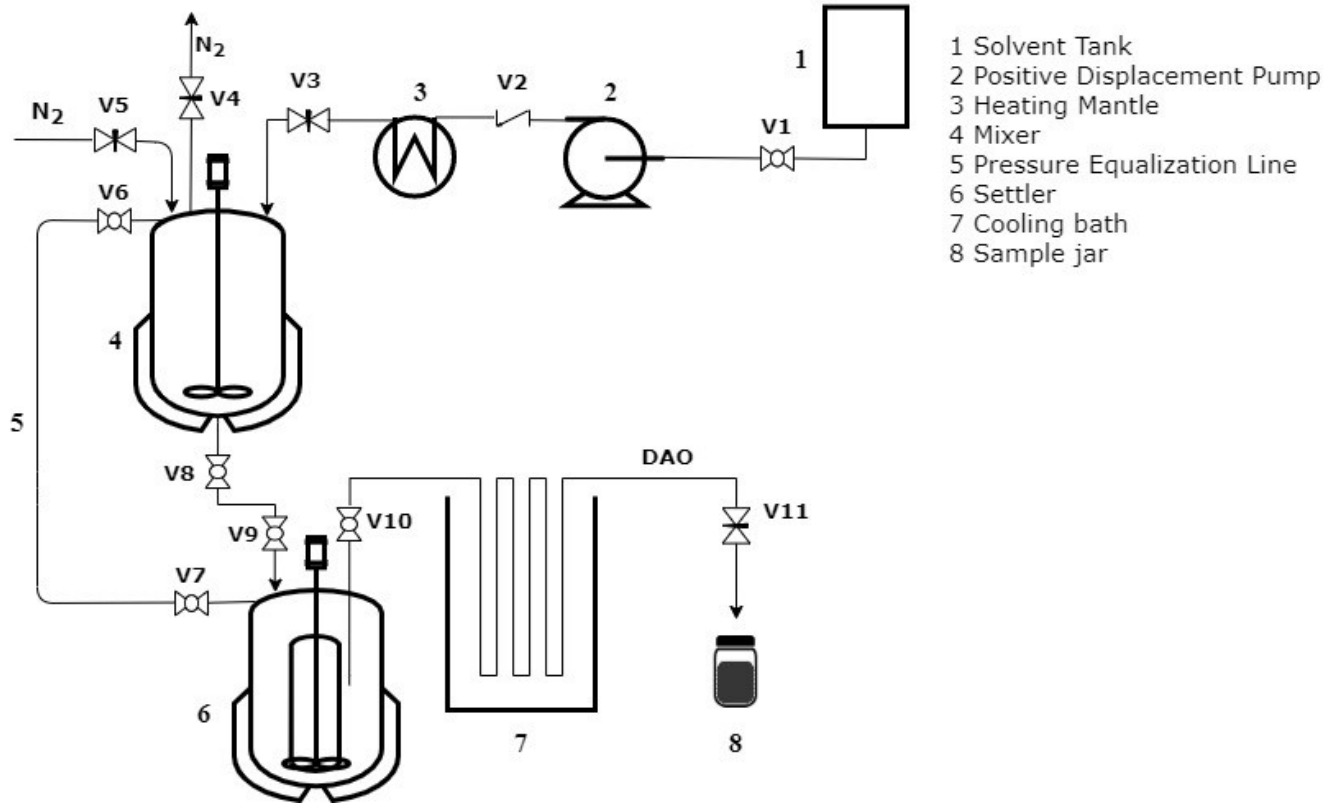

Figure 3. 3. Process flow diagram for the bench-scale solvent deasphalting of bitumen emulsion

3.5.1 Procedures for the PB-A set

The experimental setup for the PB-A set consists of a reactor. In Figure 3.3, shutting V7, V9, and V10 valves, the reactor (6) is isolated from the rest of the system. The steps followed on each day to perform the experiments of this set are as follows:

First day of experiments

1.1. Bitumen emulsion can is heated inside an ethylene glycol bath for about 1.5 hours to reduce bitumen emulsion viscosity for ease of transfer in the reactor.

1.2. Both windows of the reactor are silanized inside the fume hood with 5 wt. % dimethylchlorosilane in heptane solution.

1.3. The reactor is positioned on the stand built to hold the reactor.

1.4. Using a ladle some of the hot bitumen emulsion is transferred into a 100 ml beaker and weighed on a digital scale.

1.5. Immediately after weighing, the hot bitumen emulsion from the beaker is poured in the reactor and the beaker is weighed to determine the leftover bitumen emulsion inside the beaker. By subtracting the beaker mass before and after pouring bitumen emulsion in the reactor, the mass of bitumen emulsion transferred inside the reactor is calculated.

1.6. Based on the specified SOR, the required free water mass is calculated, weighed, and loaded to the reactor.

1.7. Based on the specified S/B ratio, the required solvent mass is calculated, weighed, and loaded to the reactor.

1.8. The reactor is sealed by putting the clamps on and tightening the compression bolts.

1.9. Parr 4848B controllers and software (SpecView) are turned on to monitor the pressure and temperature in the reactor.

1.10. The pressure inside the vessel is raised to 55 bar by injecting nitrogen and the system is tested for any leaks.

1.11. The system is considered to be pressure tight once the pressure of the system does not drop more than 5 psi per hour.

Second day of experiments

2.1. The required initial system pressure is estimated based on the materials in the reactor.

2.2. The system pressure is reduced to the estimated pressure by releasing some of the nitrogen injected the previous day.

2.3. Insulation jackets are placed onto the reactor and the heater is turned on.

2.4. The reactor pressure and temperature are recorded in an excel file every 5 mins.

2.5. The camera and the lights are placed and adjusted to record the mixing and settling processes through the window.

2.6. The heating of the reactor contents continues until the system temperature reaches the specified operating temperature (164 ℃ for most of the experiments).

2.7. The mixer is turned on and set to the target mixing speed. Mixing is allowed to continue for the specified time.

2.8. The mixer is stopped and settling is allowed to take place for the specified time (60 mins) at the operating temperature and pressure.

2.9. Once the specified settling time is up, the heater is turned off, insulation jackets are removed, and the reactor is allowed to cool down overnight.

Third day of experiments

3.1. The system is depressurized by releasing all the nitrogen from the reactor.
3.2. The reactor is unsealed and moved into the fume hood.
3.3. The DAO is withdrawn with a clean syringe and collected in a pre-weighed sample jar.
3.4. The water is withdrawn with a clean syringe and collected in a pre-weighed sample jar.
3.5. The pitch is removed with a clean spatula and collected in a pre-weighed sample jar.
3.6. The reactor is washed with some amount of toluene and left inside the fume hood to dry.

3.5.2 Procedures for the PB-B set

The PB-B set experiments were conducted in semi-batch mode, which involved sampling of DAO at operating pressure and temperature. In Figure 3.3, closing V7 and V9 valves will isolate the PB-B setup from the rest of the system. Figure 3.4 demonstrates the experimental setup that was used for the PB-B runs.

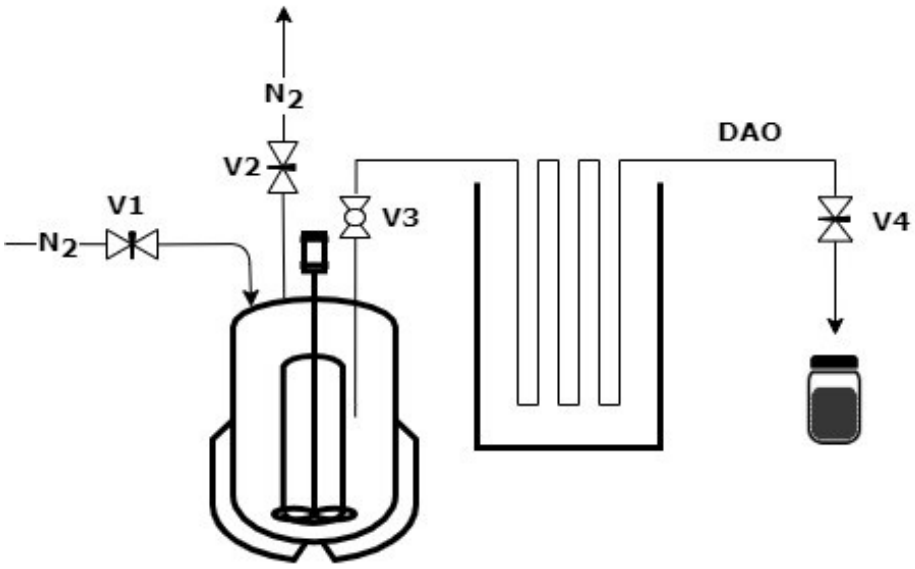

Figure 3. 4. Process flow diagram of the solvent deasphalting setup for the PB-B experiments

The steps followed on each day to perform the PB-B set experiments are as follows:

First day of experiments

1 – 11: The same as the procedures followed for the PB-A set.

Second day of experiments

2.1 – 2.8: The same as the procedures followed for the PB-A set.

2.9. The cooling bath is filled with icy water and the temperature of the bath is allowed to drop below 5 ℃.

2.10. The valve connected to the dip tube (V3) is opened to fill the tube with DAO (Figure 3.4).

2.11. By gradually opening the choke valve (V4) the DAO is sampled (Figure 3.4).

2.12. After the sampling, the heater is turned off, insulation jackets are removed, and the reactor is allowed to cool down overnight.

Third day of experiments

3.1 – 3.6: The same as the procedures followed for the PB-A set.

3.7. The DAO sampling line is disconnected from the setup and washed with toluene and left inside the fume hood to dry.

3.5.3 Procedures for the PB-D set

The PB-D set experiments were conducted in semi-batch mode, which involves all the process units illustrated in Figure 3.3. The steps followed on each day to perform the experiments of this set are as follows:

First day of experiments

1.1 – 1.11: The same as the procedures followed for the PB-A set, except 1.7. Step 1.7 was omitted, and the solvent was not loaded to the reactor on the first day of the experiments.

Second day of experiments

2.1 – 2.6: The same as the procedures followed for the PB-A set.

2.7. When the system temperature reaches the specified operating temperature, the solvent is injected using the positive displacement pump.

2.8. After the required solvent amount has been injected, the pump is turned off and V9 is closed to prevent the solvent flow from the mixer (4) into the reactor (6) (Figure 3.3).

2.9. The mixer is turned on and set to the target mixing speed.

2.10. After the specified mixing time is over, the mixer is immediately stopped, and reactor contents are allowed to settle.

2.11. Two DAO samples are retrieved following the steps 2.9 – 2.11 from the PB-B set.

2.12. The heater is turned off and the reactor is allowed to cool down overnight.

Third day of experiments

3.1 – 3.8: The same as the procedures followed for the PB-B set.

3.6 Sampling

3.6.1 DAO sampling

Deasphalted oil samples were taken through a dip tube installed inside the reactor. After the vessel contents were mixed for the specified duration, the mixture was allowed to settle and separate into DAO, asphaltenes-rich, and water phases. The DAO, being the lightest of the three phases, forms as the top phases and was pulled through the dip tube (Figure 3.1) at the specified settling time. It is important to ensure that the external lines that carry DAO are submerged into the cooling bath, as illustrated in Figure 3.3. Prior to sampling, the DAO inside the tubes has to be cooled down below the room temperature in order to prevent excessive solvent evaporation. As soon as the required amount of DAO was retrieved, the sample jar was tightly closed with a cap to avoid material loss.

Depending on the experiment, one to three samples were taken and the samples were named based on the time they were retrieved. For example, DAO-10 corresponds to the sample taken in the 10^{th} minute of settling time, DAO-60 corresponds to the sample taken in the 60^{th} minute of settling time, and DAO-24 corresponds to the sample taken 24 hours after the start of the settling process. Table 3.6 demonstrates the number of samples retrieved from each experiment. For instance, from the PB-A-002 run only one sample (DAO-24) was taken and from PB-B-005 run three samples (DAO-10, DAO-60, and DAO-24) was taken. The number of samples taken from the reactor depends on the amount of bitumen emulsion and solvent fed. For PB-A set, a low S/B ratio was

used and it was performed in complete batch mode; consequently, only one sample could be taken which occurred at the end of the experiment. The other sets were performed in semi-batch mode and thus more than one sample could be retrieved. For the PB-B set, initially, only two samples could be taken. Gradually, the S/B ratio was increased and the SOR was decreased; therefore, more DAO was produced and taking three DAO samples became feasible.

Table 3. 6. DAO samples taken from each SDA experiment

Runs	Solvent used	Pentane equivalent S/B (wt/wt)	DAO-10	DAO-60	DAO-24
PB-A-001	Batch 1	0.9	-	-	+
PB-A-002	Batch 1	0.9	-	-	+
PB-B-001	Batch 1	0.9	-	+	+
PB-B-002	Batch 1	1.3	-	+	+
PB-B-003	n-pentane	1.7	-	+	+
PB-B-004	Batch 2	1.8	-	+	+
PB-B-005	Batch 3	1.9	+	+	+
PB-B-006	Batch 3	1.9	+	+	+
PB-B-007	Batch 3	1.9	+	+	+
PB-B-008	Batch 3	1.9	+	+	+
PB-D-001	Batch 3	2.0	+	+	+
PB-D-002	Batch 3	2.2	+	+	+

3.6.2 Pitch and water sampling

Pitch samples were taken on the third day of experiments, after complete cooling of the reactor. To obtain these samples, the reactor was unsealed, moved into the fume hood, and placed on the stand to keep the reactor steady and upright. The remaining DAO was then withdrawn with a syringe and discharged into a sample jar. Similar to the DAO sampling, water was displaced and collected in a sample jar. Finally, the pitch was removed from the reactor using a clean spatula and collected in a sample jar.

Under laboratory conditions, there is a limitation to the amount of pitch that can be collected. Some of the pitch sticks to the walls of the reactor and cannot be removed unless washed with toluene. Unfortunately, washing with a known mass of toluene also causes a significant mass error, due to evaporation. Therefore, the reactor walls were wiped with weighed clean paper towels many times and the change in the total mass of the paper towels indicated the amount of pitch left in the reactor. It was determined that the amount of unrecoverable pitch is approximately 2 grams and this value is approximately the same for every experiment. This error in pitch mass collected has been indicated using error bars in the pitch yield graphs provided in the following chapters.

Since asphaltene could not be obtained separately, the asphaltene yield assessment was not performed. However, because asphaltenes are the main ingredient of pitch and the experimental results of pitch can easily be applied to asphaltenes, the pitch yield was calculated. The pitch yield was estimated based on the ratio of the mass of pitch collected to the mass of the dry bitumen fed to the reactor.

3.7 Sample analysis

After all the sampling processes were complete, sample jars were thoroughly shaken to create a homogenous mixture. Approximately 2 grams DAO were used for each water analysis and tests were performed in duplicates. The water content of DAO samples was measured in the PTP laboratory using Mettler Toledo, InMotion KF Pro Oven Autosampler. Care was taken to perform the sampling for water content measurement as quickly as possible so as not to lose material and cause composition change in the DAO samples. The remaining samples were sent to an external laboratory for asphaltene content analyses.

The volume of each DAO sample remaining after KF analysis was sent to an external laboratory at University of Alberta to evaluate the asphaltene content of samples. The standard operating procedure for ASTM D6560 was followed to analyze the samples. The complete testing procedure for calculating pentane insolubles can be found in the ASTM D6560 standard.[102] Briefly, DAO asphaltene analysis consists of three stages: solvent evaporation, treatment of sample remnants, and filtration of pentane insolubles.

First, the light fractions in DAO are evaporated off the sample in an oven under 60 ℃ and 700 mbar conditions. This process may take over two weeks depending on the light fractions content of the sample. The evaporation continues until the sample mass is essentially constant. About 1 gram of the remaining sample is then taken and mixed with n-pentane in 1:40 ratio. The solution is mixed for an hour at 350 RPM to strip the sample of remaining light fractions. Finally, this solution is filtered with a pre-weighed 0.22 μm pore sized filter paper and the mass percentage of the pentane insolubles is calculated based on

$$C5 - \text{insolubles} = \frac{\text{Grams of insolubles}}{\text{Grams of the sample used}} \times 100\ \% \tag{3.1}$$

The densities of DAO and water samples were measured using a 10 ml pipette tube. For this reason, the pipet tube was filled with the liquid up to the marked level and the liquid is then discharged into a tared beaker to weigh the mass of the displaced liquid. The density of the sample is calculated from

$$\rho = \frac{m}{V} \tag{3.2}$$

where m is the sample mass (g), V is the sample volume (ml), and ρ is the sample density (g/ml).

3.8 Mixing method

Mixing intensity and mixing energy were the two parameters calculated to quantify the mixing process. These parameters will be used to estimate the mixing characterization for the scaled-up SDA process. Recall from Section 2.3.7 that mixing intensity is the ratio of total mixing power to the total mixture mass. The mixing intensity for the experiments of the current study was calculated based on

$$\varepsilon_{mix} = \frac{N_P \rho N^3 D^5}{\rho V} = \frac{N_P N^3 D^5}{V} \quad (3.3)$$

where ε_{mix} stands for the mixing intensity (W/kg), N_P is the impeller power number, ρ is the density of the mixture (kg/m^3) , N is the speed of the impeller (rev/s), D is the diameter of the blades (m), and V is the mixture volume inside the reactor.[88]

All the parameters required for the calculation were taken from the experiments, except the power number. The power number for the combination of the impellers is 3.37.[103] A timer was used to record the mixing time, which then was used to calculate the mixing energy using

$$E = \varepsilon_{mix} \times t_{mix} \quad (3.4)$$

where E stands for the mixing energy (kJ/kg) and t_{mix} is the mixing time (s).[88]

3.9 Settling calculations

Due to the limited visibility through the reactor window, individual and hindered settling of asphaltene aggregates could not be performed. Using the camera images taken during the experiments, the settling rate of asphaltene aggregates was calculated based on the zone settling method. Three phases form during the settling process and with the zone settling method, the rate of phase separation is calculated by tracking the change in the levels of the interfaces. A MATLAB program was written to study the images and accurately track the interface levels. For this reason, images had to be taken at regular intervals (dt = 2 s) and they had to be indicated by a number. By default, the camera generated the image names by adding one to the previous image name. For example, for three consecutive images corresponding names were IMG45, IMG46, IMG47. All

the settling images were transferred to the computer and kept in a separate folder. The folder was called from the MATLAB program, which received the folder and brought to the screen one image at a time and provided the viewer with different colours to mark the interfaces. The MATLAB program interpreted the marked points as the height of the corresponding interface from the bottom of the reactor. Finally, it generated a phase separation graph, base on the interface levels and the time images were taken.

Figure 3.5 describes how phase separation occurs for the solvent deasphalting of bitumen emulsions. The calibration on the left-hand side of columns is used to track the height of the interfaces over time and calculate the aggregate settling distance, which is then used to estimate aggregates settling rate. The column at the far-left corner (t_0) corresponds to the time when the mixer is stopped, immediately after which the settling and the phase separation start. Three phases form over time: the top layer is the solvent-rich DAO phase, the bottom layer is the water phase, and the thinning middle layer is the asphaltenes-rich pitch phase. As a result of asphaltene aggregates and water droplets settling, the water and DAO phases grow bigger and the pitch phase becomes more packed and less porous over time.

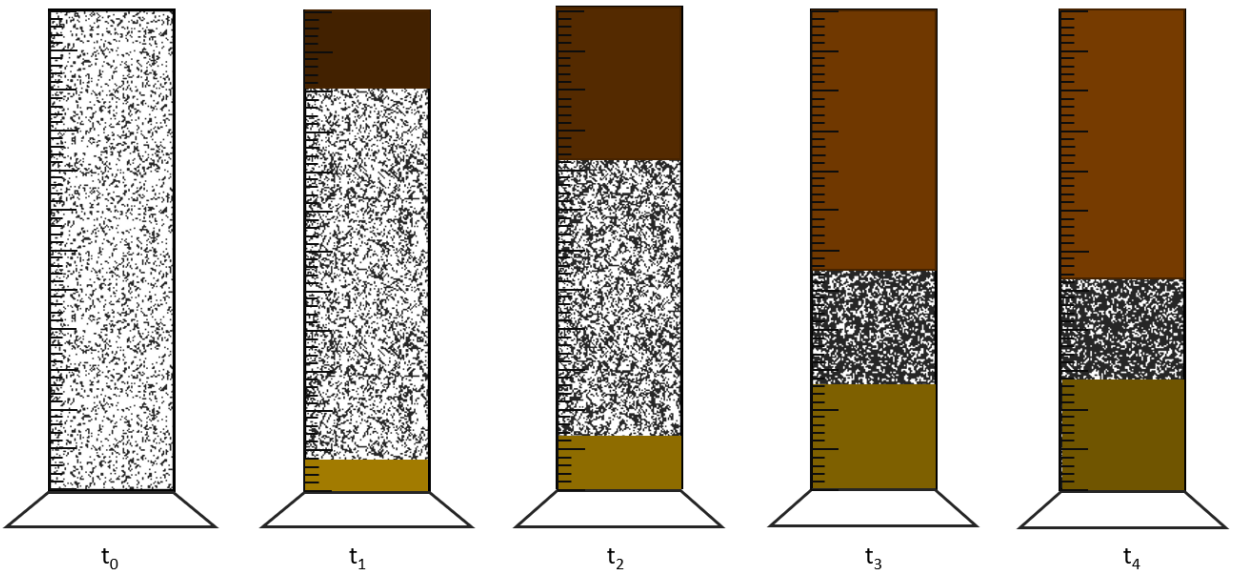

Figure 3. 5. Schematic illustration of the phase separation for solvent deasphalting of SAGD product. DAO phase (top), pitch phase (middle), water phase (bottom)

Figure 3.6 demonstrates the predicted phase separation trend for the solvent deasphalting of bitumen emulsion. The Y-axis corresponds to the height of the settling vessel and the X-axis corresponds to the settling time. As it can be seen from Figure 3.6, the tangent of the line indicating the change in the DAO interface gives the instantaneous aggregate settling rate. For actual experiments, however, since the DAO interface cannot be tracked with the required precision at any moment over the time axis, the instantaneous aggregate settling rate was not calculated.

The average aggregate settling rate was calculated for the experiments performed in the current study. For that reason, the separation of the phases was taken as the reference point. In Figure 3.6, the required time for phase separation is t3, after which the levels of water and DAO phases essentially do not change. Furthermore, since mixing creates homogeneity in the system and aggregates settle though the DAO phase, the settling distance of the asphaltene aggregates was considered to be from the top of the DAO phase to the bottom of the DAO phase. In other words, it was assumed that aggregates start settling from the very top of the mixture in the reactor. Finally, the average aggregate settling rate was calculated by diving the settling distance to the settling time. For example, the average aggregate settling rate based on Figure 3.6 is

$$\text{Average aggregate settling rate} = \frac{(80 - 40)\ \text{mm}}{(t_3 - t_0)\ \text{mins}}$$

where the numerator corresponds to the aggregate settling distance and the denominator corresponds to the aggregates settling time. Aggregate settling graphs for all the experiments that have been performed in the present study are provided in Appendix C.

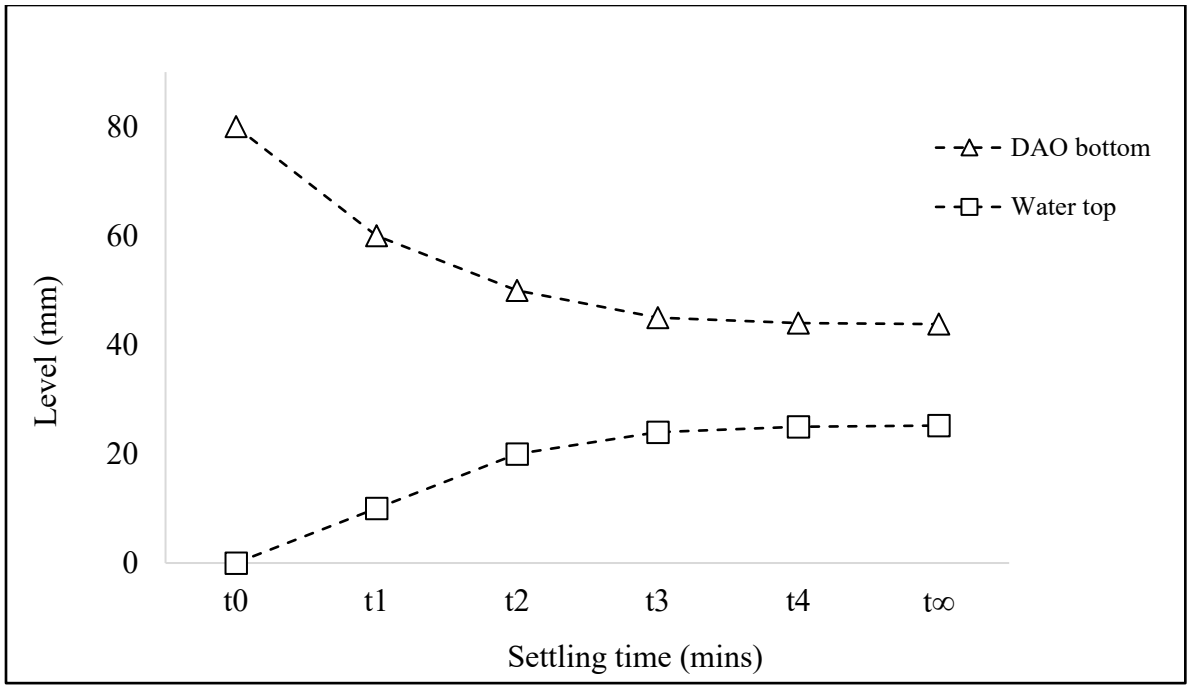

Figure 3. 6. Phase separation process for the solvent deasphalting of bitumen emulsions

4. Effects of S/B Ratio on Asphaltene Precipitation

4.1 Introduction

This chapter analyzes and discusses the experiments performed to study the effects of changing S/B ratio on solvent deasphalting of bitumen emulsion. The asphaltenes and water content of DAO samples are the major analysis results that will be discussed in detail and compared to the literature. Also, results for the pitch yield and DAO density will be used to verify the drawn conclusions and to support the analysis results for DAO samples. To clearly observe the impact of the S/B ratio on the SDA products, merely a different S/B ratio was used for each experiment while keeping all the other parameters fixed. All the experiments discussed in this chapter have been performed under the same mixing speed (515 RPM). Detailed information in regard to the operating conditions of the experiments can be found in Table 3.5.

4.2 Performed experiments

This section introduces the experiments that have been performed to study the impact of different S/B ratios on asphaltene precipitation from bitumen emulsions. Overall, nine experiments across three different sets have been conducted. Table 4.1 contains detailed information about the experiments and their mixing conditions. The S/B ratios studied here range from 0.9 to 2.2 (pentane equivalent basis). The same mixing conditions have been applied to the experiments, except for the last three experiments given in Table 4.1. As will be discussed in Chapter 5, the mixing time has an imperceptible impact on asphaltene precipitation. Therefore, experiments with different mixing times were also included in the discussion in this chapter because any difference in product quality can mainly be attributed to the S/B ratio.

In the PB-A and PB-B sets, the reactor was loaded batch-wise and the exact mass of the calculated solvent amount was poured in. For the PB-D set, however, due to the injection procedure that involves a positive displacement pump (Figure 3.3), the pumped solvent mass was determined to deviate from the calculated solvent amount (Table 3.4). These deviations have also been reflected in the graphs with the results obtained from the PB-D runs.

Table 4. 1. Experiments performed to study the effects of varying S/B ratios on the asphaltene precipitation. All the experiments have been performed at 515 RPM mixing speed

Runs	Solvent used	S/B (wt/wt)		Mixing time (mins)
		Actual	Pentane equivalent	
PB-A-001	Batch 1	1.2	0.9	60
PB-A-002	Batch 1	1.2	0.9	60
PB-B-001	Batch 1	1.2	0.9	60
PB-B-002	Batch 1	1.7	1.3	60
PB-B-003	n-pentane	1.7	1.7	60
PB-B-004	Batch 2	2.4	1.8	60
PB-B-005	Batch 3	2.4	1.9	30
PB-D-001	Batch 3	2.5[a]	2.0	10
PB-D-002	Batch 3	2.7[a]	2.2	30

[a] ± 0.1 deviation is applicable for the PB-D set experiments, due to the solvent injection method

4.3 Pitch yield

This section provides the pitch yield results calculated from each experiment for the experiments given in Table 4.1. The experimental results for the pitch yield are the first stage to investigate the impact of S/B ratio. Section 2.3.5 provides detailed information about what could be observed in an SDA process as S/B ratio is varied, and it is clearly mentioned in the literature that increasing the S/B ratio leads to more asphaltenes precipitation.[44,51] Besides, since asphaltenes are the primary constituent of the pitch, higher pitch yield is an indication of more asphaltenes precipitation.[9,34,51]

Figure 4.1 demonstrates the pitch yield (wt. %) obtained for a range of different S/B ratios. It is evident from the graph that increasing diluent mass in bitumen emulsion-solvent mixture leads to an increase in the pitch yield. Of the nine experiments that have been performed to investigate the impact of S/B ratio on the pitch formation, only six are demonstrated in Figure 4.1. That is because no quantifiable pitch was collected at low S/B ratios. In other words, the first three experiments in Table 4.1 have been conducted at the same S/B ratio and based on the results, it is believed that the loaded solvent amount was very close to (or below) the onset of asphaltene precipitation under the given operating conditions. Based on the literature,[9,44] the onset of asphaltene precipitation for

paraffinic solvents may vary between 0.8 – 1.6. Since the S/B ratio for these three experiments (S/B = 0.9) is within this range, no pitch retrieval for these experiments is a predictable result.

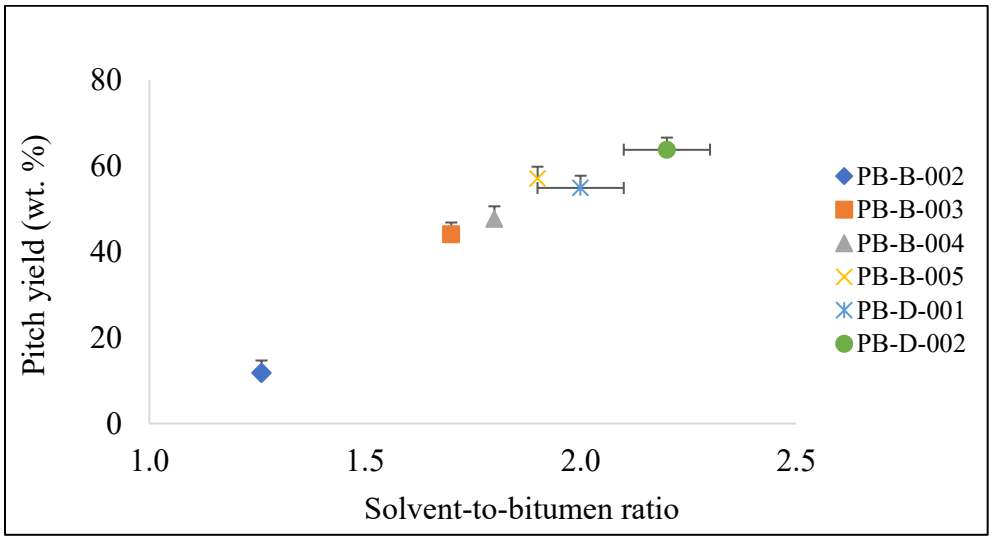

Figure 4. 1. Effects of S/B ratio on pitch yield for solvent deasphalting of bitumen emulsions under the operating conditions provided in Table 4.1

PB-B-002 is the next lowest S/B ratio that was studied. With an S/B ratio of 1.3, only about 4 grams pitch was retrieved, which corresponds to 12 wt. % pitch yield in Figure 4.1. This means that the employed S/B ratio was still too small to cause any significant asphaltene precipitation. At the same time, the results of this run also reveal that the onset of asphaltene precipitation for the used solvent blend is below 1.3.

Above the onset of asphaltene precipitation, the S/B ratio has a dramatic impact on pitch formation. A huge leap in the pitch yield is observed when the S/B ratio is raised from 1.3 (PB-B-002) to 1.9 (PB-B-005) such that the pitch yield increases more than 7 folds between these two runs.

Above an S/B ratio of 1.8, as the S/B ratio is raised further, little difference is observed in the pitch yield. This is because few heavy fractions remain in the oil and after a certain S/B value no significant precipitation can be obtained with adding more solvent. This deduction complies with the literature data. Based on the literature,[51] above a certain S/B ratio, adding more solvent does not cause any significant change in the asphaltene precipitation process and the pitch yield reaches a plateau.

The pitch samples were not sent to a laboratory for composition analysis; however, qualitative observations suggest that samples taken from the PB-B runs contain more solvent and are less viscous compared to the samples taken from the PB-D runs. This conclusion was reached as a result of a simple experiment. First, the pitch sample jars were weighed and recorded. Then, the caps of the sample jars were removed, and the sample jars were left inside the fume hood for 24 hours open to the atmosphere. After 24 hours, sample jars were sealed with caps and weighed. On average, 10 wt. % drop in mass was observed for the samples taken from the PB-B set and only 4 wt. % drop in the mass of the PB-D set samples was observed. This implies that pitch samples taken from the PB-B runs have higher solvent content compared to the pitch samples from the PB-D runs. This observation is believed to be a consequence of the way the solvent was loaded to the reactor.

As explained in Section 3.5, for the PB-D set experiments, the solvent was injected into the settler using a positive displacement pump (Figure 3.3). Because the solvent was pumped in a semi-continuous mode, it is suspected that the solvent composition might have changed during the pumping process. Recall from Section 3.5.3 that the solvent injection was stopped once the required solvent mass had been injected and immediately after the valve connecting the mixer (4) and settler (6) were closed. The most likely scenario is that solvent may have built up in the mixer (4) during the pumping process and due to the density difference, more heavy solvent fractions might be discharged into the settler (6) (Figure 3.3). Therefore, the pitch samples retrieved from the PB-B set contain more light fractions compared to the samples taken from the PB-D set. Consequently, the sample that contains more light fractions will evaporate more and lead to a higher mass drop. Nevertheless, this outcome is not expected to occur for a pilot-scale (or commercial-scale) process that operates continuously, due to the fact that a solvent buildup is an unlikely situation for a steady-state, continuous process.

4.4 Asphaltene content of DAO

This section provides the analysis results obtained for the DAO samples taken to study the impact of varying S/B ratios on the asphaltene precipitation and deasphalted oil quality. The asphaltene content of DAO samples is the major parameter that was attempted to be minimized in this study, which defines the deasphalted oil quality. The detailed DAO sampling process has been described in Section 3.6.1 and Table 3.6 demonstrates how many DAO samples have been taken from each experiment. This section mainly focuses on the DAO-10 and DAO-60 samples and on the basis of them, investigates the impact of S/B ratio on the deasphalted oil quality.

Figure 4.2 demonstrates the results for asphaltene content analysis of the deasphalted oil samples taken in the 10^{th} minute of settling time. Results for the asphaltene content and solvent content of DAO-10 samples were studied only for a small range of S/B ratios. From Figure 4.2, it is evident that there is little difference between the asphaltene content of the three samples because the employed S/B ratios are very close.

Nevertheless, higher asphaltene content for the deasphalted oil samples from the PB-D runs is a counterintuitive result because of the fact that a higher S/B ratio has been used for the PB-D runs than for the PB-B. It seems as if more asphaltenes have remained in DAO when the bitumen was treated with more diluent. This is believed to happen due to the difference in solvent injection methods between the two sets. As explained at the end of Section 4.3, as a result of pumping solvent in semi-batch mode using a positive displacement pump, the solvent loaded to the reactor in the PB-D set contains more heavy hydrocarbons compared to the solvent loaded in the PB-B set. From the discussion in Section 2.3.4, it is clear that if a heavy hydrocarbon is used as the solvent, fewer asphaltenes will precipitate and more asphaltenes will remain in oil compared to the case that light hydrocarbon is used as the solvent.[9,34,50]

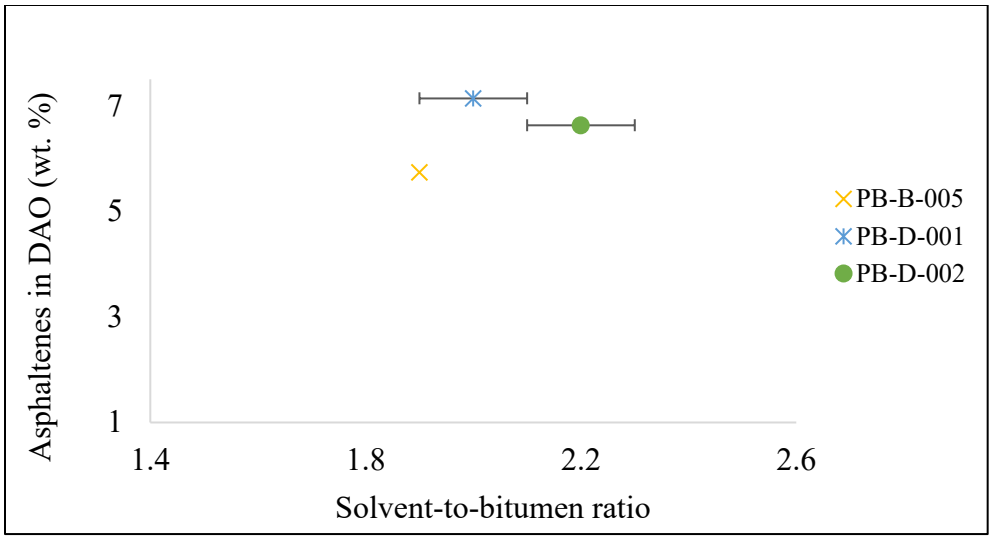

Figure 4. 2. Effects of S/B ratio on the asphaltene content of DAO-10 samples for solvent deasphalting of bitumen emulsions under the operating conditions given in Table 4.1

Figure 4.3 provides a comprehensive description of the asphaltene content in regard to the deasphalted oil samples taken in the 60th minute of the settling process. It is evident from Figure 4.3 that the asphaltene content of DAO samples decreases with increasing S/B ratio. Moreover, this decrease is more dramatic at low S/B ratios. Comparing PB-B-002 and PB-B-004 experiments, increasing the S/B ratio from 1.3 to 1.8 (~40 % increase) leads to a sharp decrease in the asphaltene content of deasphalted oil, from 23.2 wt. % to 5.3 wt. %. Recall from Section 3.2.1 that the asphaltene content of bitumen feed was 20.2 wt. %; therefore, it is believed that there is an analysis error associated with the PB-B-002 sample. Nonetheless, the observed trend is correct and the pitch yield results discussed in Section 4.3 corroborate this trend. That means, the observed difference in pitch yield of these two runs (Figure 4.1) is expected to be accompanied by a similar difference between the asphaltene content of the corresponding DAO samples.

Above an S/B ratio of 1.8, the change in asphaltene content is less noticeable. This is because most of the asphaltenes have already precipitated, and therefore a minor impact is observed with increasing S/B ratio. This interpretation agrees with the literature data and with the deductions from Section 4.3. The literature[51] reports that greater jumps in S/B ratios might be required to observe noticeable changes in the product quality at high S/B ratios. However, a substantial increase in diluent addition may not be a viable option to improve the deasphalted oil quality

because such an increase in diluent addition will reduce the production capacity and increase the cost of operation.

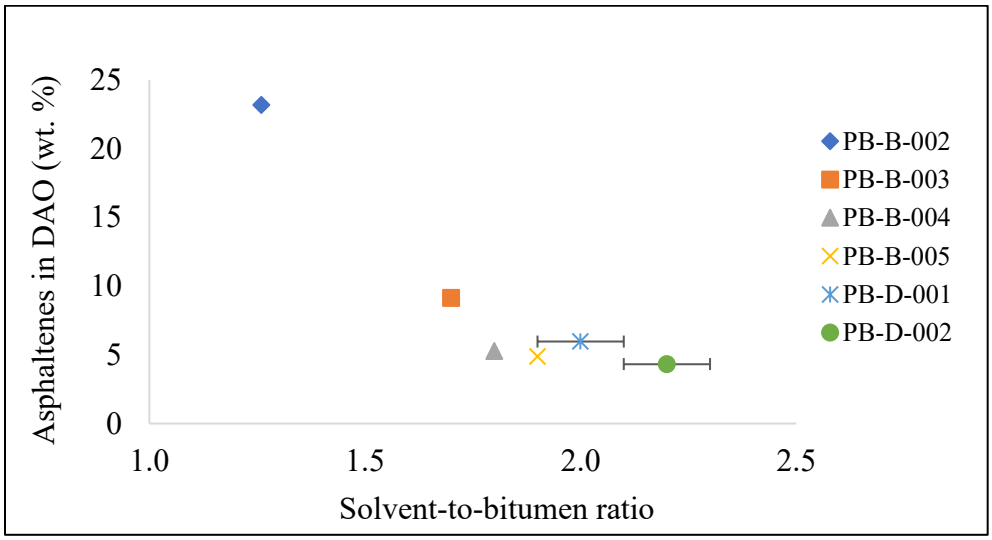

Figure 4. 3. Effects of S/B ratio on the asphaltene content of DAO-60 samples for solvent deasphalting of bitumen emulsions under the operating conditions given in Table 4.1

Despite the considerable decrease in the asphaltene content of the deasphalted oil sample, the remaining asphaltenes fraction still violates the requirements of most refineries.[34] There are three possible options to further minimize the asphaltene content in oil. First, treating bitumen with much lighter hydrocarbons such as propane and butane. It is a firmly established fact that lighter paraffinic solvents precipitate more asphaltenes and reduce the asphaltene content of oil more significantly.[9,44,50,51] Second, employing a very high S/B ratio, possibly three or four times more than the values mentioned in this study, that will increase the contact between the solvent and heavy oil fractions and enable the precipitation of asphaltenes.[30,34] Third, employing a multi-stage solvent deasphalting process. As explained in Section 2.2, injecting solvent in different stages and washing the obtained pitch significantly decreases the asphaltene content of deasphalted oil and improves process efficiency.[61,104]

Of the three options, the first two are very uneconomic and infeasible to be implemented in an industrial-scale plant; therefore, they can only be used in laboratory-scale experiments to obtain high-quality deasphalted oil samples. The third option, however, can readily be implemented to a

commercial-scale solvent deasphalting plant to obtain oil with minimum asphaltenes content. Indeed, it is one of the widely used methods in the petroleum industry for vacuum residue and heavy oil upgrading processes.

4.5 DAO density

This section introduces the density results obtained for the DAO-60 samples and investigates how the density of deasphalted oil changes with an increasing S/B ratio. As the asphaltene content of DAO changes, its physical and chemical properties also change. Since asphaltenes are the heaviest fraction of oil, the density and the average molecular weight of deasphalted oil becomes higher with its increasing asphaltenes content.

Figure 4.4 demonstrates the impact of S/B ratio on the densities of DAO-60 samples. As it can be clearly seen in Figure 4.4, the deasphalted oil density decreases with the increasing diluent amount. The derived results agree with the literature,[105] which states that bitumen treated with a low S/B ratio is denser because of the remaining large asphaltenes fraction compared to the oil treated with a large S/B ratio. The reason for this trend is that most of the asphaltenes cannot be precipitated at low S/B value and heavy oil fractions that remain dissolved inside the deasphalted oil increases both its average molecular weight and density.[105]

At above 1.7 S/B ratio, the density curve flattens and that is where the density of deasphalted oil is very close to that of the light paraffinic solvents, which means no significant asphaltene precipitation is observed with the further addition of diluent. The lower boundary of the attainable oil density is the density of the used precipitant. The average densities of the prepared solvent blends were approximately 0.7 g/ml. From Figure 4.4, it is evident that the DAO density decreases and approaches this value as the loaded solvent mass increases.

Although compared to the bitumen emulsion feed there is a significant density reduction in PB-B-001 and PB-B-002 samples, whereas no pitch was removed from the PB-B-001 run and very little pitch was taken from the PB-B-002 run. Therefore, it is assumed that solvent at low S/B ratios behave as a diluent rather than a precipitant and that is why the density of oil decreases when mixed with light solvents.

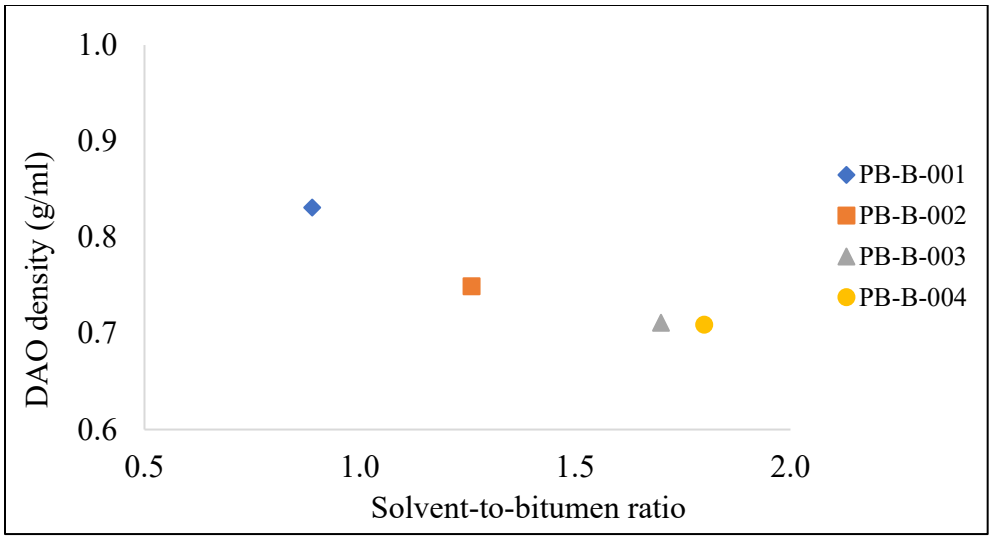

Figure 4. 4. Effects of S/B ratio on the density of DAO-60 samples for solvent deasphalting of bitumen emulsions under the operating conditions given in Table 4.1

4.6 Water content of DAO

As mentioned in Section 3.2.1, the bitumen extracted from the SAGD process contains about 12.5 wt. % emulsified water which is very detrimental to the oil quality and diminishes its product value. In this section, the impact of S/B ratio on the water content of DAO samples will be investigated and the obtained results will be compared to the literature results to date. From the literature,[9,30] it is evident that above the asphaltene precipitation onset, water droplets start to coalesce and precipitate with asphaltene aggregates. Furthermore, the amount of paraffinic solvent significantly affects the coalescence of water droplets and thus the water content of oil.[9]

Figure 4.5 demonstrates the water content of DAO-60 samples retrieved. It is evident from Figure 4.5 that the S/B ratio has a profound impact on the DAO's water content. The bitumen emulsion was fed with an initial water content of about 12.5 wt. % and it dropped below 2 wt. % for every sample studied. Additionally, the water content dropped more than twice when the S/B ratio was increased from 0.9 (PB-B-001) to 1.3 (PB-B-002). When the S/B ratio gets over 2.0, the water content of oil drops below 0.2 wt. % which is a substantial improvement in oil quality.

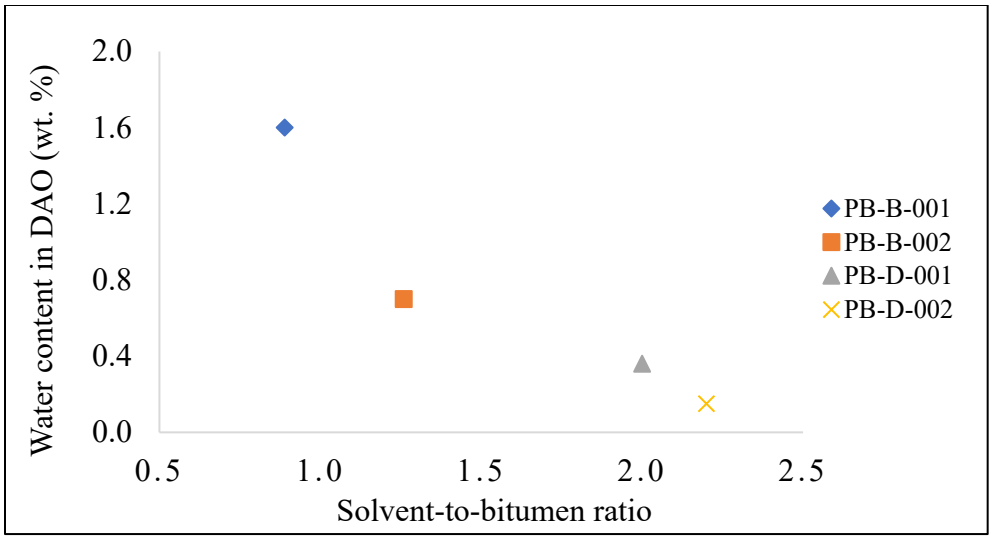

Figure 4. 5. Effects of S/B ratio on the water content of DAO-60 samples for solvent deasphalting of bitumen emulsions under the operating conditions given in Table 4.1

Long et al.[9] states that water removal starts only after the onset of asphaltene precipitation and water is removed within the asphaltene aggregates. Therefore, based on Figure 4.5, despite not observing any pitch formation in the PB-B-001 experiment, asphaltene precipitation had started. However, since the amount of the precipitated asphaltene aggregates was very little, it did not form a separate layer and thus it could not be removed from the reactor as a separate sample. This also implies that the onset of asphaltene precipitation for the prepared solvent batches could be below 0.9. The onset of asphaltene precipitation is the S/B value at which the first asphaltene aggregate precipitation is observed, which is a good method to determine the best precipitant among many available options. However, as demonstrated by the experimental findings, the onset of asphaltene precipitation is not a favourable S/B value for a solvent deasphalting process therefore much higher S/B value is required to precipitate most of the asphaltenes.[9,32]

Since water almost completely can be removed from bitumen emulsion at around an S/B ratio of 2, then the first objective of an industrial-scale SDA process must be separating water and removing a significant portion of it from the process in the initial stages of an SDA process. By means of this, the production capacity of the later stages can be fully harnessed, and the cost of operation can be minimized.

4.7 Conclusions

The conclusions of Chapter 4 can be summarized as follows:

- The onset of asphaltene precipitation for the solvent batches used in this study was below 0.9 S/B ratio. Nevertheless, no pitch sample was recovered at this value because the precipitated asphaltenes mass was little, and it did not form a separate phase in the reactor to be removed as a separate sample.

- Asphaltene precipitation directly depends on the S/B ratio and increasing the S/B ratio gives rise to an increase in the asphaltene aggregate precipitation. Above 1.8, the observed precipitation is much less pronounced, which agrees with the literature that asphaltene precipitation does not proportionally increase with the increasing S/B ratio.

- The operation mode and the solvent injection method have an impact on the composition of the loaded solvent. In other words, the PB-D setup operates in a semi-batch mode and gives rise to more heavy solvent fractions injection into the reactor, which in turn affects the composition of the retrieved products. Nevertheless, it is believed that for a continuous process this issue is a very unlikely scenario.

- It was proven that the asphaltene content of deasphalted oil could be decreased to approximately 5 wt. %. For a laboratory-scale SDA process, the asphaltene content can be further minimized by using a much higher S/B ratio or employing lighter paraffinic solvents such as propane and butane. For a commercial-scale scale SDA process, however, a multistage partial bitumen upgrading plant is a more favourable option.

- Close to the precipitation onset and below that, the solvent acts as a diluent and simply reduces the density and viscosity of bitumen. The density of deasphalted oil sample decreases with increasing S/B ratio and it asymptotically approaches the density of the solvent used.

- Alongside precipitating asphaltenes, paraffinic solvents are also believed to destabilize the water emulsions and promote the coalescence of water droplets. However, the water

removal starts only after the onset of asphaltene precipitation which leads to believe that there is a connection between the initiation of the asphaltene precipitation process and the start of water removal. When the injected solvent amount is just above the onset value of the S/B ratio, more than 95 wt. % of the emulsified water is rejected from bitumen. The emulsified water content can be dropped below 0.2 wt. % at around an S/B ratio of 2, which can be used to remove the majority of emulsified water from the process at early stages of partial upgrading process to harness the maximum capacity of the process units and increase the production rate.

5. Effects of Mixing Conditions on Asphaltene Precipitation

5.1 Introduction

In this chapter, the experimental results obtained under different mixing conditions are introduced, discussed, and compared to the limited literature data available. As explained in Section 2.3.8, the effect of mixing intensity and mixing energy is a point of dispute among many researchers. Therefore, the impact of these parameters will be investigated in terms of the data obtained for the pitch yield and DAO content and then, the obtained results will be compared with the research done on the SDA field to date. To better observe the effect of mixing conditions on the SDA products, the S/B ratio will essentially be kept constant and different combinations of the mixing parameters will be used for each experiment.

5.2 Performed experiments

Here, the experiments performed to study the impact of mixing intensity and mixing energy on the pitch yield and DAO quality are introduced and their respective operating conditions are illustrated. Table 5.1 demonstrates the experiments conducted to investigate the impact of varying mixing conditions on the obtained SDA products. Table 3.5 in Section 3.4 gives a detailed illustration of experimental conditions for the experiments given in Table 5.1. From the discussion in Chapter 4, it is clear that above the S/B ratio of 1.8, a small difference at the S/B ratio does not cause any appreciable change in the SDA product specifications; therefore, the PB-D-001 run was also included to the discussion in this chapter with a slightly higher S/B value. That means, for the experiments given in Table 5.1, any considerable compositional difference in the obtained products can mainly be attributed to the employed mixing conditions.

Overall, five experiments will be analyzed across two different sets of experiments. Two different mixing powers (0.45 and 0.06 W/kg) and four different mixing time lengths (2, 10, 30, and 60 mins) were used to study the solvent deasphalting of the SAGD extracted bitumen emulsion across an energy input range of 0.1 – 1.6 kJ/kg.

Table 5. 1. Experiments performed to study the impact of mixing conditions on asphaltene precipitation

Runs	Pentane equivalent S/B ratio (wt/wt)	Mixing Power (W/kg)	Mixing Time (mins)	Mixing Energy (kJ/kg)
PB-B-005	1.9	0.45	30	0.81
PB-B-006	1.9	0.45	60	1.62
PB-B-007	1.9	0.45	2	0.05
PB-B-008	1.9	0.06	60	0.20
PB-D-001	2.0[a]	0.45	10	0.27

[a] ± 0.1 deviation is applicable for PB-D set experiments, due to the solvent injection method

5.3 Mixing environment

This section aims to shed some light upon the mixing process of the bench-scale solvent deasphalting process. It explains how the mixing process was performed and based on what parameters the completion of mixing was defined. As explained in Section 3.3, a combination of two different impellers (PBT and RT) were used to achieve a well-mixed environment in the reactor. The terms well-mixed, complete mixing, and thorough mixing refer to the same phenomenon in the thesis and indicate the steadiness of the operating parameters and the uniform distribution of the vessel contents.

Figure 5.1 gives a good illustration of the mixing that was performed. The first image (Figure 5.1a) corresponds to the loaded reactor description during 100 RPM mixing. As clearly seen from the figure, although low RPM mixing had continued for about an hour, no noticeable mixing and turbulence was observed for the low RPM speed, which is a good indication of how important the mixing intensity is to achieve a well-mixed solution. Under the low RPM mixing speed about 0.01 kJ/kg energy was added to the system which was substantially low to cause any significant turbulence and aggregation process in the reactor. That means, with low mixing speed, significantly longer mixing time is required to achieve complete mixing. For instance, under 515 RPM mixing speed, 2 minutes of mixing was sufficient to achieve a well-mixed solution; however, under 258 RPM speed, it took over 15 minutes to achieve complete mixing of the reactor contents.

Therefore, depending on the allowed residence time, the optimum mixing speed and therefore the mixing intensity may vary.

Figure 5.1 demonstrates the mixing pattern that was observed for the PB-B-008 run, however, the observed mixing pattern is applicable to all the experiments that were conducted in the current study. In Figure 5.1a, the top impeller is visible at the solvent/water interface at below 45 mm height. Another interesting observation from Figure 5.1a is that only solvent and water is detectable through the window at the operating temperature and pressure. That is because based in Table 3.1, the bitumen has the highest density of all the materials loaded to the reactor and therefore it has settled to the bottom of the reactor.

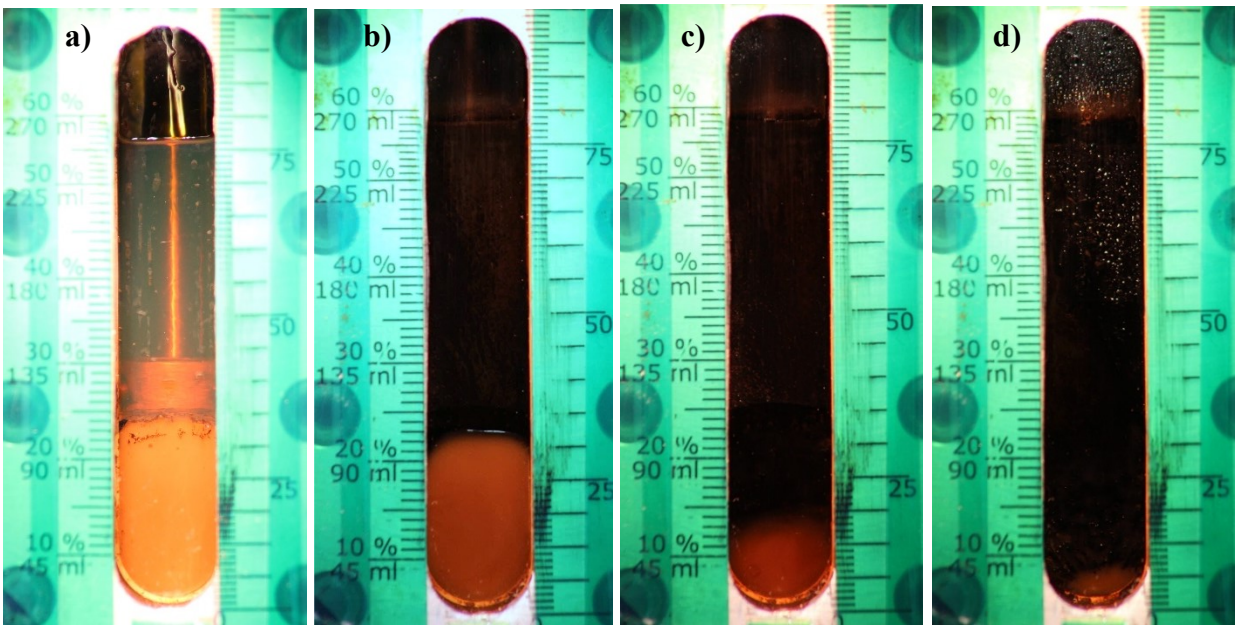

Figure 5. 1. The mixing process observed for the PB-B-008 experiments. From left to right, images illustrate the reactor contents a) 0 min, b) 2 mins, c) 10 mins, and d) 30 mins after the start of 258 RPM mixing process

Figure 5.1b corresponds to the initial few minutes of the high RPM mixing, where the solvent phase, as a result of mixing with bitumen emulsion, gets dark black colour. The difference between Figures 5.1a and 5.1b also illustrates the importance of the mixing intensity. That means, even though no mixing is observed after 1 hr of 100 RPM mixing speed, considerable turbulence has been attained with only 2 mins of mixing at 258 RPM speed. In Figure 5.1c, as the mixing

continues, the water phase gradually disappears and more of the reactor contents is observed as a unit black colour. Finally, Figure 5.1d corresponds to the end of the mixing process, where the reactor contents observed through the window are essentially uniform in its colour and no stationary free water is detected at the bottom of the reactor. The observed pattern in Figure 5.1d is the indication that well-mixed reactor contents have been achieved. The environment given in Figure 5.1d was observed for all the experiments before shutting down the mixer. That is, the mixer was not stopped unless a well-mixed environment has been achieved.

5.4 Pitch yield

This section provides the experimental results and data interpretation for the experiments that were performed to study the impact of the mixing conditions on the pitch yield. As discussed in Section 4.3, the pitch yield is an important parameter to determine the effectiveness of the asphaltene precipitation process. Since the pitch is mainly comprised of asphaltenes, the amount of pitch formed gives a good indication about how much asphaltene has precipitated and how much the DAO quality has improved.

Figure 5.2 demonstrates the trend between pitch yield and mixing time for the constant mixing intensity of 0.45 W/kg. For the given mixing intensity, changing mixing time, and therefore mixing energy, shows no perceptible impact on the obtained pitch yield. For instance, compare the data points for the PB-B-007 and PB-B-006 runs; as a result of increasing mixing energy by 30 times, the pitch yield only increases by about 3 wt. %. Zawala et al.[52] and Cheung[8] stated in their studies that increasing mixing energy leads to an increase in aggregate diameter, and therefore it is expected to increase the formed pitch mass. However, the results do not agree with this deduction. Consequently, it is reasonable to assume that aggregates become larger at the expense of the already formed small aggregates and not because of the rejection of more asphaltenes from bitumen. That is to say, larger aggregates form as a result of the collision between smaller aggregates and this only increases the aggregate precipitation rate not the overall mass of the asphaltenes rejected from the bitumen.[52,53]

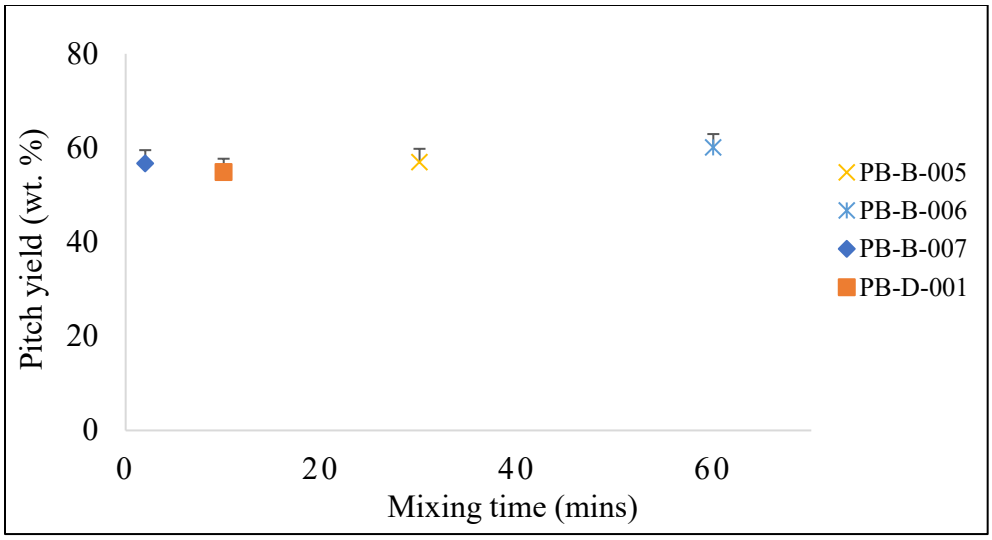

Figure 5. 2. Effects of increasing mixing time on pitch yield for solvent deasphalting of bitumen emulsion under constant mixing intensity of 0.45 W/kg

Figure 5.3 demonstrates the obtained pitch yield results for multiply mixing energy points. From the wide range of mixing energies that have been studied, the pitch yield shows insignificant change with changing mixing energy. For instance, at the constant mixing time (60 mins), increasing mixing intensity from 0.06 (PB-B-008) to 0.45 W/kg (PB-B-006) seems to make an imperceptible difference in the pitch yield. There is diversion between researchers in terms of the interpretation of the effects of mixing intensity on asphaltene aggregates formation. According to Zawala et al.[52] and Casas et al.[53], increasing mixing intensity does not affect the size of the formed aggregates and only increases the density of the asphaltene aggregates which is explained to happen through the entrainment of water and solid particles within the aggregates. According to Rahmani et al.[35] and Cheung[8], increasing mixing intensity leads to a reduction in aggregate size.[35,93,94]

If increasing mixing intensity resulted in a higher aggregate density due to water and solids entrainment, it must have led to a heavier pitch formation and higher pitch yield. Since the obtained pitch yield does not change appreciably, it cannot be justified that aggregates are denser and heavier. However, smaller aggregates formation, as explained by Rahmani et al.[35] and Cheung[8], is more explicable based on the observed experimental results. Small aggregates may form as a result

of the fragmentation of large aggregates that do not change the overall mass of the pitch precipitated.

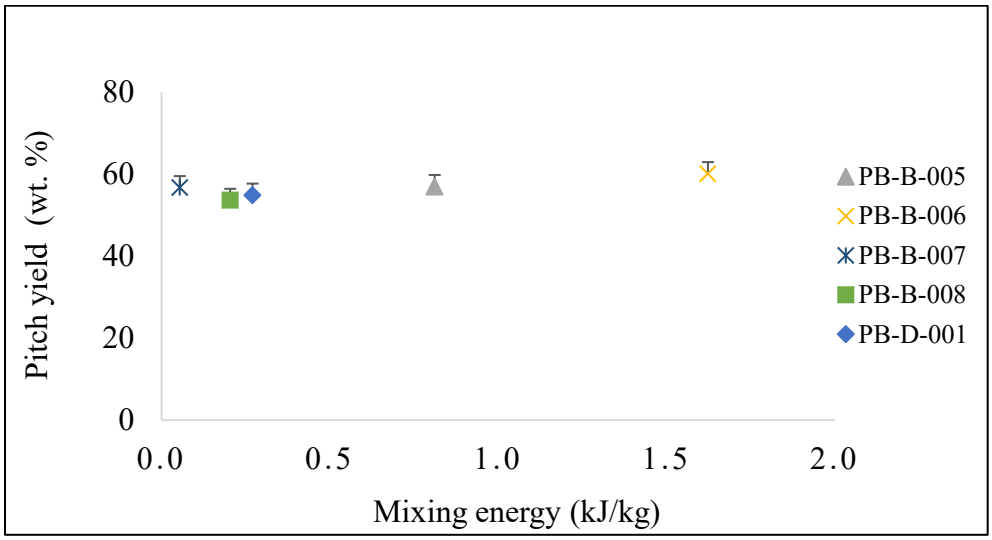

Figure 5. 3. Effects of varying mixing energies on pitch yield for solvent deasphalting of bitumen emulsion. The experimental conditions for each run are provided in Tables 3.5 and 5.1

To summarize, the literature results suggest that changing mixing intensity and mixing energy may lead to a change in aggregate properties and aggregate size. From Figures 5.2 and 5.3, it can be concluded that mixing conditions have an insignificant impact on the overall asphaltene precipitation and pitch yield for the studied mixing range. It is noteworthy that thorough mixing was ensured for each experiment (Figure 5.1d). Therefore, based on the range of the mixing parameter that has been studied, as long as a well-mixed environment has been achieved, any combination of mixing power and mixing energy will lead to essentially the same result in the pitch yield. From a commercial-scale SDA perspective, an optimization point here would be to reduce the length of residence time in the mixer. To be more precise, for most of the experiments in the study, mixing has been performed for 60 minutes; however, from Figure 5.1, it is evident that well-mixed reactor content can be achieved in a much shorter time.

5.5 Asphaltene content of DAO

This section introduces results for the analysis performed on the DAO samples that were taken from the experiments conducted to study the impact of mixing parameters on the SDA process. DAO-10 and DAO-60 are the two samples that were taken to investigate the impact of mixing intensity and mixing energy on the deasphalted oil obtained from the bench-scale solvent deasphalting of bitumen emulsion.

Figures 5.4 and 5.5 demonstrate the asphaltene content analysis results for DAO samples retrieved in the 10^{th} and 60^{th} minutes of the settling process. The asphaltene content results for the DAO samples also agree with the deductions from Section 5.4. In other words, there is little difference in the asphaltene content of the samples taken at different mixing conditions. The only outlier is the DAO-10 test result for PB-B-007 which indicates that the asphaltene content of the sample is just below 4 wt. %; however, that is suspected to be a testing error (Figure 5.4).

Figure 5.5 also illustrates the same trend between the mixing time and the DAO-60 samples' asphaltene content for the same experiments given in Figure 5.4. A higher asphaltene content in DAO-60 of the PB-B-007 run verifies the above deduction that the DAO-10 testing result is not correct. As will be explained in Chapter 6, the asphaltene content of DAO decreases for longer settling time; therefore, for a given SDA experiment, due to the continuous aggregate precipitation, any DAO sample always has less asphaltene content than the preceding DAO sample.

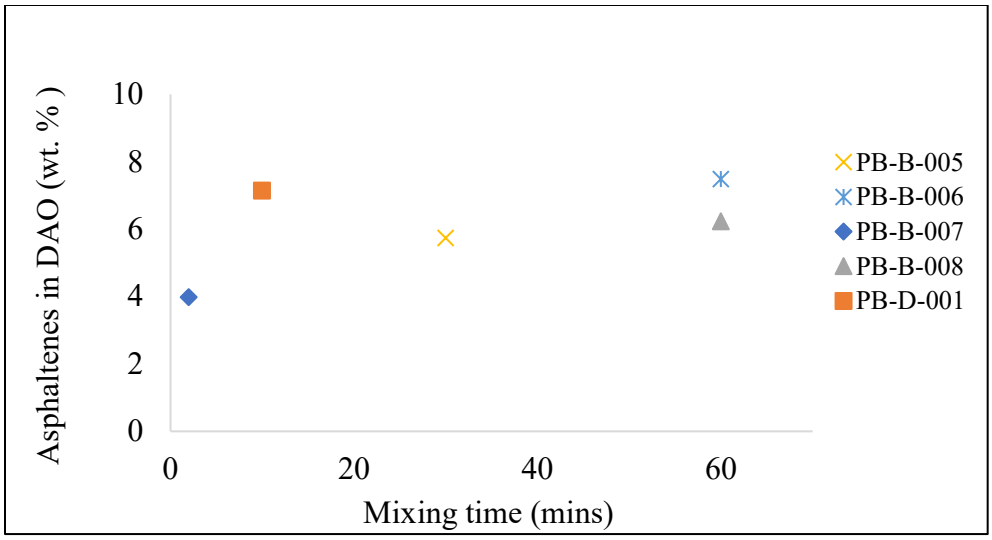

Figure 5. 4. Asphaltene content of DAO-10 samples at varying mixing times and constant mixing intensity. The experimental conditions for each run are given in Tables 3.5 and 5.1

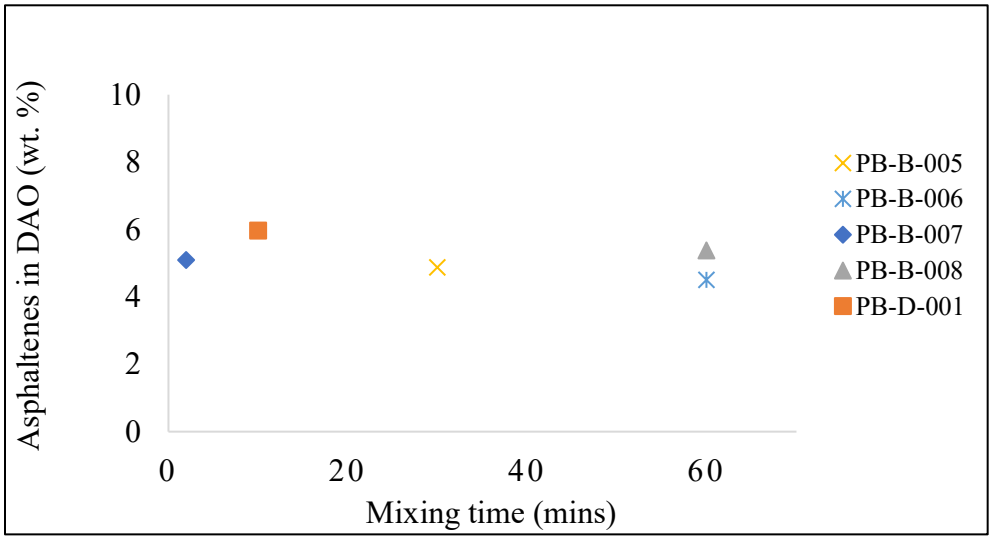

Figure 5. 5. Asphaltene content of DAO-60 samples at varying mixing times and constant mixing intensity. The experimental conditions for each run are given in Tables 3.5 and 5.1

5.6 Conclusions

The main conclusions of Chapter 5 are as follows:

- A well-mixed bitumen emulsion-solvent mixture is essential to increase the efficiency of the solvent deasphalting process. For this study, "well-mixed" was defined as the complete dispersion of water within the mixture and the uniformity in the colour of the obtained reactor contents. Complete mixing can be achieved through either increasing mixing intensity or performing mixing for a sufficiently long duration.

- The impact of mixing parameters on asphaltenes aggregate properties and size are unclear and conflicting; However, both pitch yield and DAO sample results revealed that as long as a well-mixed environment has been achieved, the mixing intensity and mixing energy do not have an appreciable impact on the asphaltene removal from bitumen, for the studied range of mixing conditions. Since no noticeable change was detected on the SDA product specifications by varying mixing parameters, it is assumed that the observed changes in the aggregate properties and the change in aggregate diameter that were reported by other researchers are a consequence of aggregation/fragmentation among the existing small aggregates and not because of the removal of more asphaltenes from bitumen.

- For a commercial-scale solvent deasphalting process, short residence time in the mixer is favourable because it will increase the production rate and improve the process economics. It can be achieved by employing a high mixing intensity that provides the system with sufficient mixing in a short duration.

6. Settling of Asphaltene Aggregates

6.1 Introduction

This chapter introduces and explains the results for the asphaltene aggregates precipitation in terms of the asphaltene content of DAO samples. Based on the images of the settling process, the asphaltene aggregates settling trend is determined, the average aggregate settling rate is calculated for each experiment, and the effects of experimental conditions on aggregates settling process are elaborated. Additionally, the analysis results of the DAO samples taken at different settling times are used to evaluate the optimum residence time in the settler and investigate the asphaltene aggregates settling after the complete phase separation. Finally, the implications of these results to a commercial-scale solvent deasphalting process are discussed.

6.2 Aggregate settling rate

Here, the aggregates settling process is described and the calculation results for aggregates settling rate in terms of the recorded settling process are provided. As mentioned in Section 3.9, the settling rate of asphaltene aggregates was performed based on the zone settling method, where the change in interface level is recorded over time in order to estimate the average aggregate settling rate.

Figure 6.1 demonstrates the settling dynamics observed for the PB-B-004 experiment for the initial 2 minutes of the settling process. The illustrated settling trend is applicable to all the experiments conducted in the study. The reactor window is calibrated on both sides. The calibration on the left-hand side corresponds to the volume (ml) from the bottom of the vessel and on the right-hand side corresponds to the height (mm) from the bottom of the vessel.

Time zero in Figure 6.1a corresponds to the moment of shutting down the mixer, immediately after which the settling of the asphaltene aggregates starts. Although care was taken to illuminate the inside of the reactor with two flashlights as much as possible, the taken photos are still mostly opaque and provide limited insight on the settling dynamics. Only the water level can explicitly be detected because of the sharp colour differences between the water and DAO phases. Since both DAO and asphaltene aggregates are black and non-transparent, it is challenging to track individual aggregates within the DAO phase and calculate the settling rate for the individual aggregates.

Therefore, the water level was taken as the main reference to track the phase separation, and from which the average aggregate settling rate was calculated.

In Figure 6.1a, no phase separation is observed. As the settling continues, initially, the rising water level is detected. 25 seconds after the start of the settling process, the water level is at 15 mm height (Figure 6.1b) and it is not increasing evenly across the window. From Figure 6.1c, it is more evident that the water level has started to increase unevenly and that is because aggregates have settled and occupied some of the space on top of the water phase; consequently, the creeping water can only fill the pores in the pitch and cause an uneven increase in the water level across the window. The last settling image (Figure 6.1d) demonstrates that pitch is on top of the water phase, however, pores of the pitch have totally been occupied by water, and thus the region between 15 – 30 mm looks like a mixture of water and pitch.

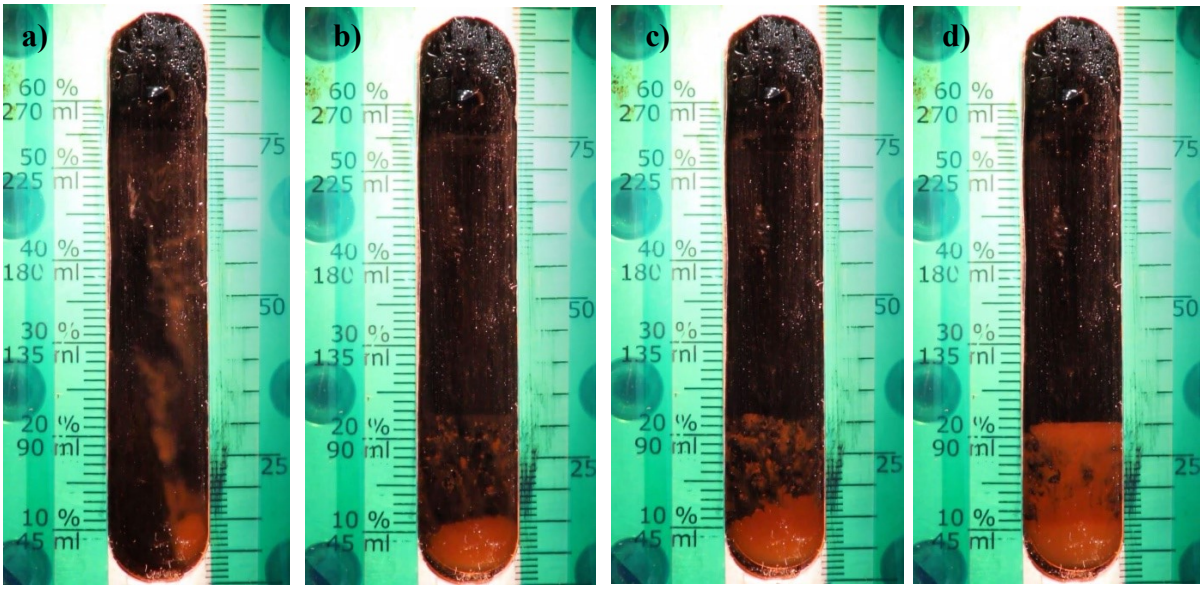

Figure 6. 1. Aggregate settling process for the PB-B-004 run under the operating temperature and pressure of 164 ℃ and 41 bar. From left to right, images have been taken a) 0 s, b) 25 s, c) 60 s, and d) 120 s from the start of the settling process

It is critical to note that the levels of the interfaces were tracked based on the water phase. For instance, the levels of all three phases can be evaluated from Figure 6.1 by simply observing the water phase. From Figure 6.1b, the water level is at about 15 mm height because that is up to where

the water phase is observed as an undisturbed uniform orange colour. From Figure 6.1d it is evident that the pitch layer is between 15 – 30 mm height because between these heights the colour of the water becomes slightly red and the dark spots are observed because of the presence of the pitch. It is assumed that all the fluid above 30 mm height is practically DAO because of the sharp and smooth interface between the water and DAO phases.

While in Figure 6.1d the DAO/water interface can clearly be detected at 30 mm height, the same interface was also slightly visible in Figure 6.1b too and as water filled the pores, the settling images became much sharper. Therefore, it could be inferred that aggregate settling had already been finalized in the first 25 seconds of the settling process (Figure 6.1b). In some experiments, the pitch level was completely indistinguishable from the DAO phase; therefore, stabilization of water level was important to define the aggregate settling time, which led to errors in aggregates settling rate calculations.

It is noteworthy that the observed DAO/water interface is not an indication of the termination of the aggregates settling process. Small aggregates may take much longer time to settle which cannot be detected from the settling images. To verify this argument, DAO samples at different settling times have been taken to analyze their asphaltenes content. Based on the asphaltene content of DAO samples taken at different settling times, it will be determined whether the settling of asphaltene aggregates continues even after the complete phase separation.

From Figure 6.1, it is also observed that continuous evaporation and condensation of light solvent fractions give rise to mist formation on the window above the DAO phase at around 80 mm height (or 270 ml). This may happen due to the small disturbances in the pressure and temperature of the system during the settling process.

Figure 6.2 illustrates how the asphaltene aggregates settling rate was calculated using the zone settling method. The Y-axis corresponds to the height of the fluid level and the X-axis is the time length that settling of asphaltene aggregates was studied or. As demonstrated in the legend of Figure 6.2, three fluid levels were tracked for each experiment: top (top of the overall mixture inside the reactor), DAO bottom (bottom level of the DAO phase), and water top (top level of the water phase). From the calibration in Figure 6.1 on the right-hand side of the window, it is evident

that the minimum observable liquid height through the window is 5 mm (or 45 ml), and thus the water level could only be tracked from that level upward. Also, in all the aggregate settling graphs, the water level starts from 5 mm height. As explained in Section 3.9, since the individual aggregate settling could not be tracked, it was assumed that aggregate settling starts from the very top of the solution in the reactor; consequently, the settling distance of aggregates was assumed to be from the top of the overall liquid level to the bottom of the DAO phase.

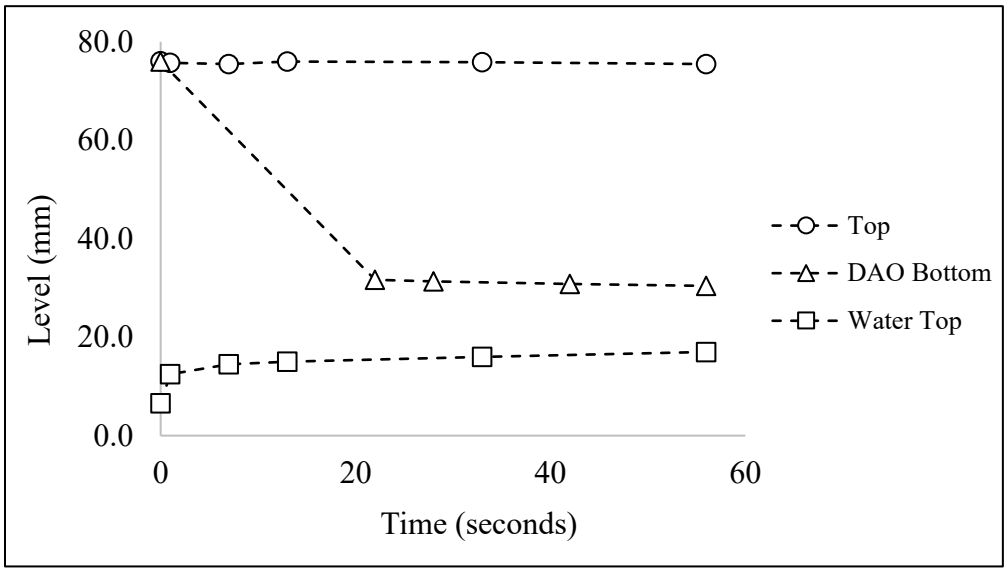

Figure 6. 2. Asphaltene aggregates settling trend for the PB-B-004 run based on the zone settling method. The experiment was performed under the conditions provided in Table 3.5

From Figure 6.2, it is evident that more interface readings have been taken for the water level compared to the DAO level. That is because the water phase is more visible through the window and easier to track, which can clearly be seen in Figure 6.1. Therefore, calculations of the aggregates settling rate are mainly based on the change in the water level, and the accuracy of the results depends on how clearly the interface can be detected. Moreover, these calculations are only valid for the large aggregates settling and it is believed that aggregate settling continues for small aggregates, even after observable interface formations. Therefore, the sharp interface formations are referred to as the end of the observable settling process.

Long et al.[64] studied aggregate settling for solvent diluted bitumen streams. They calculated that at an S/B ratio of 2 and a mixing temperature of 30 ℃, the aggregates settling rate is 23.6 mm/min.

The paper also states that aggregate settling significantly depends upon the operating temperature; consequently, the aggregates settling rate reaches 97 mm/min at the mixing temperature of 100 ℃.[64]

As discussed in Section 2.3.1, the aggregation of asphaltene particles increases and the viscosity of the medium decreases with increasing operating temperature, both of which facilitate the aggregates settling process.[52,53] It is also evident From Table 3.1 that the viscosity of the bitumen employed for the current study drops about an order of magnitude as the temperature rises from 100 ℃ to 160 ℃. Therefore, considering that the operating temperature of the current study (164 ℃) is much higher than the one employed by Long et al.[64], it is anticipated that a higher aggregate settling rate will be obtained. Even though the calculated average aggregate settling rate (120 mm/min) for the PB-B-004 run that is described in Figure 6.2 is slightly higher than the results obtained by Long et al.[64], it is significantly lower than the predicted result. In other words, such a substantial drop in bitumen viscosity with increasing temperature was expected to be accompanied by a corresponding rise in aggregates settling rate. Nevertheless, it is believed that this is a consequence of uncertainties in the interface detection and the method that aggregates settling rate was calculated.

The results of the performed experiments show that the main aggregate settling takes place within the initial few minutes of the settling process; however, for some experiments, a longer duration was required to explicitly detect the DAO/water interface, which led to erroneous settling rate calculation results. In addition, since similar results were observed in terms of the settling trend of all the experiments, the figures for the remaining experiments will be provided in Appendix C.

Table 6.1 demonstrates the aggregate setting rate and the essential operating conditions for all the performed experiments. For the first three experiments, the aggregate settling rate has been omitted, due to the fact that no pitch was retrieved in these runs. Different S/B ratios and mixing conditions seem not to affect the aggregates settling process in an explicable manner. For instance, for the same mixing conditions and essentially the same S/B ratio, the aggregate settling rate appears to decrease 4 times from PB-B-004 to PB-B-006 run, which is very irrational and implies that aggregates settling may have finished before the phase separation was complete. Therefore, it

can be concluded that taking phase separation as the reference point leads to an underestimate in the aggregates settling rate.

Table 6. 1. Average aggregate settling rate calculated based on the zone settling method

Runs	Pentane equivalent S/B ratio (wt/wt)	Mixing time (mins)	Mixing energy (kJ/kg)	Average aggregate settling rate (mm/min)
PB-A-001	0.9	60	1.62	-
PB-A-002	0.9	60	1.62	-
PB-B-001	0.9	60	1.62	-
PB-B-002	1.3	60	1.62	30
PB-B-003	1.7	60	1.62	40
PB-B-004	1.8	60	1.62	120
PB-B-005	1.9	30	0.81	20
PB-B-006	1.9	60	1.62	30
PB-B-007	1.9	2	0.05	20
PB-B-008	1.9	60	0.02	90
PB-D-001	2.0	10	0.27	50
PB-D-002	2.2	30	0.81	60

From a pilot-scale SDA plant standpoint, a high aggregate settling rate is important and according to Zawala et al.[52], the aggregate settling rate for a pilot-scale process is in a range of 600 – 900 mm/min, which is about an order of magnitude greater than the results obtained in this study. However, the results obtained for bench-scale and pilot-scale experiments also show some inconsistencies in their study. For the bench-scale experiments, they also observed a significantly low aggregate settling rate that ranged between 50 – 700 mm/min, based on the individual aggregate settling rates that were calculated by extracting some asphaltene aggregate samples from the reactor and observing their settling in a separate transparent column filled with diluent. Besides, there is a standard deviation of more than ± 100 mm/min involved with most of the aggregates settling rate results. Therefore, based on the literature[52] and the experimental results of the current study, it can be inferred that the bench-scale SDA experiments seem to underestimate

the settling rate by about an order of magnitude. However, despite the underestimates in the bench-scale aggregate settling rate results, they are good reference points and suggest that a much higher aggregate settling rates will be observed for a pilot-scale solvent deasphalting process.

6.3 Effects of settling time on DAO quality

This section explains the significance of the settling time on the asphaltene content of DAO samples. Three DAO samples taken 10 mins, 60 mins, and 24 hrs after the start of the settling process will be analyzed to determine the impact of settling time on the DAO quality. Depending on the size and physical properties of the aggregates, they may settle at different rates and their settling rates define the quality of the deasphalted oil and feasibility of the SDA process. Therefore, the impact of settling time on the DAO quality will be investigated and its potential implications to the SDA process will be clarified.

Figure 6.3 demonstrates the trend for the asphaltene aggregates settling over time, on a logarithmic scale. The ordinate of the graph corresponds to the asphaltene content (wt. %) of deasphalted oil and the abscissa corresponds to the settling time. Five experiments have been performed to study the impact of settling time on the asphaltene content of the DAO samples. Recall from Section 3.2.1 that the bitumen feed used for all the experiments contains 20.2 wt. % asphaltenes. It is evident from the graph that with longer settling time the asphaltene content of DAO decreases, which means that aggregates precipitation continues after both DAO-10 and DAO-60 sampling processes. Furthermore, in all the cases, asphaltene content drops below 8 wt. % just after 10 minutes of the settling time which corresponds to more than 60 wt. % asphaltenes removal from the bitumen.

Excluding DAO-10 of the PB-B-007 run, all the results follow the same decreasing asphaltene content trend with longer settling time. From the obtained results, it can be inferred that primary aggregate settling takes place at the initial 10 minutes of the settling time. Even though longer settling time leads to a cleaner and better quality deasphalted oil, whereas the change in the asphaltene content of the DAO samples is insignificant compared to the time allowed for the settling. For instance, from the analysis results of the PB-B-006 experiment, it is clear that even though there is about 3 wt. % drop in asphaltene content from DAO-10 to DAO-60, whereas only

about 0.5 wt. % decrease in asphaltene content is observed from DAO-60 to DAO-24. That means, 50 minutes of settling time gave rise to 6 times more asphaltene aggregate precipitation than the succeeding 23 hours of settling time.

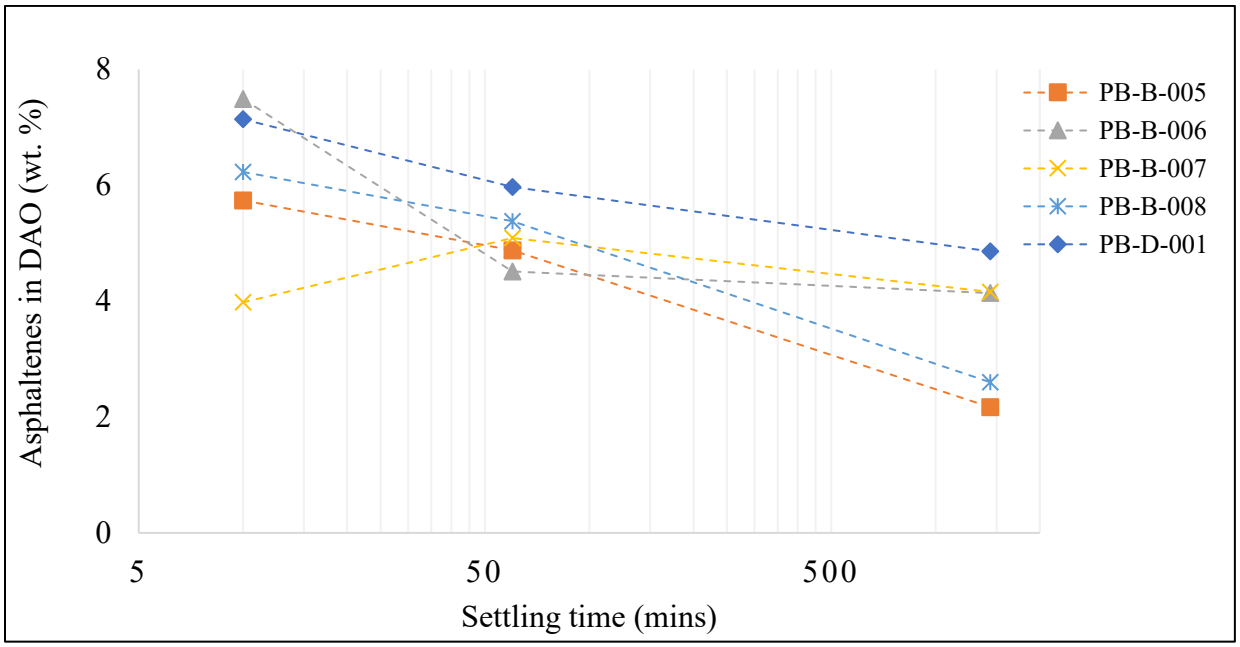

Figure 6. 3. Asphaltene content of deasphalted oil at different settling times. For each experiment three DAO samples have been taken: DAO-10, DAO-60, and DAO-24

From a commercial plant perspective, it may be inefficient and unprofitable to allow settling to take place for 24 hours or longer just to achieve a small improvement in the deasphalted oil quality because longer settling time requires significantly larger settling vessels that will result in a higher capital cost. Besides, even after 24 hours of the allowed settling time, there is about 4 wt. % asphaltenes remaining in DAO. Thus, as proposed in Section 4.4, a multistage solvent deasphalting process has to be used to minimize the time spent for the settling, and thus, to increase deasphalted oil quality and improve the overall process efficiency.

6.4 Conclusions

The main conclusions of Chapter 6 can be summarized as follows:

- Aggregate settling calculations were performed in terms of the zone settling model and it was found that the reliability of the results strictly depends on the visibility of the DAO/water interface through the reactor window and the accuracy in detecting the interface heights. Due to the challenges in tracking the DAO interface for the whole length of settling time, the instantaneous aggregates settling rate could not be calculated and only the average asphaltene aggregate settling rate was determined. It was revealed that the aggregate settling rate based on the phase separation can lead to underestimations.

- It was proved that the aggregate settling rate is a function of temperature and the increasing temperature gives rise to an increase in aggregates settling rate. For the bench-scale and pilot-scale experiments, substantially different aggregate settling rates can be obtained that may differ by an order of magnitude. Furthermore, in both bench-scale and pilot-scale processes, the aggregate settling rate results involve significant standard deviations due to the uncertainties associated with determining asphaltene aggregates properties and calculating the aggregates settling rate.

- For a given experiment, several DAO samples were taken at different settling times and each DAO sample had more asphaltenes and water content than the succeeding sample which indicates that aggregates settling continues even after the phase separation is over.

- The DAO obtained with longer settling time is slightly cleaner and has higher quality. Since the asphaltene content of deasphalted oil decreases approximately 2 wt. % with an additional 23 hours of settling time, for a commercial-scale plant it would be uneconomic to allow settling to take place for so long to attain such a small product advancement. Therefore, a multistage SDA process is believed to be a better alternative to minimize the settling time and improve process economics.

7. Conclusions and Recommendations for Future Work

7.1 Introduction

The main conclusions of the study are summarized in this chapter. It explains the objectives that were met within this study and what are the implications of them for the SDA process in both laboratory-scale and commercial-scale operations. The significance of this study to the solvent deasphalting process is explained and the major contributions are laid out. It also provides critical ideas and directions for the further improvement of the solvent deasphalting process.

7.2 Conclusions

There is a critical S/B ratio at which the asphaltene precipitation is first detected and this is referred to as the onset of asphaltene precipitation. Below which, any amount of solvent acts merely as a diluent and does not cause any asphaltene aggregation or precipitation. The precipitation onset depends on the solvent nature and solvent molecular weight. For the studied solvent blends, this critical value was determined to be just below 0.9.

Above the onset of asphaltene precipitation, small increments in S/B ratio give rise to significant asphaltene rejection from bitumen; however, at high enough values of S/B, significant jumps in S/B ratio is required in order to observe noticeable changes in pitch yield and asphaltene content of DAO.

Although paraffinic solvents also have an impact on the emulsified water content of bitumen, it is unclear whether water removal and asphaltene precipitation are interdependent. The water removal also appears to start at the asphaltene precipitation onset, which raises the question of whether asphaltene precipitation is a pre-condition for the destabilization of the emulsified water droplets or this is merely a simultaneous co-occurrence of two events. It was determined that the emulsified water content in bitumen emulsion can be minimized down to trace amounts as a result of the solvent deasphalting of bitumen emulsion.

The composition of the solvent employed has an enormous impact on the retrieved sample's asphaltene and solvent content. Since light paraffinic solvents are superior to heavy paraffinic solvents in regard to asphaltene precipitation capacity, a solvent that contains mostly light

hydrocarbons will lead to a deasphalted oil containing fewer asphaltenes compared to a solvent that has relatively heavier hydrocarbons.

A well-mixed bitumen emulsion and solvent mixture has to be achieved for an efficient solvent deasphalting process. For the studied mixing parameters range, it was determined that as long as a well-mixed environment has been achieved, mixing intensity and mixing energy do not have a significant impact on pitch yield and asphaltene content of DAO samples. However, based on the literature, the mixing conditions are believed to affect the aggregate properties and size which in turn affects the aggregates settling rate. Moreover, the residence time in the mixer is considered to be an optimization point for a commercial-scale solvent deasphalting process. That means, with sufficiently high mixing intensity the required mixing time can drastically be reduced that will lead to an increased production rate and improved process profitability.

Aggregate settling rate calculations were performed based on the rising water level. The stabilized water level was accepted as an estimation of the required time for aggregate settling. Due to the challenges in detecting the DAO interface at the beginning of the settling process, the instantaneous aggregate settling rate could not be calculated. Thus, only the average aggregate settling rate was estimated for the experiments. Aggregate settling calculations based on the zone settling method indicate that the obtained aggregate settling rate (120 mm/min) may not be applicable to a pilot-scale SDA process, due to the slow aggregate settling rate. However, it is also believed that bench-scale aggregate settling calculations may underestimate results for larger-scale processes.

The settling images show that phase separation takes place within the first few minutes of the allowed settling time. Nevertheless, the analyses of DAO samples taken at different settling times indicate that aggregate settling continues for a much longer time than the phase separation due to the presence of small aggregates. However, from an industrial process point of view, longer settling time implies a larger settling vessel to keep up with the production capacity, which will be accompanied by higher capital costs. Thus, there is a trade-off to be made between the required product quality and the cost of production. Furthermore, it is believed that a multistage solvent deasphalting process will considerably improve the process efficiency and minimize the deasphalted oil quality.

7.3 Implications for the design of future SDA pilots

In a single-stage solvent deasphalting process, a high S/B ratio and long settling time have to be employed in order to obtain a deasphalted oil with high purity. Therefore, the feasibility of a multistage solvent deasphalting process has to be assessed. A multistage solvent deasphalting process will minimize the diluent requirement and also reduce the residence time in the settler. In addition, asphaltene precipitation does not proportionally increase with the addition of more diluent that is why the optimum S/B value has to be determined and employed for a given solvent deasphalting process. For this study, the optimum value was approximately 1.8, above which asphaltene precipitation still occurs, however, the asphaltene precipitation rate drops significantly.

The operating temperature used in the study seems to give desirable results in terms of the asphaltene precipitation. Based on the literature (Figure 2.3), a sufficiently high temperature reduces the solubility of asphaltenes which means an even higher temperature than the one employed in this study can be investigated to minimize the solvent requirement and increase the production capacity. However, a detailed evaluation of each process parameter has to be performed to ensure that changing one variable does not compromise the safety and feasibility of the overall partial upgrading process. Furthermore, as long as thorough mixing of bitumen emulsion and solvent mixture has been achieved, mixing intensity and mixing energy do not have an appreciable impact on either the pitch formation or the asphaltene content of deasphalted oil; therefore, as high mixing intensity as physically possible can be employed to minimize the residence time in the mixer and increase the production rate.

7.4 Significant contributions of this study

It was verified that the amount of solvent has a substantial impact on asphaltene aggregate formation and DAO quality, and this impact is not always proportional to the mass of solvent; therefore, the optimum S/B ratio has to be evaluated for each SDA process. Depending on the solvent mass, the solvent may act as a diluent or a precipitant. To be more precise, below the onset of asphaltene precipitation solvent acts as a diluent, and thus a high enough S/B ratio has to be used in order to precipitate asphaltenes. Additionally, it was proven that a one-stage solvent deasphalting process has limitations in terms of the DAO quality that can be attained, which may reduce the profitability of the SDA process significantly.

Based on the observed results, it can be stated that mixing conditions do not affect the product specifications, provided that a well-mixed environment has been achieved. Thus, low residence time can be employed with a high mixing intensity so as to increase the production rate and process economics. Moreover, it was also demonstrated that settling time must also be optimized for a pilot-scale process because long settling time does not seem to benefit the DAO quality appreciably therefore the residence time in the settler can greatly be reduced to improve the process viability.

It was revealed that through the solvent deasphalting process emulsified water content in bitumen can be reduced to almost 0 wt. %. Additionally, since the emulsified water can readily be separated from bitumen with paraffinic solvent treatment, it is favourable to separate and remove a significant portion of the water in the early stages of the SDA process in order to fully harness the capacity of the process units.

7.5 Future work

Using the solubility model approach in Section 2.3.4, different classes of hydrocarbons can be studied to test their abilities on the asphaltene precipitation. Additionally, there exist more advanced models to theoretically assess the precipitant capability of organic solvents and those models can be utilized to determine a range of solvents that can be employed for a pilot-scale process and then through experimental methods the best option can be identified. Mixtures with certain hydrocarbon ratios can be used to make a new and superior blend that will reject asphaltenes and water from heavy oils more effectively.

New techniques and methods should be developed to be able to study aggregate properties and individual aggregate settling rate. This can be done by taking small aggregate samples and investigating their properties. Also, in glass reactors, the hindered settling rate of the asphaltene aggregates can be studied more effectively under intense light. Multiple DAO samples can be taken to narrow down the optimum settling duration to reduce the production time and increase the efficiency of the partial upgrading process.

Based on the literature results, the impact of mixing conditions on asphaltene aggregates settling rate and aggregate properties is uncertain. A wide range of mixing intensity and mixing energy

can be studied to draw a more comprehensive conclusion about the impact of mixing parameters on the aggregate settling rate, pitch yield, and DAO quality. In this study, aggregate properties were not investigated; however, the researches performed to date imply that the aggregate properties and diameter strongly depend on the mixing intensity and mixing energy. Consequently, the aggregate settling rate may be impacted by the mixing conditions, which in turn will affect the DAO quality and the optimum residence time in the settler. Taking DAO samples under different mixing conditions and studying both aggregate properties and the aggregate settling rate will shed some light upon the importance of the mixing intensity and mixing energy on the asphaltenes removal process.

The relationship between the water removal and the asphaltene precipitation can be studied for a wide range of solvent types in small transparent reactors to find out how a solvent affects the molecular stability of both compounds. Under different operating conditions the onset of asphaltene precipitation can be studied and it can be determined whether in all the cases water removal follows the asphaltene precipitation or it may occur sooner than the asphaltene precipitation.

References

1. Bentley, R. W. Global oil and gas depletion: An overview. Energy Policy **30**, 189–205 (2002).
2. Hallock, J. L., Wu, W., Hall, C. A. S. & Jefferson, M. Forecasting the limits to the availability and diversity of global conventional oil supply: Validation. Energy **64**, 130–153 (2014).
3. Colyar, J. Has the time for partial upgrading of heavy oil and bitumen arrived? Petrol. technol. quart. (2009).
4. Qi, Z. Microfluidic and Nanofluidic Study of Solvent-based Unconventional Hydrocarbon Processes. (University of Toronto, 2019).
5. Curley, M. Effects of Cyclical Load Conditions on Wear Rate and Wear Scar in a Modified ASTM G65 Abrasion Test. (University of Alberta, 2016).
6. Stringham, G. Energy Developments in Canada's Oil Sands. Alberta Oil Sands Energy, Ind. Environ. **11**, 19–34 (2012).
7. Masliyah, J. H., Czarnecki, J. & Xu, Z. Handbook on theory and practice of bitumen recovery from Athabasca oil sands, Volume I: Theoretical basis. (Kingsley Knowledge Publishing, 2011).
8. Cheung, A. EFFECTS OF MIXING ON SOLVENT ADDITION TREATMENT PROCESSES. (University of Alberta, 2019).
9. Long, Y., Dabros, T. & Hamza, H. Selective Solvent Deasphalting for Heavy Oil Emulsion Treatment. in Asphaltenes, Heavy Oils, and Petroleomics (eds. Mullins, O. C., Sheu, E. Y., Hammami, A. & Marshall, A. G.) 511–547 (Springer New York, 2007).
10. Czarnecki, J., Masliyah, J. H., Xu, Z. & Dabros, M. Handbook on Theory and Practice of Bitumen Recovery from Athabasca Oil Sands Volume II: Industrial Practice. vol. II (Kingsley Knowledge Publishing, 2013).
11. Söderbergh, B., Robelius, F. & Aleklett, K. A crash programme scenario for the Canadian oil sands industry. Energy Policy **35**, 1931–1947 (2007).
12. Engelhardt, R. & Todirescu, M. An introduction to development in Alberta's oil sands. (2005).
13. Wang, Z., Gao, D., Diao, B. & Zhang, W. The influence of casing properties on performance of radio frequency heating for oil sands recovery. Appl. Energy **261**, (2020).
14. Chindo, M. Environmental risks associated with developing oil sands in southwestern Nigeria. Singap. J. Trop. Geogr. **36**, 3–22 (2015).
15. Samsonov, S. V., Czarnogorska, M. & Charbonneau, F. Selecting Optimal RADARSAT Constellation Mission Beams for Monitoring Ground Deformation in Alberta's Oil Sands.

Can. J. Remote Sens. **41**, 390–400 (2015).

16. Banerjee, D. K. Oil sands, heavy oil & bitumen: from recovery to refinery. (PennWell Books, 2012).

17. Yeh, S. et al. Land use greenhouse gas emissions from conventional oil production and oil sands. Environ. Sci. Technol. **44**, 8766–8772 (2010).

18. Shah, A. et al. A review of novel techniques for heavy oil and bitumen extraction and upgrading. Energy and Environmental Science vol. 3 700–714 (2010).

19. Nenniger, J. Methods and apparatuses for SAGD hydrocarbon production. U.S. Patent 8596357B2. (2013).

20. Chung, T., Bae, W., Lee, J., Lee, W. & Jung, B. A Review of Practical Experience and Management of the SAGD Process for Oil Sands Development. Energy Sources, Part A Recover. Util. Environ. Eff. **34**, 219–226 (2011).

21. Kawaguchi, H., Li, Z., Masuda, Y., Sato, K. & Nakagawa, H. Dissolved organic compounds in reused process water for steam-assisted gravity drainage oil sands extraction. Water Res. **46**, 5566–5574 (2012).

22. Kumasaka, J., Sasaki, K., Sugai, Y., Alade, O. S. & Nakano, M. Measurement of Viscosity Alteration for Emulsion and Numerical Simulation on Bitumen Production by SAGD Considering In-situ Emulsification. J. Earth Sci. Eng. **6**, 10–17 (2016).

23. Strausz, O. P. & Lown, E. M. The Chemistry ofAlberta Oil Sands, Bitumens and Heavy Oils. (Alberta Energy Research Institute, 2003).

24. Santos, R. G., Loh, W., Bannwart, A. C. & Trevisan, O. V. An overview of heavy oil properties and its recovery and transportation methods. Braz. J. Chem. Eng. **31**, 571–590 (2014).

25. Mochinaga, H. et al. Properties of Oil Sands and Bitumen in Athabasca. (2015).

26. Mullins, O., Sheu, E., Hammami, A. & Marshall, A. Asphaltenes, heavy oils, and petroleomics. (Springer, 2007).

27. Mehrotra, A. K. & Svrcek, W. Y. Viscosity of compressed athabasca bitumen. Can. J. Chem. Eng. **64**, 844–847 (1986).

28. Robinson, L. H. & Garcia, J. Drillers Knowledge Book: Creative Solutions for Today's Drilling Challenges. (International Association of Drilling Contractors (IADC), 2015).

29. Speight, J. G. Handbook of Petroleum Analysis. Wiley-Interscience (2001).

30. Yeung, C. K. System for the decontamination of asphaltic heavy oil and bitumen. U.S. Patent 7.625,466 B2. (2009).

31. Gray, M. R., Zhao, Y., McKnight, C. M., Komar, D. A. & Carruthers, J. D. Coking of hydroprocessing catalyst by residue fractions of bitumen. Energy and Fuels **13**, 1037–1045 (1999).

32. Soleymanzadeh, A., Yousefi, M., Kord, S. & Mohammadzadeh, O. A review on methods of determining onset of asphaltene precipitation. J. Pet. Explor. Prod. Technol. **9**, 1375–1396 (2019).

33. Subramanian, S., Simon, S. & Sjöblom, J. Asphaltene Precipitation Models: A Review. J. Dispers. Sci. Technol. **37**, 1027–1049 (2016).

34. Zhao, Y. & Wei, F. Simultaneous removal of asphaltenes and water from water-in-bitumen emulsion. I. Fundamental development. Fuel Process. Technol. **89**, 941–948 (2008).

35. Rahmani, N. H. G., Masliyah, J. H. & Dabros, T. Characterization of asphaltenes aggregation and fragmentation in a shear field. AIChE J. **49**, 1645–1655 (2003).

36. Gray, M. R. Upgrading oilsands bitumen and heavy oil. (University of Alberta Press, 2015).

37. Gray, M. R. Fundamentals of Partial Upgrading of Bitumen. Energy & Fuels (2019).

38. Fukuyama, H., Nakamura, T. & Ikeda, A. Partial upgrading of bitumen at SAGD wellsite. in Canadian Unconventional Resources and International Petroleum Conference vol. 1 274–285 (2010).

39. Klerk, A. De, Reques, N. G. Z., Xia, Y. & Omer, A. A. Integrated central processing facility (CPF) in oil field upgrading (OFU). U.S. Patent 9,650,578 B2. Google Patents (2017).

40. Zachariah, A. & De Klerk, A. Partial upgrading of bitumen: Impact of solvent deasphalting and visbreaking sequence. Energy & Fuels (2017).

41. Wiehe, I. A. Process chemistry of petroleum macromolecules. (CRC Press, 2008).

42. Turuga, A. S. S. Effect of solvent deasphalting process on the properties of deasphalted oil and asphaltenes from bitumen. (University of Alberta, 2017).

43. Rana, M. S., Sámano, V., Ancheyta, J. & Diaz, J. A. I. A review of recent advances on process technologies for upgrading of heavy oils and residua. Fuel **86**, (2007).

44. Xu, Y. Asphaltene Precipitation in Paraffinic Froth Treatment: Effects of Solvent and Temperature. Energy & Fuels **32**, 2801–2810 (2018).

45. Johnston, K. A., Schoeggl, F. F., Satyro, M. A., Taylor, S. D. & Yarranton, H. W. Phase behavior of bitumen and n-pentane. Fluid Phase Equilib. **442**, 1–19 (2017).

46. Duran, J. A. et al. Nature of Asphaltene Aggregates. Energy & Fuels (2018).

47. Yarranton, H. . W., Schoeggl, F. F. & Baydak, E. N. Deasphalting Related Phase Behavior and Properties. (2016).

48. Speight, J. G., Long, R. B. & Trowbridge, T. D. Factors influencing the separation of asphaltenes from heavy petroleum feedstocks. Fuel (1984).

49. Speight, J. G. Fouling in Refineries. (Gulf Professional Publishing, 2015).

50. Calles, J. A. et al. Properties of asphaltenes precipitated with different n-Alkanes. A study to assess the most representative species for modeling. Energy & Fuels **22**, 763–769 (2008).

51. Luo, P., Wang, X. & Gu, Y. Characterization of asphaltenes precipitated with three light alkanes under different experimental conditions. Fluid Phase Equilib. (2010).

52. Zawala, J., Dabros, T. & Hamza, H. Settling properties of aggregates in paraffinic froth treatment. Energy & Fuels **26**, 5775–5781 (2012).

53. Casas, Y. A., Duran, J. A., Schoeggl, F. F. & Yarranton, H. W. Settling of Asphaltene Aggregates in n-Alkane Diluted Bitumen. Energy & Fuels (2019).

54. Gieseman, J. & Keesom, B. Bitumen Partial Upgrading Whitepaper AM0401A. (2018).

55. Meyers, R. Handbook of petroleum refining processes. (2004).

56. Richard, H. L. & Philip, R. B. Solvent-deasphalting residual oil containing asphaltenes. (1999).

57. Aitani, A. M. Oil Refining and Products. (2004).

58. Magomedov, R. N., Pripakhaylo, A. V., Maryutina, T. A., Shamsullin, A. I. & Ainullov, T. S. Role of Solvent Deasphalting in the Modern Oil Refining Practice and Trends in the Process Development. Russian Journal of Applied Chemistry vol. 92 (2019).

59. Arciniegas, L. M. Asphaltene Precipitation During Solvent Injection at Different Reservoir Conditions and Its Effects on Heavy-Oil Recovery from Oilsands. (University of Alberta, 2014).

60. Corscadden, T., Bruce, G., Diduch, G., Hocking, D. & Remesat, D. Enhcaned methods for solvent deasphalting of hydrocarbons. U.S. Patent 20130098735A1. (2013).

61. Yves Jacquin, S., Manuel Gimenez-Coronado, C., Dai-Nghia, H. & Malmaison, R. Process for solvent deasphalting heavy hydrocarbon fractions. (1984).

62. Krasuk, J., Solari, R. B., Aquino, L. G., Rodriguez, J. V & Granados, A. Solvent deasphalting in solid phase. U.S. Patent 4572781A. (1986).

63. Aytan, A. Persistent free radicals in asphaltenes and their reactions. (University of Alberta, 2019).

64. Long, Y., Dabros, T. & Hamza, H. Structure of water/solids/asphaltenes aggregates and effect of mixing temperature on settling rate in solvent-diluted bitumen. (2004).

65. Torkaman, M., Bahrami, M. & Dehghani, M. R. Influence of Temperature on Aggregation and Stability of Asphaltenes. II. Orthokinetic Aggregation. Energy & Fuels (2018).

66. Mehrotra, A. K. & Svrcek, W. Y. Viscosity of compressed cold lake bitumen. Can. J. Chem. Eng. **65**, 672–675 (1987).

67. Lee, J. M. et al. Separation of solvent and deasphalted oil for solvent deasphalting process. Fuel Process. Technol. **119**, 204–210 (2014).

68. Joshi, N. B., Mullins, O. C., Jamaluddin, A., Creek, J. & McFadden, J. Asphaltene precipitation from live crude oil. Energy and Fuels **15**, 979–986 (2001).

69. Hirschberg, A., DeJong, L. N. J., Schipper, B. A. & Meijer, J. G. Influence of temperature and pressure on asphaltene flocculation. Soc. Pet. Eng. J. **24**, 283–293 (1984).

70. Buenrostro-Gonzalez, E., Lira-Galeana, C., Gil-Villegas, A. & Wu, J. Asphaltene precipitation in crude oils: Theory and experiments. AIChE J. **50**, 2552–2570 (2004).

71. Speight, J. G. The chemistry and technology of petroleum. (CRC Press, 2014).

72. Mehrotra, A. K. & Svrcek, W. Y. Correlation and prediction of gas solubility in cold lake bitumen. Can. J. Chem. Eng. **66**, 666–670 (1988).

73. Hansen, C. M. 50 Years with solubility parameters - Past and future. Prog. Org. Coatings **51**, 77–84 (2004).

74. Buckley, J. S., Wang, J. & Creek, J. L. Solubility of the Least-Soluble Asphaltenes. in Asphaltenes, Heavy Oils, and Petroleomics 401–437 (2007). doi:10.1007/0-387-68903-6_16.

75. Thomas, F. B., Bennion, D. B., Bennion, D. W. & Hunter, B. E. Experimental And Theoretical Studies Of Solids Precipitation From Reservoir Fluid. J. Can. Pet. Technol. **31**, (1992).

76. Chung, T. Thermodynamic modeling for organic solid precipitation. (1992).

77. De Boer, R. B., Leerlooyer, K., Eigner, M. R. P. & Van Bergen, A. R. D. Screening of crude oils for asphalt precipitation: theory, practice, and the selection of inhibitors. SPE Prod. Facil. **10**, 55–61 (1995).

78. Yarranton, H. W. & Masliyah, J. H. Molar mass distribution and solubility modeling of asphaltenes. AIChE J. **42**, (1996).

79. Martin, A., Newburger, J. & Adjei, A. Extended hildebrand solubility approach: Solubility of theophylline in polar binary solvents. J. Pharm. Sci. **69**, 487–491 (1980).

80. Park, K. A., Kim, K. H. & Hong, I. K. Comparison of solubility parameters for alkane family obtained using cubic equation of state. J. Ind. Eng. Chem. **17**, 213–217 (2011).

81. Yaws, C. L. Yaws' Thermophysical Properties of Chemicals and Hydrocarbons (Electronic Edition) - Knovel. (2010).

82. Oh, K. & Deo, M. D. Effect of organic additives on the onset of asphaltene precipitation. Energy and Fuels **16**, 694–699 (2002).

83. Zhao, Y. & Wei, F. Simultaneous removal of asphaltenes and water from water-in-bitumen emulsion. II. Application feasibility. Fuel Process. Technol. **89**, 941–948 (2008).

84. Clarke, P. F. & Pruden, B. B. Asphaltene precipitation from Cold Lake and Athabasca bitumens. Pet. Sci. Technol. **16**, 287–305 (1998).

85. Shelfantook, W. E. A Perspective on the Selection of Froth Treatment Processes. Can. J. Chem. Eng. **82**, 704–709 (2008).

86. Yang, X. & Czarnecki, J. The effect of naphtha to bitumen ratio on properties of water in diluted bitumen emulsions. Colloids Surf., A **211**, 213–222 (2002).

87. Yang, X., Hamza, H. & Czarnecki, J. Investigation of Subfractions of Athabasca Asphaltenes and Their Role in Emulsion Stability. Energy & Fuels (2004).

88. Paul, E. L., Atiemo-Obeng, V. A. & Kresta, S. M. Handbook of Industrial Mixing. Handbook of Industrial Mixing (2004).

89. Harrison, S. T. L., Kotsiopoulos, A., Stevenson, R. & Cilliers, J. J. Mixing indices allow scale-up of stirred tank slurry reactor conditions for equivalent homogeneity. Chem. Eng. Res. Des. **153**, 865–874 (2020).

90. Machado, M. B. & Kresta, S. M. When mixing matters: choose impellers based on process requirements. Chem. Eng. Prog. (2015).

91. Machado, M. B., Bittorf, K. J., Roussinova, V. T. & Kresta, S. M. Transition from turbulent to transitional flow in the top half of a stirred tank. Chem. Eng. Sci. **98**, 218–230 (2013).

92. Liné, A. Energy consumption to achieve macromixing revisited. Chem. Eng. Res. Des. **108**, 81–87 (2016).

93. Rahmani, N. H. G., Dabros, T. & Masliyah, J. H. Evolution of asphaltene floc size distribution in organic solvents under shear. Chem. Eng. Sci. **59**, 685–697 (2004).

94. Soleimani-Khormakala, H., Torkaman, M. & Bahrami, M. The Effect of Shear Rate on Aggregation and Fragmentation of Asphaltene Aggregates. J. Dispers. Sci. Technol. **40**, 836–845 (2019).

95. Duran, J. A., Schoeggl, F. F. & Yarranton, H. W. Kinetics of asphaltene precipitation/aggregation from diluted crude oil. Fuel (2019).

96. Johnson, C. P., Li, X. & Logan, B. E. Settling velocities of fractal aggregates. Environ. Sci. Technol. **30**, 1911–1918 (1996).

97. Demirbas, A., Alidrisi, H. & Balubaid, M. A. API Gravity, Sulfur Content, and Desulfurization of Crude Oil. Pet. Sci. Technol. **33**, 93–101 (2015).

98. Analysis report. University of Alberta. (2019).

99. Prefontaine, A. Test report. Innnotech Alberta. (2019).

100. Certificate of Analysis. Bureau Veritas Laboratories, Edmonton. (2019).

101. Liquid hydrocarbon analysis. Bureau Veritas Laboratories, Edmoton. (2019).

102. ASTM D6560-00: Standard Test Method for Determination of Asphaltenes (Heptane Insolubles) in Crude Petroleum and Petroleum Products. Pet. Prod. Lubr. Foss. Fuels (2013).

103. Breakey, D. Autoclave conditions calculations. University of Alberta. (2019).

104. Kiersted, J. W. Removal of asphaltic constituents from hydrocarbon oil. U.S. Patent 2,500,757. (1950).

105. Shin, S. et al. Physical and rheological properties of deasphalted oil produced from solvent deasphalting. Chem. Eng. J. **257**, 242–247 (2014).

Appendix A Solvent Composition

Tables A.1, A.2, and A.3 demonstrate the detailed composition of each solvent blend used for the study. These tables are the more detailed version of Table 3.3 given in Chapter 3.

Table A. 1. Detailed composition of solvent Batch 1

Component	Boiling Point (℃)	Mole Fraction	Mass Fraction	Volume Fraction
Methane	-162	0	0	0
Ethane	-89	0	0	0
Propane	-42	Trace	Trace	Trace
Iso-Butane	-12	Trace	Trace	Trace
n-Butane	0	0.0072	0.0054	0.006
Iso-Pentane	28	0.6213	0.5767	0.5981
n-Pentane	36	0.1693	0.157	0.1615
Hexanes	37-69	0.0841	0.0932	0.091
Heptanes	70-98	0.0612	0.0724	0.0642
Octanes	99-126	0.034	0.0451	0.0385
Nonanes	127-151	0.0091	0.0136	0.0114
Decanes	152-174	0.0038	0.0066	0.0057
Undecanes	175-196	0.0019	0.0039	0.0034
Dodecanes	197-216	0.0012	0.0026	0.0023
Tridecanes	217-236	0.0011	0.0026	0.0022
Tetradecanes	237-253	0.0008	0.002	0.0017
Pentadecanes	254-271	0.0007	0.0018	0.0016
Hexadecanes	272-287	0.0005	0.0016	0.0012
Heptadecanes	288-302	0.0005	0.0014	0.001
Octadecanes	303-317	0.0003	0.0011	0.0008
NonaDecanes	318-331	0.0002	0.0009	0.0006
Eicosanes	332-343	0.0002	0.0009	0.0006
Heneicosanes	344-357	0.0002	0.0008	0.0006
Docosanes	358-369	0.0002	0.0007	0.0006
Triacosanes	370-380	0.0002	0.0007	0.0005
Tetracosanes	381-391	0.0002	0.0007	0.0005
Pentacosanes	392-402	0.0002	0.0005	0.0004
Hexacosanes	403-412	0.0001	0.0005	0.0003
Heptacosanes	413-422	0.0001	0.0005	0.0004
Octacosanes	423-432	0.0002	0.0006	0.0004
Nonacosanes	433-441	0.0002	0.001	0.0007
Triacontanes+	442-449+	0.0010	0.0052	0.0038

Table A. 2. Detailed composition of solvent Batch 2

Component	Boiling Point (℃)	Mole Fraction	Mass Fraction	Volume Fraction
Methane	-162	0	0	0
Ethane	-89	Trace	Trace	Trace
Propane	-42	Trace	Trace	Trace
Iso-Butane	-12	Trace	Trace	Trace
n-Butane	0	0.0062	0.0047	0.0052
Iso-Pentane	28	0.5954	0.5567	0.574
n-Pentane	36	0.1824	0.1707	0.1745
Hexanes	37-69	0.0937	0.1047	0.1016
Heptanes	70-98	0.0676	0.0806	0.073
Octanes	99-126	0.0366	0.0491	0.0426
Nonanes	127-151	0.0093	0.0144	0.0124
Decanes	152-174	0.0037	0.0065	0.0057
Undecanes	175-196	0.0017	0.0034	0.003
Dodecanes	197-216	0.0008	0.0019	0.0017
Tridecanes	217-236	0.0007	0.0016	0.0014
Tetradecanes	237-253	0.0003	0.0008	0.0007
Pentadecanes	254-271	0.0002	0.0007	0.0006
Hexadecanes	272-287	0.0002	0.0005	0.0004
Heptadecanes	288-302	0.0002	0.0006	0.0005
Octadecanes	303-317	0.0002	0.0004	0.0003
NonaDecanes	318-331	0.0001	0.0003	0.0003
Eicosanes	332-343	0.0001	0.0004	0.0003
Heneicosanes	344-357	0.0001	0.0003	0.0003
Docosanes	358-369	0.0001	0.0003	0.0003
Triacosanes	370-380	0.0001	0.0002	0.0002
Tetracosanes	381-391	0.0001	0.0002	0.0001
Pentacosanes	392-402	Trace	0.0001	0.0001
Hexacosanes	403-412	Trace	0.0001	0.0001
Heptacosanes	413-422	Trace	0.0001	0.0001
Octacosanes	423-432	Trace	0.0001	0.0001
Nonacosanes	433-441	Trace	Trace	Trace
Triacontanes+	442-449+	0.0002	0.0006	0.0005

Table A. 3. Detailed composition of solvent Batch 3

Component	Boiling Point (℃)	Mole Fraction	Mass Fraction	Volume Fraction
Methane	-162	0	0	0
Ethane	-89	Trace	Trace	Trace
Propane	-42	Trace	Trace	Trace
Iso-Butane	-12	0.0001	0.0001	0.0001
n-Butane	0	0.0245	0.019	0.0208
Iso-Pentane	28	0.6506	0.6275	0.6411
n-Pentane	36	0.1832	0.1767	0.179
Hexanes	37-69	0.0662	0.0763	0.0735
Heptanes	70-98	0.0435	0.0528	0.0458
Octanes	99-126	0.0221	0.0301	0.025
Nonanes	127-151	0.0054	0.0084	0.0069
Decanes	152-174	0.002	0.0038	0.0032
Undecanes	175-196	0.0009	0.0019	0.0017
Dodecanes	197-216	0.0005	0.0011	0.0009
Tridecanes	217-236	0.0004	0.0009	0.0008
Tetradecanes	237-253	0.0002	0.0006	0.0005
Pentadecanes	254-271	0.0002	0.0004	0.0004
Hexadecanes	272-287	0.0001	0.0001	0.0001
Heptadecanes	288-302	0.0001	0.0002	0.0001
Octadecanes	303-317	Trace	0.0001	0.0001
NonaDecanes	318-331	Trace	Trace	Trace
Eicosanes	332-343	Trace	Trace	Trace
Heneicosanes	344-357	Trace	Trace	Trace
Docosanes	358-369	Trace	Trace	Trace
Triacosanes	370-380	Trace	Trace	Trace
Tetracosanes	381-391	Trace	Trace	Trace
Pentacosanes	392-402	Trace	Trace	Trace
Hexacosanes	403-412	Trace	Trace	Trace
Heptacosanes	413-422	Trace	Trace	Trace
Octacosanes	423-432	Trace	Trace	Trace
Nonacosanes	433-441	Trace	Trace	Trace
Triacontanes+	442-449+	Trace	Trace	Trace

Appendix B Experimental Data

Table B.1 demonstrates the results that were obtained from each experiment and used to generate graphs provided in Chapter 4 and 5. The cells that contain minus (-) sign indicate that no sample were retrieved for that case from the corresponding experiment. It is either because it was not part of the experimental procedure for that experiment or because no sample could be recovered under those operating conditions. For instance, in PB-A experiments, DAO-10 and DAO-60 sample do not exist because it was a batch process and they were not part of the experimental procedure. Besides, for the same set of experiments, pitch yield results also do not exist because under the given operating conditions no pitch was observed. The cells that contain plus (+) sign indicate that samples were retrieved, however, were not sent for analysis either because were too little to be able perform asphaltene content analysis or because were not to the interest of the project.

Table B. 1. Analysis results for the samples taken from the present investigation

Runs	Pitch yield (wt. %)	DAO-10 Asph. (wt. %)	DAO-60 Asph. (wt. %)	DAO-24 Asph. (wt. %)
PB-A-001	-	-	-	+
PB-A-002	-	-	-	+
PB-B-001	-	-	+	+
PB-B-002	12	-	23.18	+
PB-B-003	44	-	9.14	+
PB-B-004	48	-	5.28	+
PB-B-005	57	5.74	4.88	2.17
PB-B-006	60	7.49	4.51	4.14
PB-B-007	57	3.98	5.09	4.16
PB-B-008	54	6.23	5.38	2.60
PB-D-001	55	7.14	5.97	4.86
PB-D-002	64	6.63	4.33	+

Appendix C Asphaltene Aggregates Settling

The following figures (Figure C.1 – Figure C.12) are the derived aggregates settling trends for each experiment based on the recorded camera images of the setting process. Detailed operating conditions for each experiment have been provided in the captions. For the PB-A set experiments and the first two PB-B set experiments no pitch was observed or sampled; therefore, in Figures C.1, C.2, and C.3 the DAO and water phases almost coincide in each graph and verifies that no appreciable amount of pitch was formed in order to create a separate phase. Moreover, substantially more data points for these experiments prove that interfaces could readily be tracked and no obstruction by pitch was observed. Since both DAO and water have low viscosity, they easily settled and formed separate phases. The rest of the experiments, however, may involve some errors in terms of aggregates settling time and much fewer data points at the beginning of the settling process are an indication of difficulty to determine the phase level.

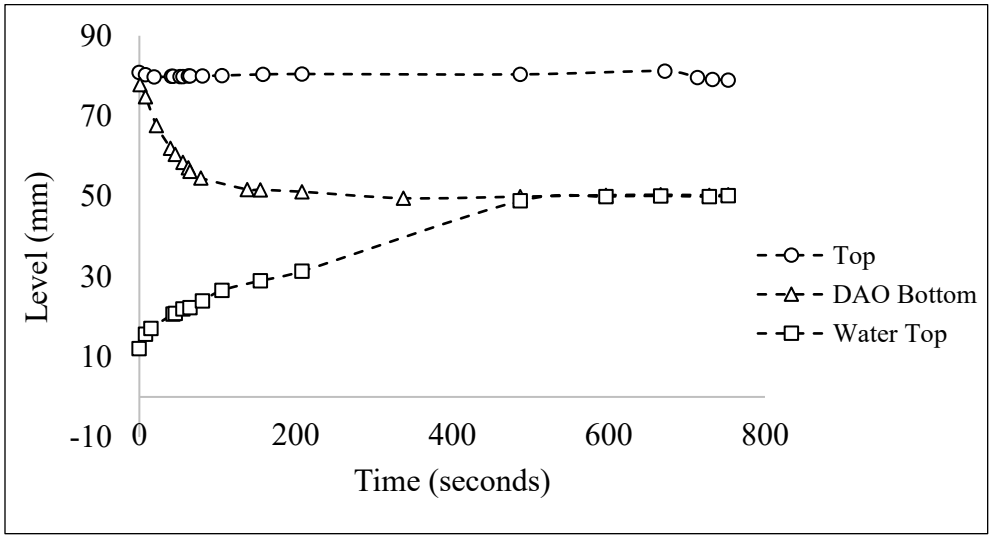

Figure C. 1. Aggregate settling trend for the PB-A-001 run. The mixing was performed for 1 hour at 515 RPM mixing speed and the settling continued for 24 hours. The other operating conditions are S/B = 0.9, SOR = 3.0, P = 46 bar, T = 165 ℃

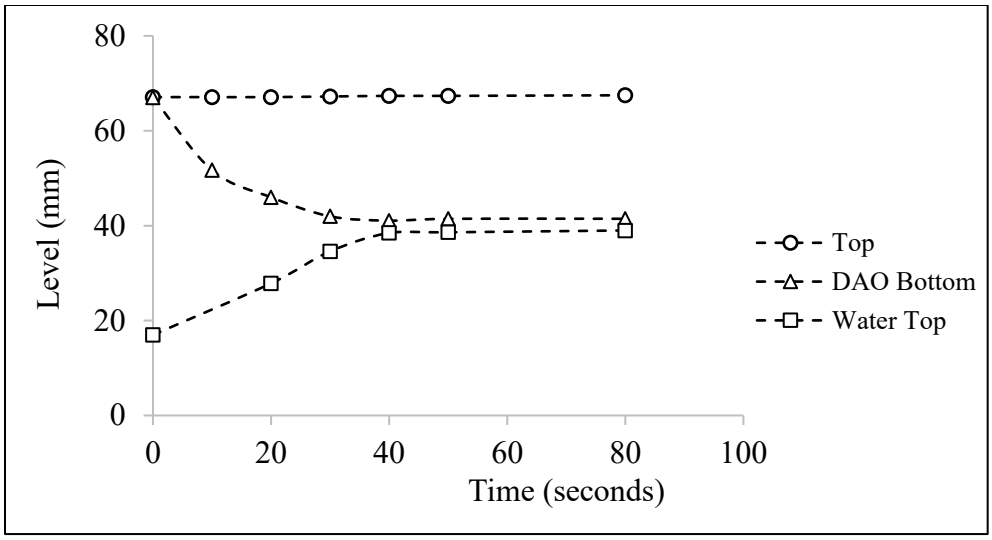

Figure C. 2. Aggregate settling trend for the PB-A-002 run. The mixing was performed for 1 hour at 515 RPM mixing speed and the settling continued for 24 hours. The other operating conditions are S/B = 0.9, SOR = 3.0, P = 33 bar, T = 165 ℃

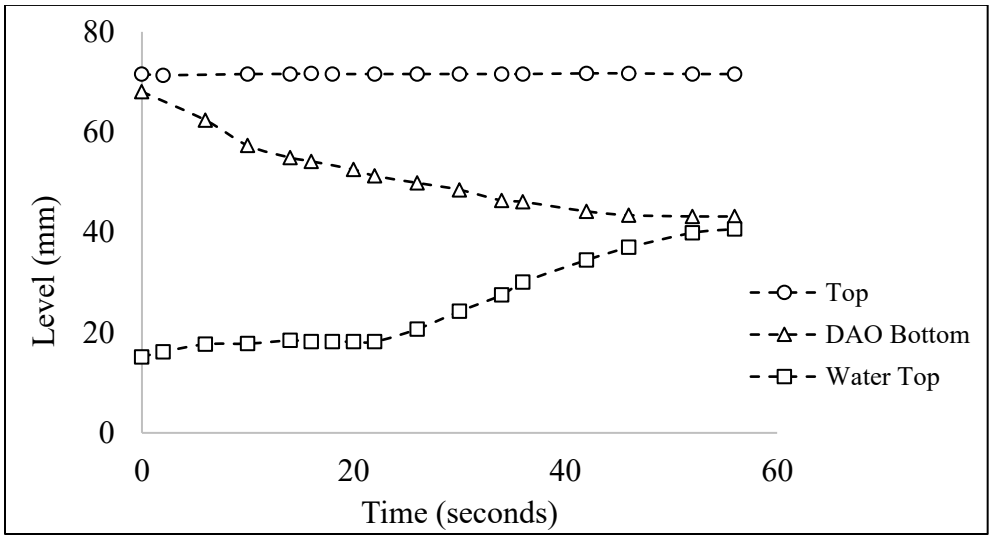

Figure C. 3. Aggregate settling trend for the PB-B-001 run. The mixing was performed for 1 hour at 515 RPM mixing speed and the settling continued for 24 hours. The other operating conditions are S/B = 0.9, SOR = 3.0, P = 31 bar, T = 165 ℃

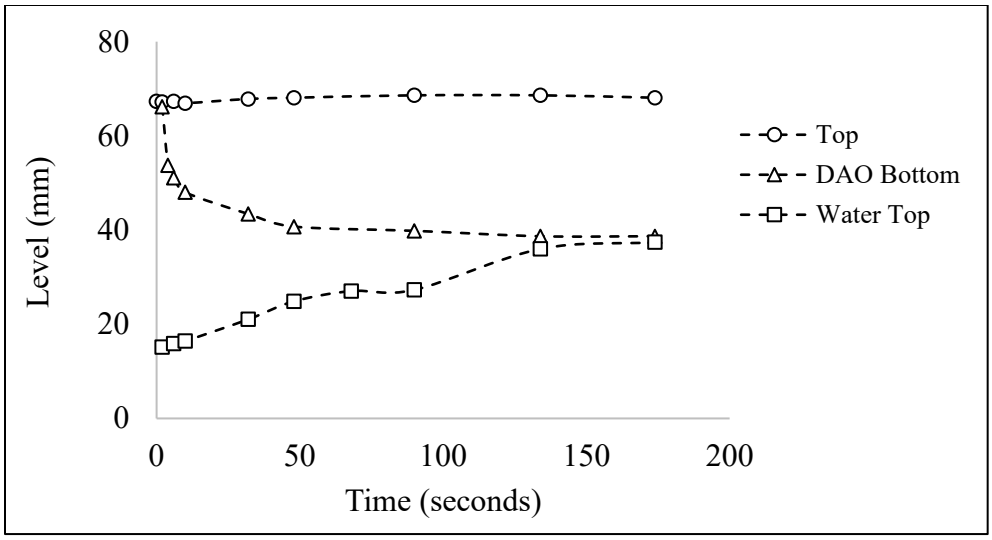

Figure C. 4. Aggregate settling trend for the PB-B-002 run. The mixing was performed for 1 hour at 515 RPM mixing speed and the settling continued for 24 hours. The other operating conditions are S/B = 1.3, SOR = 3.0, P = 41 bar, T = 164 ℃

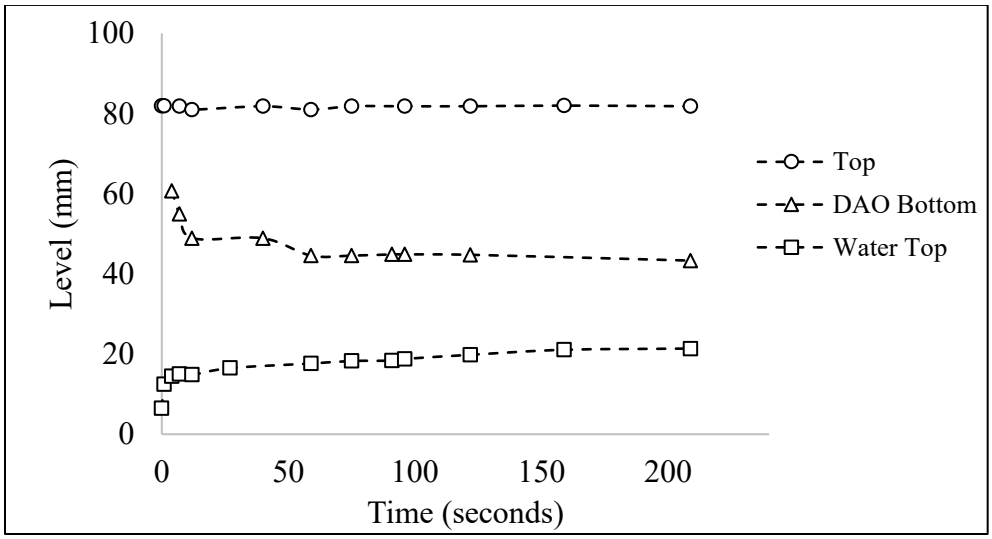

Figure C. 5. Aggregate settling trend for the PB-B-003 run. The mixing was performed for 1 hour at 515 RPM mixing speed and the settling continued for 24 hours. The other operating conditions are S/B = 1.7, SOR = 3.0, P = 42 bar, T = 164 ℃

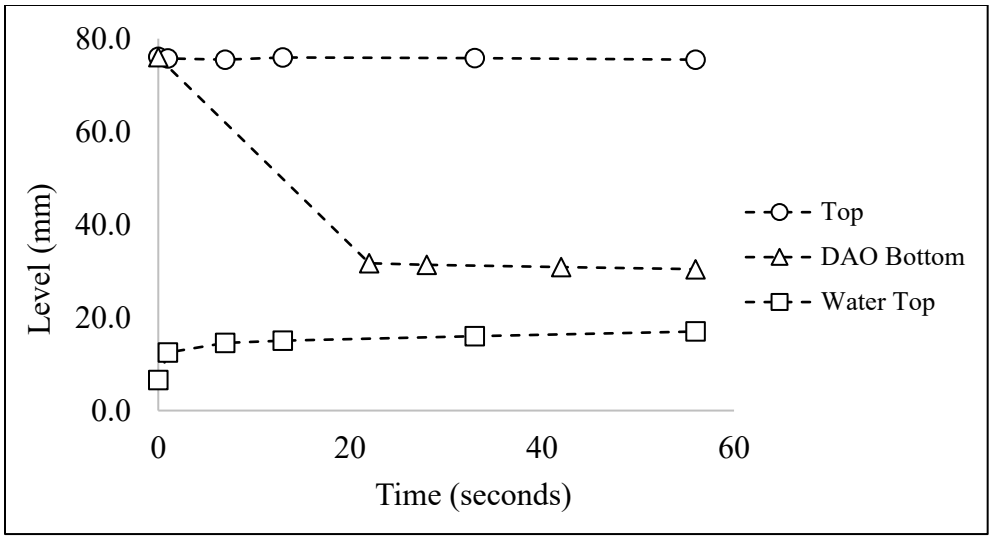

Figure C. 6. Aggregate settling trend for the PB-B-004 run. The mixing was performed for 1 hour at 515 RPM mixing speed and the settling continued for 24 hours. The other operating conditions are S/B = 1.7, SOR = 2.0, P = 41 bar, T = 164 ℃

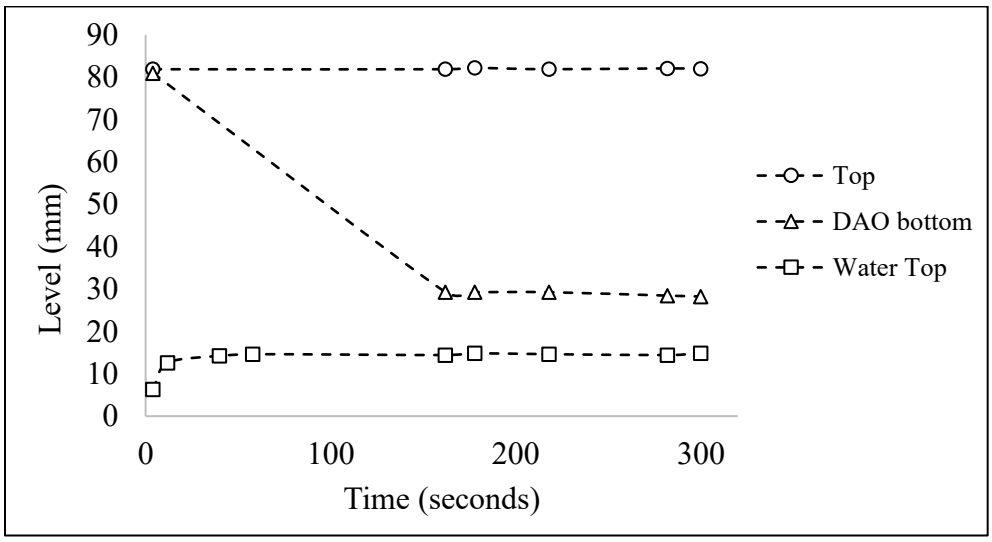

Figure C. 7. Aggregate settling trend for the PB-B-005 run. The mixing was performed for 1 hour at 515 RPM mixing speed and the settling continued for 24 hours. The other operating conditions are S/B = 1.9, SOR = 1.9, P = 38 bar, T = 164 ℃

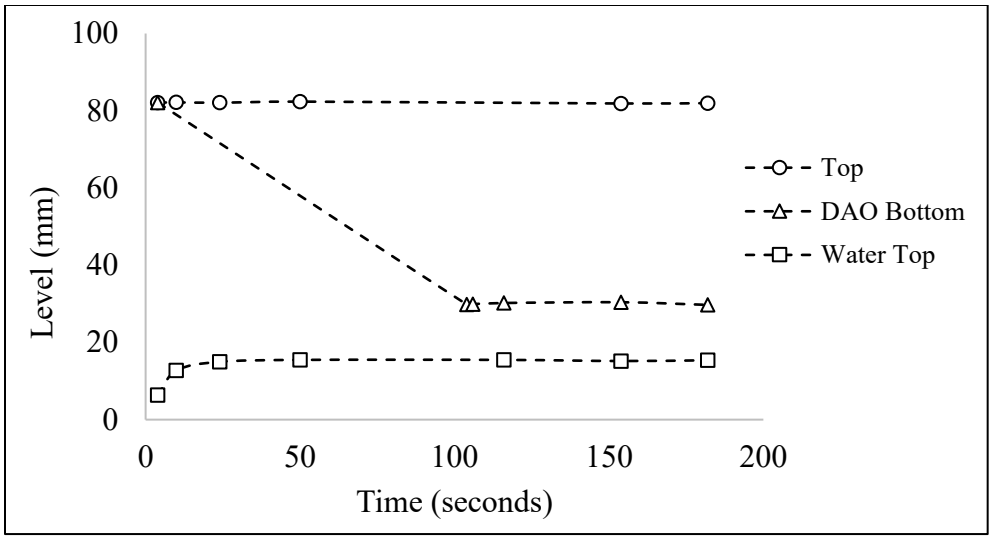

Figure C. 8. Aggregate settling trend for the PB-B-006 run. The mixing was performed for 1 hour at 515 RPM mixing speed and the settling continued for 24 hours. The other operating conditions are S/B = 1.9, SOR = 1.9, P = 38 bar, T = 164 ℃

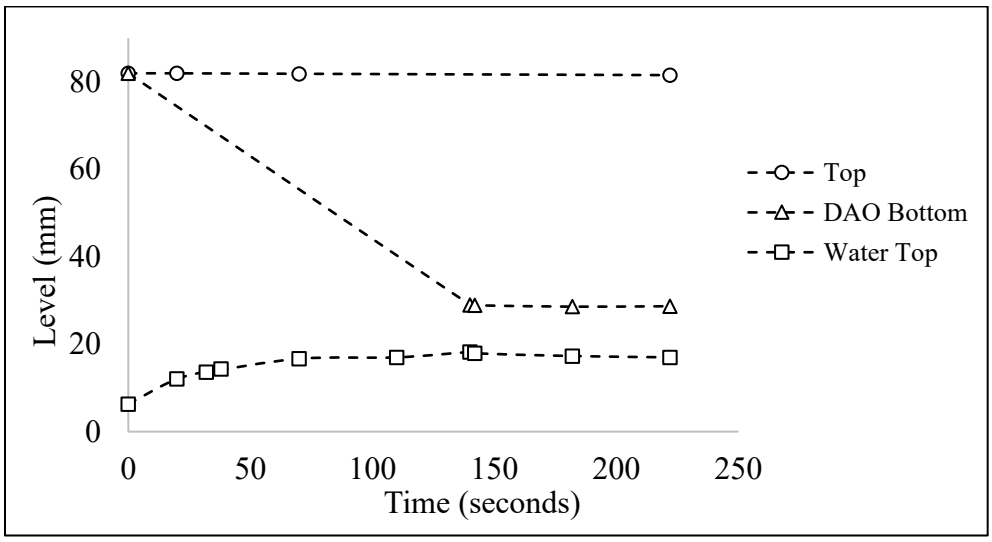

Figure C. 9. Aggregate settling trend for the PB-B-007 run. The mixing was performed for 1 hour at 515 RPM mixing speed and the settling continued for 24 hours. The other operating conditions are S/B = 1.9, SOR = 1.9, P = 36 bar, T = 164 ℃

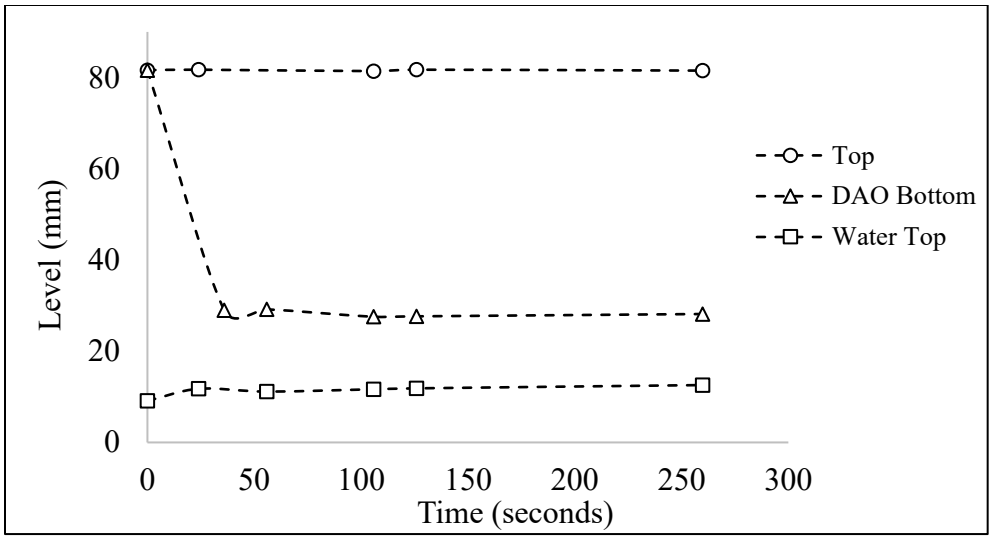

Figure C. 10. Aggregate settling trend for the PB-B-008 run. The mixing was performed for 1 hour at 515 RPM mixing speed and the settling continued for 24 hours. The other operating conditions are S/B = 1.9, SOR = 1.9, P = 43 bar, T = 164 ℃

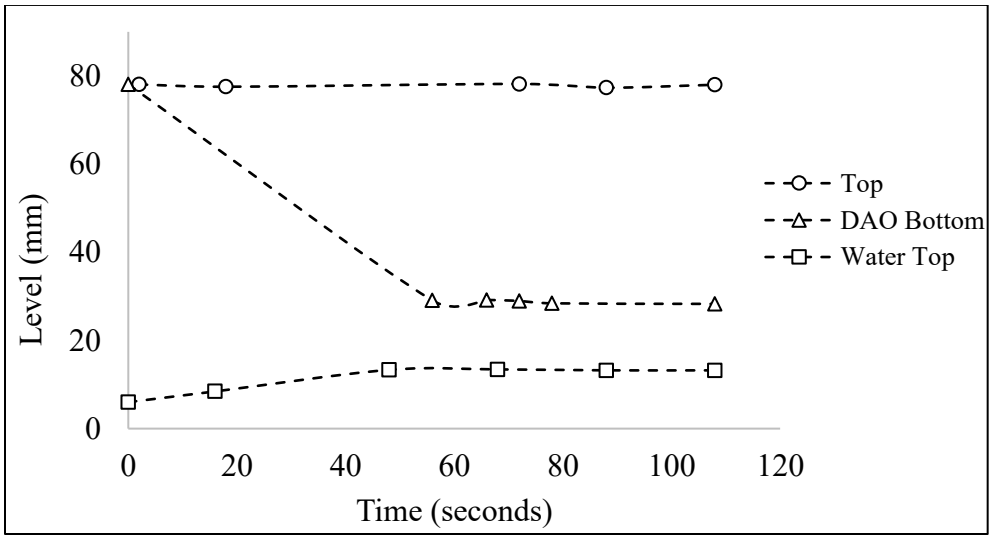

Figure C. 11. Aggregate settling trend for the PB-D-001 run. The mixing was performed for 1 hour at 515 RPM mixing speed and the settling continued for 24 hours. The other operating conditions are S/B = 2.0, SOR = 1.9, P = 37 bar, T = 164 ℃

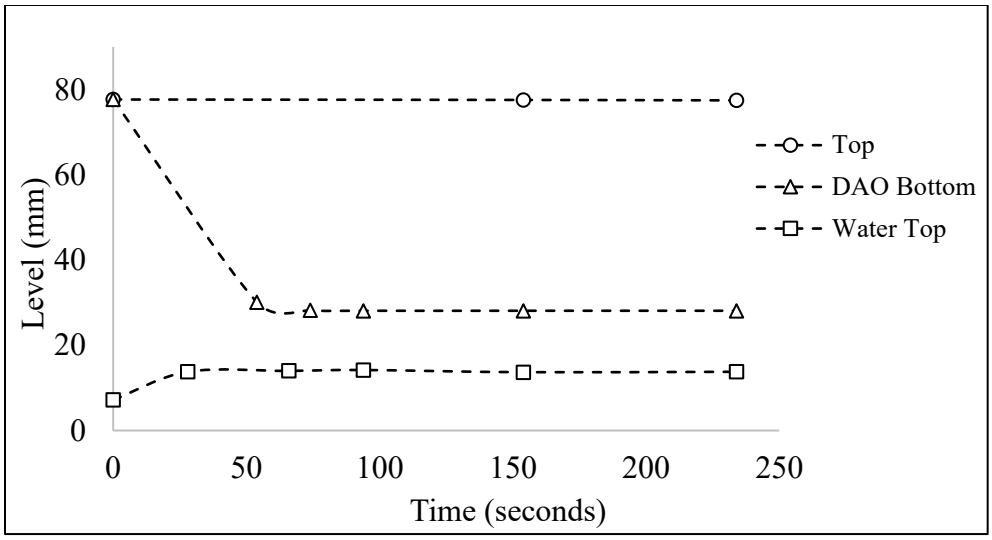

Figure C. 12. Aggregate settling trend for the PB-D-002 run. The mixing was performed for 1 hour at 515 RPM mixing speed and the settling continued for 24 hours. The other operating conditions are S/B = 2.2, SOR = 1.9, P = 37 bar, T = 164 ℃

Appendix D Safe Work Procedure

Since the PB-D set has the most complex experimental setup, the safe work procedure (SWP) for PB-D set experiments is provided below. Figure D.1 was used as the reference to the SWP. The safe work procedure for the other sets (PB-A and PB-B) can be obtained by simply omitting the sections that are not part of the experimental procedure. The basic experimental procedures have been provided in Section 3.5, where it demonstrates the experimental setup for each set. The SWP consists of four parts: Silanization of the reactor, loading the reactor, pressure testing, performing the experiment, and shutting down and cleaning.

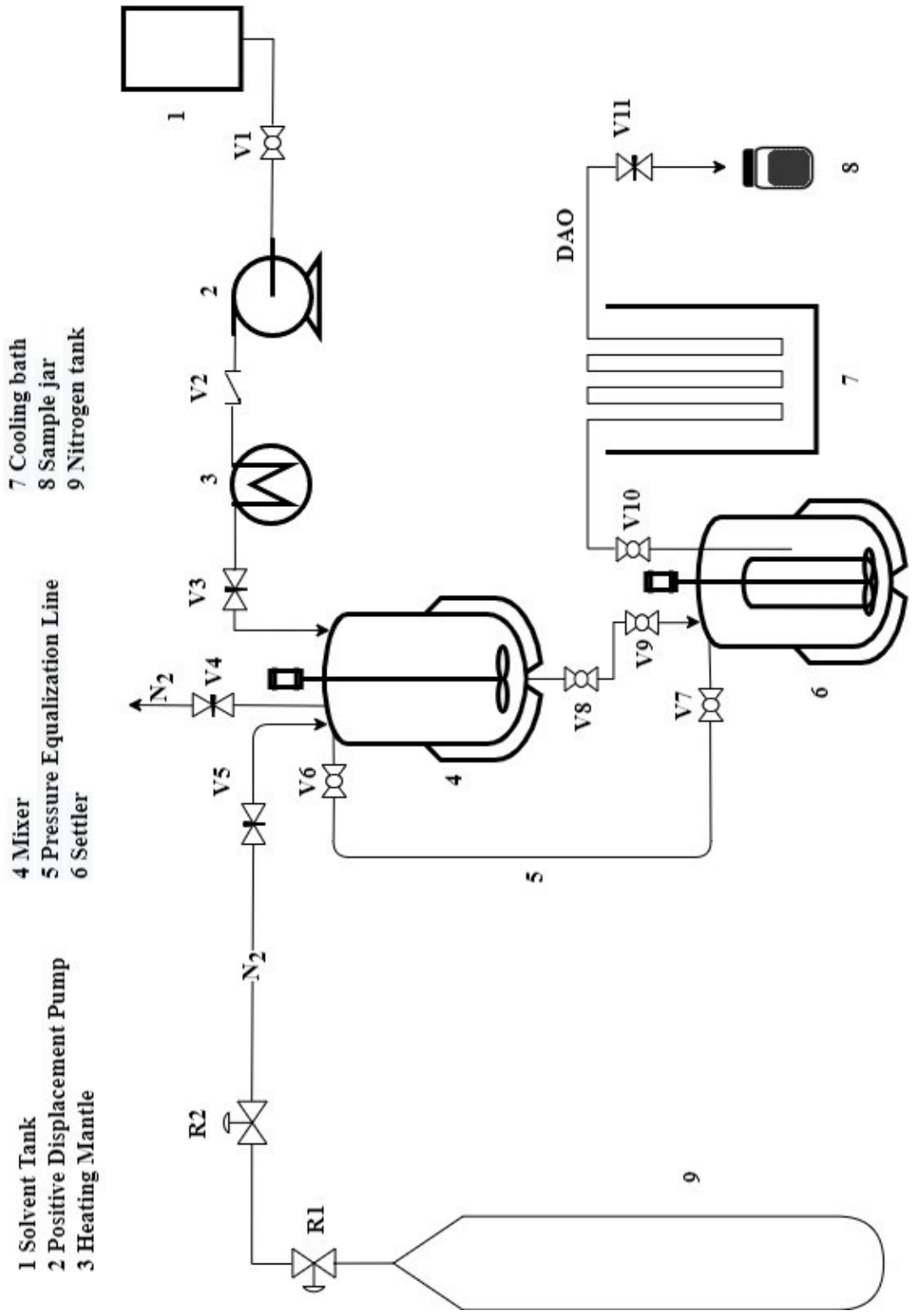

Figure D. 1. Experimental setup for the PB-D experiments

Table D. 1. Safe work procedure (SWP) for the PB-D setup

Job title: Semi batch (PB-D set) – DAO and pitch sampling at pressure & temperature	Date: 27 January 2020
Written by Aaron Cheung Edited by Aligulu Alili	Conducted by: Aligulu Alili, Marcio Machado,
Required Protective Equipment: Closed-toe shoes, flame-retardant lab coats, full-length pants (leg covers are recommended to protect against splashes), nitrile gloves, heat-resistant gloves, full-coverage safety goggles, approved and fitted respirators.	
First Aid Measures: (See MSDS for further details) If on the skin, wash with plenty of water. If inhaled, remove person to fresh air and keep comfortable for breathing. If in eyes, Rinse cautiously with water for several minutes. Remove contact lenses, if present and easy to do so. Continue rinsing. Call a poison centre or doctor if you feel unwell.	

MSDS: "Bitumen Emulsion" MSDS003, Nexen Energy ULC, September 14, 2015.
"Condensate, Sweet" NGL Natural Gas Liquid, Keyera and Affiliates.
"Pentane" C5, Keyera and Affiliates.
"Silanization solution I", Sigma-Aldrich Canada Co.

MSDS-listed emergency phone: Bitumen Emulsion - 780 334 3911; Condensate - 780 449 7910

Table D. 2. Part 1: Silanization of the reactor

Number	Sequence of safe work procedure steps	Potential hazards
1.1	Unplug the windowed reactor heater from the controller and move the cords through the lowered stand.	
1.2	Check that the stand and reactor are lowered as far as it can go.	
1.3	Lift the reactor out of the stand and into the fume hood. Lay the reactor on its side with the window to be silanized face down.	The windowed reactor cylinder is fairly heavy. If needed, have two people perform this step.
1.4	Transfer some silanization solution into a sample vial for use. Return the salinization solution bottle to storage after obtaining your sample vial amount.	Silanization solution is extremely flammable, toxic by inhalation, and can react violently with water. Be sure there is no source of ignition or moisture when using the solution. Only use small quantities of it at any time to minimize the hazard in case of a spill. Respirators should be worn when utilizing silanization solution.
1.5	Use a small transfer pipette to fill the inside of the window with a thin layer of silanization solution.	
1.6	Lower the fume hood sash and leave the solution on the window for 5 minutes.	
1.7	After 5 minutes, remove the silanization solution with the pipette and deposit it back into the sample vial.	Wear a respirator before lifting the fume hood sash.

1.8	Dry the inside of the glass window with the air hose for 5 minutes.	
1.9	Flip the reactor so that it is laying the other window.	
1.10	Repeat steps 1.5 to 1.8 on the remaining window.	
1.11	After silanization, return the reactor to the stand and plug the heater back into the 4848 controller.	The windowed reactor cylinder is fairly heavy. If needed, have two people perform this step.

Table D. 3. Part 2: Loading the reactor

Number	Sequence of safe work procedure steps	Potential hazards
2.1	Position the heating bath inside the fume hood.	
2.2	Fill the heating bath to about 80 % full with ethylene glycol.	Ethylene glycol can be harmful if inhaled. Be sure to do all filling in the fume hood or well-ventilated area.
2.3	Remove the paper label from the bitumen emulsion paint can.	
2.4	Secure the paint can with a chain clamp so it does not move around the bath during heating.	
2.5	Set the bath to temperature to 82 °C and turn ON the heating bath.	
2.6	Lower the fume hood sash as much as possible.	
2.7	Wait for the emulsion to heat to 60-80 °C (approx. 1.5 hours). While waiting, set up a balance with a 100 ml beaker in the fume hood. Zero the balance with the beaker on it.	Be careful not to touch the paint can or allow any non-heat-resistant materials to come in contact with it.
2.8	Once the bitumen is heated, use to the ladle to transfer the appropriate amount from the paint can to the 100 ml beaker. Record the weight transferred to the beaker. Initial bitumen weight = _____g	The paint can be hot. Use heat-resistant gloves when handling it.

2.9	Pour the hot bitumen from the beaker into the reactor. Weigh the leftover bitumen in the beaker. Leftover bitumen weight = _____g Bitumen transferred to reactor = _____g	Hot bitumen may release volatile gases. Be sure that everyone in the lab is wearing a suitable respirator when moving it from the fume hood to the reactor.
2.10	Shut down the heating bath.	
2.11	In clean 250 ml beakers, weigh and transfer the appropriate amounts of water into the reactor. Water weight = _____g	
2.12	Raise the reactor cylinder up until the head and cylinder are aligned.	The windowed reactor cylinder is fairly heavy. Perform this step with two people. Use the stand to raise the cylinder into place and have one person hold the neck of the cylinder to align it.
2.13	Place the split O-ring seals onto the reactor head and body. Close the latches and tighten all six cap screws by hand first.	

2.14	Tighten the screws to 15 ft-lbs of torque initially (for an operating pressure of under 1000 psi). If the operating pressure is between 1000-3000 psi, then increase torque to 25 ft-lbs. Tightening should be done in a crisscross pattern instead of going around the circle.	Do not overtorque the bolts. Overtorque may cause bolt and split O-ring damage.
2.15	Lower the stand once the reactor cell is secured onto the head.	
2.16	Power on the 4848 reactor controller.	Powering on the controller could start the heater or mixer prematurely. Ensure that the heater power and motor power are both OFF (Position O) before turning on the controller.
2.17	Start the computer and open up SpecView to begin data recording.	
2.18	Pressure test the reactor at ambient temperature. *	*See Part 3: Reactor pressure testing procedure.

Table D. 4. Part 3: Reactor pressure testing procedure

Number	Sequence of safe work procedure steps	Potential hazards / Notes
3.1	Check that the following pieces of equipment are in the appropriate starting positions: - Autoclave cylinder: Detached (160 mL, 600 mL or windowed) - N2 supply: Minimum 60 bar(g) (870 PSI(g)) available at main regulator - Valves: Capped valves OPEN. All other valves CLOSED.	N2 supply should be at least slightly higher pressure than the run pressure. Good practice for how much higher is uncertain.
3.2	Fill the autoclave cylinder to the desired condition. Note that the vessel internals reduce the total vessel volume.	The autoclave cylinder should never be filled more than 2/3 full.
3.3	Raise the autoclave cylinder up until the head and cylinder are aligned.	Autoclave cylinders can be heavy. There is potential to drop it causing a spill or injury.
3.4	Place the split O-ring seals onto the autoclave head and body. Close the latches and tighten all six cap screws by hand first. Tighten the screws to 15 ft-lbs of torque initially and then increase to **20-25 ft-lbs**. Tightening should be done in a criss-cross pattern instead of going around the circle. Lower the stand once the autoclave cell is secured onto the head.	
3.5	Check that the autoclave gas inlet valve (V5), the reactor 1 regulator valve (R2), and the N2 cylinder regulator valve (R1) are completely CLOSED.	

3.6	Open the N2 cylinder supply valve and observe the N2 supply pressure. Close the N2 cylinder supply and check the supply pressure reading. If it does not drop, move onto the next step.	N2 cylinders need to be properly secured and stored when not in use. Ensure appropriate operation of cylinder and regulator prior to pressurizing autoclave. Potential gas leak at N2 cylinder supply connection. If the N2 supply pressure drops after closing the supply valve, Snoop detection should be applied to locate the leak. Once located, depressurize the system and fix the leak.
3.7	Reopen the N2 cylinder supply valve and adjust the N2 regulator valve R1 to just above the desired test pressure.	Test pressure should be 1.25x the run pressure. (ex. 44 bar(g) run => 55 bar(g) test pressure).
3.8	Adjust the reactor regulator valves (R2) to the desired test pressure then slowly open valve V5 to apply the pressure to the autoclaves.	Potential gas leakage when applying pressure. Pressurization should be immediately stopped if gas leaks are detected. If overpressure does occur beyond 1000 PSI, the rupture disks will fail and N2 will begin escaping the autoclave. Close the N2 cylinder regulator and turn the temperature in the autoclave off. Allow vessel to depressurize and cool.
3.9	Close the N2 supply valve and monitor the pressure in the system for 30 to 60 minutes. If the system pressure drops, then a leak in the system is present.	A < 5 PSI/hr drop is OK.

3.10	If leaks are detected, use Snoop® leak detector fluid to check all pressure inlet lines and vessel connections for gas leaks. Once the leak is located, close the gas inlet valve, release the pressure and fix the leak. If there are no leaks detected, proceed onto the next step.	
3.11	Close the N2 supply valve.	
3.12	Bring the pressure in the autoclave and supply line down by **slowly** opening valve V4.	Releasing gas too quickly could cause failure of valves or lines. Discharge of fluid could occur as well if gas release is not controlled.
3.13	Observe the pressure on the controller until it reads 0 gauge pressure. Let the autoclave sit for 60 seconds afterwards to let any residual pressure escape from the vessel.	The pressure test is successful if no leaks were detected. The regular experiment can continue from this point after pressure testing.

Table D. 5. Part 4: Running the experiment

Number	Sequence of safe work procedure steps	Potential hazards
4.1	Attach the insulation jacket into place around the reactor cell.	
4.2	If not already done during the pressure test, open the N2 cylinder supply valve and adjust the N2 cylinder regulator valve R1 to just above the desired run pressure.	N2 cylinders need to be properly secured. Do NOT pressurize the reactor if the cylinder is not secured. Make sure that valves R and R2 are completely closed prior to opening the N2 supply valve. Overpressure of the system occurs at 1000 PSIG at which point rupture discs will burst.
4.3	Check that the reactor valves V1 to V11 are all are CLOSED, except V6 and V7. V6 and V7 valves are kept open to equalize the pressure in reactors.	
4.4	Adjust the vessel 1 regulator valve, R2, to the desired test pressure.	
4.5	**Slowly** open valve V5 slightly to apply the calculated starting pressure to the reactor. Starting pressure = _____PSIG	Potential gas leakage when applying pressure. Pressurization should be immediately stopped if gas leaks are detected. The gas leak should be fixed before continuing any further.
4.6	Close valve V5 then the nitrogen cylinder supply valve once pressure has been applied.	

4.7	Turn ON the motor/pressure transducer cooling water loop pump and check that all cooling water lines have flow.	
4.8	Set the both reactors temperatures on the 4848 controller to the target temperature. Target temperature = _____°C	
4.9	Turn ON the vessel 1 heater to position I (half power) and Turn ON the vessel 2 heater to position II (full power) and wait for the reactor to heat up. When the temperature is 10 °C below the target temperature, switch the vessel 2 heater to position I (half power). While heating, set the motor speed to 100 RPM, but do NOT turn on the motor.	Burns may be caused by touching the reactor heater with bare skin. Avoid contact with reactor and other components that are above room temperature. Use appropriate heat resistant gloves if contact is required.
4.10	TURN ON solvent heater to position I (half power) and TURN ON transfer line and solvent line heating tapes.	
4.11	When the reactor reaches 60 °C, on the 4848 controller, set the motor control to AUTO and power ON the motor. Use the return key to set the RPM r-S control to “Run”.	Motor speed can suddenly jump when powered on. To avoid this, check that the mixer turns freely by hand and that the motor r-S control is set to “Stop” prior to powering on the mixer.
4.12	Set up the camera and lighting in front of the reactor window during heating.	

4.13	Make solvent feed ready and turn on the pump and prime the pump by pulling at least 20 ml of solvent to remove the air from the suction tube.	The pump must be primed to remove the air bubbles. Air bubbles may cause reduced solvent flow rate and faulty flow rate readings.
4.14	Once the reactor has reached the target temperature and pressure, set the solvent flow rate and start the pump to inject solvent.	By this time, the solvent heater and solvent transfer line should have already reached the specified temperature, if not, wait till the temperature reaches the target.
4.15	After the calculated amount of solvent has been injected, increase the motor speed to the high mixing speed target using SpecView and allow the system to mix for the specified time. High mixing speed = _____RPM High RPM mixing time = _____min	
4.16	When the required solvent amount has been transferred, stop the pump and prime the pump to remove all the remaining solvent from the pump.	
4.17	Turn OFF heating mantle	After the solvent has been injected, heating mantle has to be turned off to simplify the process control and avoid energy waste.
4.18	Turn OFF reactor 1 heater and remove the insulation jacket.	For PB-D experiments, reactor 1 is used as an intermediate solvent flow-

		through unit and thus has to be disconnected from the main reactor by closing valve V7, V8, and V9. Reactor 1 heater has to be turned off to simplify the process control and avoid energy waste.
4.19	Upon completing high RPM mixing, turn OFF the motor power (position O). Set the RPM r-S control to "Stop." Switch the motor control to MANUAL and turn the speed dial fully down.	
4.20	Turn ON the camera and lighting.	
4.21	Observe and record the settling through the reactor window.	
4.22	Prepare ice baths for both the DAO and U/F collection lines.	
4.23	Prepare a clean sample jar, label, and weigh for taking DAO samples.	Make everything ready (sample jars, scale, labels, parafilm) not to waste time during sampling to ensure everything goes smoothly and sample mass does not change substantially due to delayed sampling process.
4.24	Hold a sample jar at the outlet of valve V11.	It may need to be supported with a clamp to avoid burns due to accidental DAO splash.

4.25	Fill the DAO collection line by slowly opening valve V10.	Sample coming from valve V10 to the ice bath will be HOT. Wear heat resistant gloves if necessary.
4.26	**Slowly** open valve V11 and collect the sample into the sample jar/beaker.	Fluid coming from valve V11 is under high pressure! Be sure to open valve V11 slowly and have your hand ready to close it immediately. Valve V11 should never be fully opened as it is a choke valve meant to drop the pressure.
4.27	Close valve V11 once enough sample has been collected.	Depending on the experiment, more than one DAO samples might be required. In that case, ensure that the DAO extraction line has been purged, prior to next sampling. Otherwise, following samples will be contaminated with the leftover DAO in the external lines.
4.28	Check that all the valves are fully CLOSED.	
4.29	After the last sample has been taken, turn OFF the heater (power position O) on the 4848 controller.	
4.30	Put on heat resistant gloves and remove the insulation jacket from the reactor body.	Burns may be caused by touching the reactor heater with bare skin. Avoid contact with reactor and other components that are above room temperature. Use appropriate heat resistant gloves if contact is required.

4.31	Wait for the reactor to cool down to < 100 °C.	
4.32	Once the temperature is below 100 °C, purge the pump/ pressure transducer cooling lines with air to remove all the water from the cooling lines.	
4.33	Turn OFF the cooling water pump.	
4.34	Shut OFF the controllers and leave the reactor to cool overnight.	

Table D. 6. Part 5: Shuting down and cleaning of the reactor and ancillaries

Number	Sequence of safe work procedure steps	Potential hazards
5.1	Once cooled, release the pressure by **slowly** opening valve V4. Leave valve V4 open part way and wait for the pressure to drop in the reactor.	Releasing gas too quickly could cause the failure of valves or lines. Discharge of fluid could occur as well if gas release is not controlled.
5.2	Once the reactor is depressurized, check that the N2 cylinder supply valve is closed and the regulator valves R1 and R2 are still open.	
5.3	Open valve V5 **slowly** to allow pressure to be released from the N2 feed lines.	
5.4	Observe the pressure on the controller until it reads 0 gauge pressure. Wait an additional 60 seconds afterwards to let any residual pressure escape from the vessel.	
5.5	Close valve V5.	
5.6	Raise the stand to support the reactor.	
5.7	Unplug the reactor heater from the controller and put the wires through the stand such that they do not get in the way when lifting the reactor.	
5.8	Raise the fume hood sash so it is high enough to move the entire reactor into it.	
5.9	Position the reactor stand in the fume hood.	
5.10	Turn ON the snorkel and position it near the reactor head.	
5.11	Loosen the six bolts and undo the latches to remove the split O-ring seals. Lower the reactor cylinder slowly while one hand is	Ensure that everyone in the lab is wearing a suitable respirator before the reactor is opened.

	holding the lip of the cylinder firmly until it is clear of all of the reactor head internals (such as impellers, thermowells, etc.).	
5.12	Lift the reactor out from the rig stand and into the stand inside the fume hood.	The windowed reactor cylinder is fairly heavy. If necessary, perform this step with two people.
5.13	Lower the fume hood sash as much as possible.	
5.14	Sample the reaming materials	Reactor should contain, pitch water and the reaming DAO. Ensure to perform this stage without any delays to avoid excessive solvent evaporation that may cause significant errors in mass balance.
5.15	Displace DAO using a clean syringe and collect it in a labeled and weighed sample jar.	
5.16	Displace all the water with a clean syringe and collect it in a labeled and weighed sample jar.	
5.17	Remove all the pitch from the bottom of the reactor using a clean spatula and collect it in a labeled and weighed sample jar.	
5.18	After sampling all the materials, weigh the taken samples and record the results.	

5.19	Clean the reactor and all dirty lines with toluene.	Perform cleaning in the fume hood and ensure that nitrile gloves are worn. Lines may have to be disassembled from the rig and cleaned in the fume hood.
5.20	Leave the reactor body in the fume hood to dry overnight.	
5.21	Save all data logs on the computer and run clone-to-drive.bat	This feature allows all the recorded data to be uploaded to an external drive.
5.22	Turn OFF the fan, snorkel, computer, and all the controllers.	